

Distribution agreement

In presenting this thesis or dissertation as a partial fulfillment of the requirements for an advanced degree from Emory University, I hereby grant to Emory University and its agents the non-exclusive license to archive, make accessible, and display my thesis or dissertation in whole or in part in all forms of media, now or hereafter known, including display on the world wide web. I understand that I may select some access restrictions as part of the online submission of this thesis or dissertation. I retain all ownership rights to the copyright of the thesis or dissertation. I also retain the right to use in future works (such as articles or books) all or part of this thesis or dissertation.

Signature:

Logan Melot

Date

Characterizing Infection of B Cells with Wild-type and Vaccine Strains of Measles Virus

By
Logan Melot
Doctor of Philosophy

Graduated Division of Biological and Biomedical Sciences
Immunology and Molecular Pathogenesis

Paul A. Rota
Advisor

David Steinhauer
Co-Advisor, Committee Member

Mandy Ford
Committee Member

Haydn Kissick
Committee Member

Mehul Suthar
Committee Member

Accepted:

Kimberly Jacob Arriola, Ph.D.

Dean of the James T. Laney School of Graduate Studies

Date

Characterizing Infection of B Cells with Wild-type and Vaccine Strains of Measles Virus

By

Logan Melot

B.S. University of Oklahoma

Advisor: Dr. Paul A. Rota

Ph.D., Michigan State University

An abstract of the dissertation submitted to the Faculty of the James T. Laney School of Graduate Studies of Emory University in partial fulfillment of the requirements for the degree of

Doctor of Philosophy in Immunology and Molecular Pathogenesis

2023

ABSTRACT

Characterizing Infection of B Cells with Wild-type and Vaccine Strains of Measles Virus

By Logan Melot

Acute infection with measles virus (MeV) causes transient immunosuppression which can lead to secondary infections, which is not observed in vaccinated individuals. MeV infection of B lymphocytes leads to changes in the antibody repertoire and memory B cell populations for which the mechanism is unknown. We characterize the infection of primary B cells with wild-type (FL-15) and vaccine (EZ) strains of MeV. EZ-GFP infected cells are characterized by a higher percentage of cells positive for viral protein, regardless of B cell subtype. Cells infected with EZ-GFP displayed higher levels of N gene transcription at 24- and 48-hours post-infection than cells infected with FL-15. Non-switched memory cells had lower levels of viral protein expression than other subtypes during EZ-GFP infection. There were slightly higher levels of viral protein detected in non-switched memory cells than in other subtypes during FL-15 infection. Despite evidence of replication, measles-infected B cells did not produce detectable virus progeny. There are measurable differences in cell viability between FL-15 and EZ infected cultures. FL-15 infected culture had lower viability as well as higher levels of MLKL phosphorylation and cleavage of caspase-3, -8, and -9. Both FL-15 and EZ infected cultures had increased expression of IL-4 and IL-6. Higher levels of IL-8 were detectable in FL-15 infected cultures than in EZ infected cultures. Higher levels of TNF- α and IL-10 were detected in EZ compared to FL-15 infected cultures. Localization of nucleoprotein on the cell surface and at sites of cellular interaction were observed in both FL-15 and EZ infected cultures. Localization of hemagglutinin and MeV receptor SLAM were observed in both FL-15 and EZ infected cultures but protein reorganization occurred earlier in the infection in EZ infected cultures. These data help us understand the differences in viral replication and cellular outcome following infection with vaccine or wild-type strains of MeV.

Characterizing Infection of B Cells with Wild-type and Vaccine Strains of Measles Virus

By

Logan Melot

B.S. University of Oklahoma

Advisor: Dr. Paul A. Rota

Ph.D., Michigan State University

A dissertation submitted to the Faculty of the

James T. Laney School of Graduate Studies of Emory University

in partial fulfillment of the requirements for the degree of Doctor of Philosophy in Immunology

and Molecular Pathogenesis

2023

ACKNOWLEDGEMENTS

I'd like to acknowledge all of my lab mates and friends that are in the Viral Vaccine Preventable Diseases Branch at the Centers for Disease Control and Prevention. They have been instrumental to my success. Thank you Paul, Bettina, and Melissa for being my mentors over the years and putting up with my hard-headed nature. I am grateful for their guidance and the lessons they have taught me that have helped me develop into an independent scientist. I would also like to thank all of my friends I've made over the years through IMP and other GDBBS programs. They have provided comradery and friendship that really helped break up the minutia and grind that goes along with the research, making it more bearable. . I've had a lot of fun traveling with lab mates, getting to go to conferences, and experience the scientific world. My friends in Oklahoma and other friends I've stayed in contact with through gaming or other online methods have also been a great support in giving me an escape from the thesis work when it was needed. I'd also like to give a special thank you to my dog, Kevin, who has really kept me grounded and has been a light in my life since I adopted him when I first moved to Atlanta. Thank you to all of the YouTube channels I had on in the background while doing data analysis or running flow cytometry to help the mundane tasks become more bearable. I'd also like to make a special mention of my late friend Tim Hoang who sadly passed away from COVID related complications in the summer of 2022. He was a brilliant scientist and a fun guy to have a round and we all miss him dearly. I'd like to acknowledge my committee members Haydn, Mandy, Mehul, and Dave for helping guide me in the right direction when I was scrambling or lost in the project. Haydn was instrumental in helping me navigate this project and helping me deal with the struggles that came with the degree. I was not one of his students, but he treated me as a student and as someone that he cared about. He is a mentor that really stands out and goes above and beyond to help nurture the scientific minds of the students in the program. I don't think I would have made it through this without his support. Lastly, I'd like to give a special thank you to Elina, Nataliya, Katherine, Brian, Sydney, Zach, Jenna, Vincent, Mike, Eric, Maria, and all of my other close friends that have been a continuous support system over the last six and a half years. I'd also like to thank beer, so cheers to the next chapter of my life and the great things to come.

TABLE OF CONTENTS

Chapter 1: Introduction (8-23)

- Virology of Measles Virus (8-11)
- History of Measles Vaccination (12-14)
- Measles Pathogenesis (14-15)
- Measles Symptoms (15-16)
- Measles and the Immune System (16-17)
- Measles Evasion of Host Response (17-20)
- *In Vivo* Infection of B cells (20-22)
- Differences in Vaccine and Wild-type Virus (22-23)
- Gaps in Knowledge (23)

Chapter 2: Characterizing Viral Replication During the Infection of B Cells with Wild-type or Vaccine Strains of Measles Virus (25-49)

- Introduction (25-27)
- Materials and Methods (27-31)
- Results (32-36)
- Discussion (36-39)
- Figures (40-49)

Chapter 3: Assessing Cellular Characteristics of B Cells Infected with Vaccine and Wild-type Strains of MeV (50-82)

- Introduction (52-55)
- Materials and Methods (55-61)
- Results (61-64)
- Discussion (64-70)
- Figures (71-82)

Chapter 4: Discussion and Conclusions (83-94)

- BJAB Cells as a Model of Infection for MeV (83-84)
- Comparison of Wild-type and Vaccine Replication in B Cells (84-86)
- Assessing Cell Death in MeV Infected B Cell Cultures (86-87)
- Cytokine Expression in MeV Infected B Cell Cultures (87-88)
- Production of Viral Progeny and Non-canonical Viral Spread (88-91)
- Impact and Future Studies (91-93)
- Graphical Abstract (94)

References (95-102)

INTRODUCTION

Virology of Measles Virus

Measles virus (MeV) is a member of the *Paramyxoviridae* family and the type species of the *Morbillivirus* genus¹. MeV is a non-segmented, negative sense, single stranded RNA virus¹. There are currently 24 known genotypes of MeV. In 2019, five circulating genotypes were detected (B3, D4, D8, D9, and H1), but as of 2021, only two genotypes B3 and D8 were reported to the World Health Organization (WHO) Global Measles Nucleotide Sequence Database (MeaNS)². These genotypes are differentiated by mutations present in the nucleoprotein (N) and hemagglutinin (H) gene³. The several lineages of vaccine virus are all denoted as genotype A, many of which were derived from the original Edmonston-B strain developed by John F. Enders and colleagues⁴. In 1968, a weaker form of the vaccine strain called Edmonston-Enders (Moraten) was developed by Maurice Hilleman and colleagues. Common Edmonston-derived strains used in vaccines include Schwartz, Edmonston-Zagreb, and Moraten⁴. There are also some strains that did not originate from the Edmonston strain such as CAM-70, TD-97 (Tanabe), Leningrad-16, and Shanghai-191⁵. The Edmonston-derived Moraten strain is the attenuated virus used for vaccination in the United States⁴, Canada, and many European countries⁶. In addition to Moraten, the United States also uses a recently approved Schwartz strain vaccine⁷. Edmonston-Zagreb is a widely used strain in countries such as Switzerland, Mexico, and India⁸.

The genome of MeV is approximately 16,000 nucleotides which is comprised of six genes that each encode a single structural protein. These six proteins are the nucleocapsid (N) protein, phosphoprotein (P), matrix (M) protein, fusion (F) protein, haemagglutinin (H) protein and large

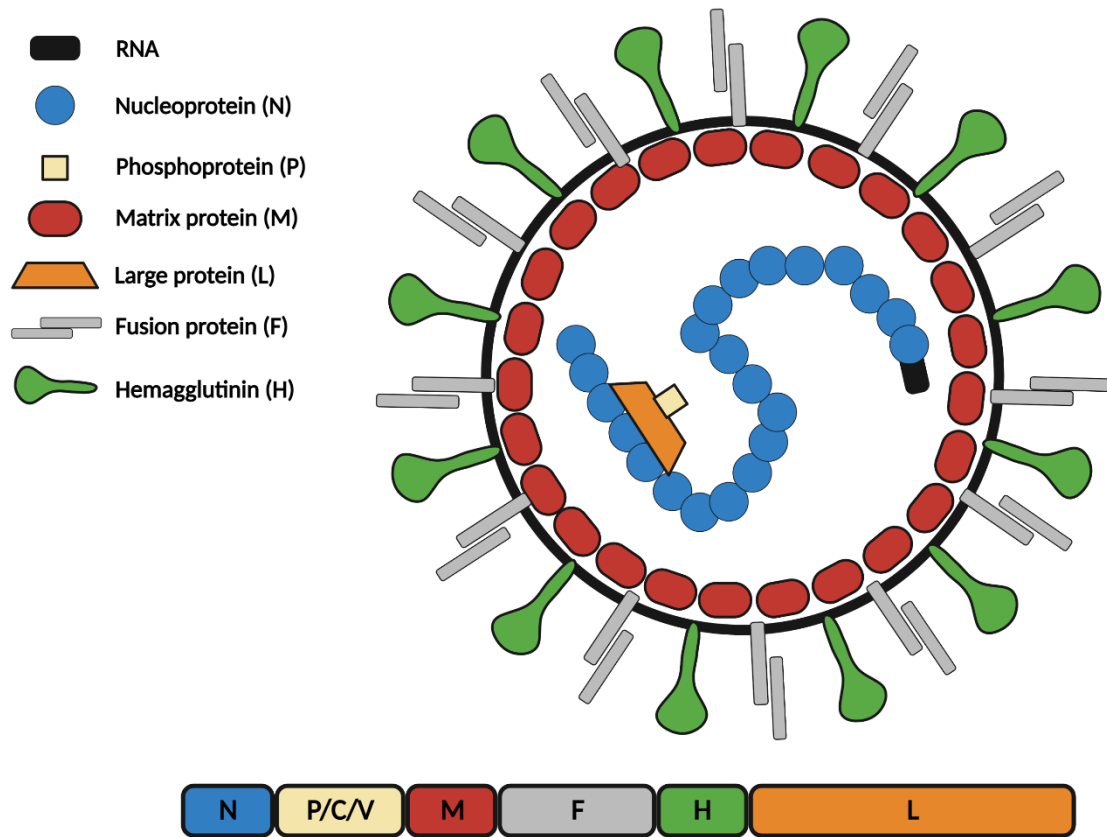


Figure 1. Visual representation of measles virion.

(L) protein (Fig. 1)¹. The P gene also encodes two non-structural proteins, the V protein and C proteins. MeV has two transmembrane glycoproteins that are exposed on the virion surface, H and F. After the viral genome enters the cell, the genome is then transcribed into positive sense and translated to generate viral proteins key for replication. After the key proteins are generated, viral replication and translation of viral protein proceeds to amplify virus related components. Due to polymerase complexes detaching from the template at intergenic regions, MeV transcription generates a gradient of mRNAs¹. The transcription gradient generates a decreasing amount of viral protein descending from N to L⁹. Lastly, MeV replication can generate sub-genomic particles that can interfere with replication called defective interfering particles¹⁰, which impact immune signaling during *in vitro* infection¹¹.

The H protein targets and binds to the host cellular receptor (CD150/SLAM) which triggers conformational changes in the F protein¹², leading to the fusion of the viral envelope with the plasma membrane of the cell and subsequent release of ribonucleoprotein complexes into the cytoplasm of the target cell. Fusion of cellular membranes also contributes to the development of the characteristic syncytia associated with MeV infection in culture and giant cell formation in lungs of measles virus infected individuals¹³. Expression of glycoproteins on the surface of infected cells allows for interaction between budding MeV virions and neighboring cell virus receptors, repeating the life cycle of the virus¹³.

The P protein is generated as a co-N terminal nested protein with the V protein. MeV V proteins are translated using P gene mRNAs which have had G nucleotides inserted at specific codons during transcription, a process called RNA editing¹⁴. C protein translation begins at a methionine initiator codon 19 nucleotides downstream from the P start codon¹. Both the insertion of G and the secondary initiator codon allow translation of three viral proteins from one gene (P, V, and C). Of the three proteins encoded by the P gene, the P protein is the only essential protein for RNA synthesis, playing a direct role in transcription by binding to L protein and acting as a bridge to link L to N within the ribonucleocapsid¹. In addition, during genome replication, P binds N protein, preventing aggregation and allowing for specificity in assembly¹. The V and C proteins encoded by the P gene have been shown to interfere with host innate anti-viral responses. The V protein interacts with molecules involved in the induction and transduction of type I IFNs (IFN α and IFN β ¹). Some of the proteins affected by this include the RNA helicases melanoma differentiation-associated gene 5 (MDA5) and LGP2¹⁵, I κ B kinase α ¹⁶, signal transducer and activator of transcription 1 (STAT1)¹⁷, STAT2¹⁸, and Janus kinase 1 (JAK1)¹⁷. While the exact mechanism of how MeV C protein interferes with the host anti-viral response is not fully

understood, experiments have shown that recombinant MeV with mutated C proteins is attenuated in cells with functional type I IFN responses¹⁹. In addition, this virus does not propagate or cause Koplik spots or rash in nonhuman primates^{20,21}. The C protein downregulates viral RNA synthesis, allowing the virus to escape detection by RIG-I and MDA5, limiting the production of interferon associated proteins²². Transfected C protein has interferes with IFN β transcription in the nucleus²³, and interferes with the formation of STAT1, leading to the attenuation of IFN γ signaling²⁴.

The MeV N protein is translated from the first gene in the viral genome¹. N is an RNA binding protein that encapsidates full length genomic and antigenomic RNAs to form the helical nucleocapsid template¹. Encapsidation protects RNA from digestion by host defenses and helps form interaction sites for assembly of progeny nucleocapsids in budding virions¹. The COOH-terminus of the N protein has been shown to bind to the Fc γ II receptor and which will then egress to the surface of B cells and dendritic cells, modulating the immune response by attenuating the production of antibodies²⁵, impairing dendritic cell functions²⁶, and limiting IL-12 production²⁷. The ribonucleoprotein complex formed with N protein is the protein complex involved in viral transcription and replication¹. MeV requires an RNA-dependent RNA polymerase for replication¹. Data has shown that the L protein contains the polymerase activity, and the P protein has an accessory role, both of which are required for replication¹. The L and P proteins are also associated with capping, methylation, and polyadenylation^{21, 24}. The measles matrix (M) protein is the most abundant protein in the membrane of the virion but is peripherally associated with the membranes and is not an intrinsic membrane protein¹. It is thought that the M protein is the organizer of viral morphogenesis by interacting with membrane proteins, the lipid bilayer, and the nucleocapsid¹. The M protein has been shown to link the ribonucleoprotein complex to viral glycoproteins²⁸. The interaction with the nucleocapsid is thought to play a role in the budding of the virus¹.

History of Measles Vaccination

One of the first written accounts of measles disease was written by a Persian doctor in the 9th century²⁹. In 1757, Francis Home demonstrated that measles was caused by an infectious agent in the blood of his patients²⁹. Starting in 1912, United States healthcare providers began to report diagnosed cases with the first decade of reporting showing an average of 6,000 measles-related deaths in the United States each year²⁹. Studies to develop a MeV vaccine began in 1954 when John F. Enders and Thomas C. Peebles began collecting blood samples from ill students during a measles outbreak in Boston²⁹. They were able to isolate MeV from one of the students, 13-year-old David Edmonston²⁹. Before John Enders and colleagues used the isolated virus in the generation of an attenuated strain in 1963, nearly all children acquired MeV by the time they were 15²⁹. Among the annual reported cases of the United States in the 1960s, estimates suggest that 400 to 500 people died, 48,000 were hospitalized, and 1,000 suffered from encephalitis²⁹. Following the development of the first vaccine in 1968, Maurice Hilleman and colleagues developed an even more attenuated strain of MeV²⁹. This new strain was called “Moraten” and is the primary strain of virus used in measles vaccines in the United States since 1968²⁹. In 1978, the Centers for Disease Control and Prevention set a goal to eliminate measles from the United States by 1982²⁹. This goal was not met; however, by 1981, the number of reported measles cases had decreased by 80% from the previous year²⁹. A MeV outbreak in 1989 among vaccinated school-aged children prompted the Advisory Committee on Immunization Practice, the American Academy of Pediatrics, and the American Academy of Family Physicians to recommend a second dose of MMR vaccine for all children. This development led to an even further decline in measles cases in the United States²⁹. Following the absence of continuous disease transmission in the

United States for longer than 12 months, measles was declared eliminated which was verified by the Pan American Health Organization (PAHO) in 2000³⁰.

In 2020, the World Health Assembly endorsed the Immunization Agenda 2030 (IA2030) that focused on vaccination and the elimination of vaccine preventable diseases (VPD) such as measles. These goals are highlighted in three sections: 1) prevent disease, 2) promote equity, and 3) build strong immunization programs. These goals highlight efforts to eliminate measles by saving lives, reducing VPD outbreaks, providing equal access to vaccination, and developing systems for distribution of vaccines such as measles vaccination³¹. Measles elimination is defined by WHO as “the absence of endemic measles transmission in a defined geographical area for more than 12 months in an area with well-performing surveillance systems,” which is verified again after 36 months³².

Vaccine implementation has had a strong impact on the number of cases in the United States. Between 2015 and 2020, there were only 2,056 reported cases of measles in the United States³³. WHO reporting shows that there were 1.9 million cases globally in the same time window, with a peak of 873,000 estimated cases in 2019³³. MeV is highly infectious with a basic reproductive number (R_0) of 12-18⁴, suggesting that in a naïve population, one infected host can infect anywhere from 12 to 18 others, requiring measles vaccination to have a high level of coverage (>90%)³⁴. A recent report stated that in 2019 there was approximately 85% first dose MeV vaccination coverage and 71% for second dose vaccination coverage globally. This level of vaccine coverage is estimated to have reduced measles mortality by 62% between 2000 and 2019, leading to an estimated 25.5 million deaths that were averted by vaccination³⁴. However, the COVID-19 pandemic has exacerbated the threat of MeV globally as surveillance and vaccination coverage have declined, with a 2% decrease in first dose measles vaccination, and a 1% decrease

in second dose vaccination globally³⁴. This coincided with a 23% decrease in the number of countries with >90% MCV1 coverage³⁴. Global reports estimate that there were 9.48 million cases of measles and approximately 128,000 measles associated deaths in 2021³⁵.

Measles Pathogenesis

Upon infection, the MeV H protein binds to its receptor, CD150 (SLAM - signaling lymphocytic activation molecule). The receptor is expressed on memory T cells³⁶, B cells³⁷, dendritic cells³⁸, alveolar macrophages³⁹, and platelets⁴⁰. *In vivo*, tissue resident dendritic cells and alveolar macrophages in the respiratory tract are the initial targets of infection. SLAM is the main receptor on dendritic cells; however, MeV can also attach to DC-SIGN on dendritic cells which can mediate SLAM-dependent MeV infection⁴¹. In addition, this attachment to DC-SIGN allows for the transmission of MeV to T cells. MeV can also infect alveolar macrophages in the lungs which can lead to trans-infection of lymphocytes. Epithelial damage in the lung can allow MeV dissemination across the mucosal barrier⁴². Vaccine strains and some laboratory-adapted strains of MeV use human membrane cofactor protein (CD46) as the primary receptor for infection⁴³. Following infection of alveolar macrophages and dendritic cells present in the lung, MeV infected-cells disseminate to the draining lymphoid tissue, the site of high levels of replication and induction of viremia by infecting lymphocytes bound for circulation⁴⁴. Analysis of lymph nodes in a non-human primate model showed high levels of replication in the B-cell follicles, generating multinucleated giant cells known as Warthin-Finkeldey cells which consist of fused B cells⁴⁵. Following the infection of cells in the lymph node, dendritic cells and circulating T cells and B cells disseminate the virus to epithelial cells that express nectin-4, the cellular receptor used for exit by wild-type MeV⁴⁶. The basolateral side of respiratory epithelial cells expresses nectin-4 and

upon entry into the epithelial cells lining the respiratory tract, coughing or sneezing causes transmission of virus to other hosts through respiratory droplets⁴⁷.

Measles Symptoms

MeV has an incubation period of 7-14 days, during which the virus replicates in myeloid and lymphoid cells to generate a systemic infection⁴⁸. Once the virus has spread to peripheral lymphoid tissues and out of the respiratory tract, a prodromal phase, or the period between the appearance of symptoms and the development of rash, starts⁴⁸. The prodromal phase is characterized by malaise, fever, and cough⁴⁸. Within 24 to 48 hours, clustered white lesions called Koplik spots can begin to form on the buccal mucosa. These spots are the pathognomonic symptom for MeV infection⁴⁹. Koplik spots are a sign of the virus disseminating to the peripheral tissues such as the skin and the submucosa of the respiratory tract, allowing for transmission to the surrounding epithelial cells and keratinocytes. The maculopapular skin rash begins after the three-to-five-day long prodromal phase, usually starting around the ears and face, spreading down the body to the trunk or extremities⁴⁸. Conjunctivitis tends to develop around the same time as the rash, both of which have been shown to be caused by immune-mediated clearance of MeV-infected cells⁴⁸. Due to the involvement of the immune system in the development of conjunctivitis and maculopapular rash, it may be difficult to diagnose measles in individuals who have attenuated immune responses^{48, 49}.

In addition to these acute symptoms, there are two long-term, more severe sequelae that can occur following MeV infection. Measles can lead to severe neurological complications such as acute post-infection measles encephalitis (APME) (0.1% of measles cases), measles inclusion body encephalitis (only immunosuppressed patients), and subacute sclerosing panencephalitis (SSPE) (6.5-11 cases per 100,000 measles cases)⁵⁰. SSPE is caused by a persistent viral infection

detected in the central nervous system of infected individuals with a latent period between 6 and 8 years. Symptoms range from involuntary muscle movements known as myoclonic jerks to seizures. Death occurs in individuals diagnosed with SSPE within 1 to 3 years⁵¹. A small percentage of diagnosed individuals will have symptoms occur more rapidly, but approximately five percent of diagnosed individuals may experience improvement and regain function^{48, 51}. MeV infection has also been shown to induce a state of immunosuppression, leading to the generation of inadequate responses to secondary infection following MeV infection causing symptoms such as diarrhea, pneumonia, or otitis media⁴⁸.

Measles and the Immune System

MeV infection can induce a state of immunosuppression which leads to the generation of inadequate responses to secondary infection following MeV infection which increases the risk of secondary infections like diarrhea, pneumonia, or otitis media. In countries lacking adequate health care, these types of illnesses can lead to death. Case fatality ratios for measles can range between 0.01% to more than 5% depending on age of infection, nutritional status, access to health care, and vaccine coverage with a peak level of 20-30% during humanitarian crises⁴⁸. Different estimates exist for the duration of MeV-induced immune suppression. The immune suppression can be limited to several months as seen in attenuated responses to tuberculin in tuberculosis tests⁵² and mathematical models have shown that suppression can cause an increase in measles associated mortality for up to 3 years⁵³. These models are supported by studies that show increases in hospitalizations, antiviral prescriptions, and antibiotic prescriptions in the UK following infection with MeV. There was a 30% increase in the prescription of anti-infective medications in children between the ages of 1-5 years following MeV infection in the UK, accompanied by a 10% increase in hospitalizations in children between the ages of 1-2 years⁵⁴. The overall mechanism of this

immune suppression is not fully understood. Due to the breadth of immune cells infected by MeV, the role of each infected cell type in the development of immune suppression is currently unknown. While effector function following MeV infection has been characterized in T cells and dendritic cells, the changes in effector function of B cells following MeV infection are not fully defined. B cells could play a large role in immunosuppression due to high levels of interaction with other immune cells.

Measles Evasion of Host Response

MeV proteins can interact with host cell function. The P, V, and C proteins of measles interact with the innate immune system, effectively preventing the ability of the infected cell to respond to the infection. The MeV V protein limits the activation of MDA5⁵⁵, inhibiting the activation of the interferon response to infection. MeV V protein interacts with NF- κ B signaling by retaining its p65 subunit in the cytoplasm⁵⁶, leading to a downregulation in transcription processes related to antiviral responses⁵⁷. MeV also interacts with other proteins in the RIG-I signaling pathway by blocking key proteins involved in the antiviral response such as blocking STAT1 phosphorylation¹⁷, STAT2 phosphorylation¹⁹, RNA helicase function¹⁵, and other proteins involved in the signaling cascades. *In vitro*, the collective impact of MeV proteins on interferon signaling is an almost complete ablation of the interferon response with infection of A549/hSLAM lung cells *in vitro* showing that 14 of 17 wild-type isolates did not generate a significant IFN β response⁵⁸. *In vivo*, IFN α , IFN β , and IFN γ remain undetectable in infected rhesus macaques⁵⁹. While there may be a lack of interferon induction during MeV infection, there is induction of RNA transcription for proteins involved in the inflammasome responses⁶⁰ as well as IL-1 β ⁶⁰, IL-6⁶¹, IL-8⁶¹, and IL-18⁶² production. Therefore, MeV can directly inhibit key antiviral pathways but not others which permits viral clearance and induction of the adaptive immune system via non-

interferon mediated pathways. These studies also show that different kinds of immune cells are impacted in different ways as well as to different degrees by MeV infection.

In addition to being the initial target cells of infection, the innate immune system plays a key role in the initial response to MeV. In rhesus macaques, dendritic cells and alveolar macrophages are the first cells infected, generally in bronchial associated lymphoid tissue, where additional infection of T and B lymphocytes occurs in draining lymph nodes⁴⁴. Infection of dendritic cells and subsequent expression of MeV H and F proteins on the cell surface leads to the dampening of the CD4 T cell response to MeV by limiting their proliferation⁶³. MeV infection impacts the expression of co-stimulatory molecules on dendritic cells, affecting the ability of T cells to mount a proper immune response⁶⁴. In addition to altered co-stimulatory molecule expression, cytokines produced by activated dendritic cells such as IL-12, IL-1 β , and IL-10 are impacted by MeV infection^{65, 66}. MeV infected dendritic cells also had suppressed TLR4 stimulation⁶⁷, potentially limiting their ability to properly respond to secondary stimulus. In addition to altered cytokines and TLR profiles, CCR7 expression is decreased, preventing migration of dendritic cells to lymphoid tissues⁶⁸. MeV H protein limits the amount of IL-2 dependent Akt activation, thus limiting proliferation in T cells. In addition, the formation of the immunological synapse, where signaling interactions occur between the dendritic and T cells, is reduced. During an immune response to viral infection, T cells tend to differentiate into Th1 cells⁶⁹; however, during a MeV infection, T cells are skewed to generate a Th2 type response⁷⁰. It is thought that MeV infection in dendritic cells limits interaction with CD8 T cells through CD40-CD40L, further dampening the T cell response⁷¹. These data show that MeV alters DC function impacting the ability of other cells to adequately respond to infection

In addition to dendritic cells, alveolar macrophages are one of the initial targets of MeV during infection⁴⁴. Similar to a dendritic cell, macrophages play a key role in transporting MeV to draining lymph nodes, allowing for infection of CD150 expressing lymphocytes residing in the lymph node. Studies done in humanized mouse models show that macrophages play a role in supporting viral replication early during infection, but are also linked to limiting infection in other cell types⁷². While both initial targets of MeV have been shown to be functionally impacted by infection, cells involved in the adaptive immune response are heavily affected by MeV infection.

The changes observed in wild-type infection are not seen in individuals vaccinated with MMR. This suggests that there are differences in wild-type and vaccine strains of MeV that may generate differences in phenotypic outcomes; however, while the clinical outcome following MeV infection is apparent, these differences and the mechanism behind the development of immune suppression are not fully understood. MeV induces a state of lymphopenia in the infected host, inherently dampening the immune system with detectable changes in lymphocyte function. T cell function is key in controlling viremia and frequency of infected cells in the periphery as depletion of CD8 T cells generates an increased severity in symptoms⁷³. Based on a study that investigated levels of T cell and B cell subsets in the peripheral blood following MeV infection, there is a decrease in the number of Th17 and Th1/17 subtypes of T cells; there is also a slight decrease in the overall levels of naïve T cells⁷⁴. Studies done in an IL-2 dependent T cell line have shown that MeV limits the ability of T cells to respond to IL-2 in addition to limiting their cytotoxic effects⁷⁵. As mentioned previously, MeV infection limited the ability of the immune system to respond to tuberculin tests in a BCG-vaccinated rhesus macaque model. Specifically, the changes in the response were characterized by the lack of infiltrating T cells to the site of tuberculin injection⁷⁶. In addition to the lymphopenia caused by the viral infection, lymphopenia is further exasperated

by death of bystander T cells, leading to cytotoxic killing in PBMCs⁷⁷. In addition to changes in cellular interactions and cytokine production, MeV limits the capacity for T cells to be activated and proliferate⁷⁸. Limited activation and proliferation were shown to be generated by an arrest in the cell cycle as well as down-regulation of costimulatory markers. In summary, not only does MeV infect and kill T cells, but it can also play a role in altering their effector function and how an immune response is produced.

Similar to T cells, B cells are arrested in their cell cycle following MeV infection and have shown an increase in size⁷⁹. Changes observed in the antibody repertoire⁷⁴ and reconstitution of B cell pools⁸⁰ following MeV infection is supported by a decrease in B cell subtypes such as IgG memory and IgA memory B cells with an increase in plasma and transitional cells was observed in infected humans⁸¹.

In Vivo Infection of B cells

Animal models have played an important role in furthering the understanding of how MeV can alter the immune profiles of infected individuals. Infections in rhesus macaques with a lab adapted B3 strain of MeV that expresses green fluorescent protein (GFP) show that both B and T cells are infected and infected cells can be isolated from PBMCs, draining lymph nodes, and tonsillar tissue with a depletion of B cells in lymphoid tissue during infection⁷⁶. B cells express the receptor required for wild-type MeV infection, CD150. B cells are the most frequently infected lymphocyte during infection *in vitro*, the most frequently infected cell out of lymphoid cells present in the tonsil of infected macaques, and the most frequently infected cell in the periphery⁸². Ferret models using a similarly pathogenic morbillivirus, canine distemper virus (CDV), show that CDV infection induces similar levels of lymphopenia, viremia, and immune suppression in animal models when compared to MeV infection⁸³. Studies were done to determine the impact of CDV

infection on an existing antibody repertoire through live-attenuated influenza virus (LAIV) vaccination as well as the ability of these ferrets to respond to secondary infection. Ferrets were vaccinated and then infected with CDV 4 weeks post vaccination. Animals infected with CDV showed a marked decrease in antibodies specific for LAIV. Additionally, ferrets were challenged with H1N1 14 weeks post vaccination to determine the impact of CDV infection on the ability of these animals to respond. The animals that were not infected with CDV saw an expected increase in antibody titer upon initial and secondary challenge with H1N1. However, animals that had been infected with CDV following LAIV vaccination, did not see an increase in antibody titer upon challenge⁸¹. These results show that not only does lymphotropic morbillivirus led to lymphopenia and a loss of immune cells, but it also generates a state of immune modulation leading to a lack of ability to respond to infections. Insights such as these have been instrumental in guiding the field to finding the mechanisms of immune suppression caused by MeV infection.

The clinical impact of MeV infection on B cells has also been assessed in humans. The immune cell profile of individuals before and after MeV infection showed changes in detectable B cell subsets following infection. Overall, there was a significant decrease in detectable memory B cells, specifically, IgG and IgA expressing memory B cells. There was also a detectable increase in transitional B cells (immature B cells) that have not gone through selection⁷⁴. Interestingly, other studies suggest that there is a skewing of the B cell repertoire to a more “naive-like” phenotype characterized by changes in the BCR repertoire on the surface of B cells following MeV infection⁸¹. This change is also characterized by a use of limited diversity of VDJ genes that tend to represent a more naive phenotype in infected individuals, preventing them from having the ability to properly respond to previously encountered pathogens. The naïve phenotype coincides with a decrease in the diversity of detectable B cell clones which suggests that there will be an

impact on the diversity of antibodies⁸¹. This hypothesis is confirmed by another study that that showed a marked loss in the diversity of the antibody repertoire of MeV infected individuals⁸⁰. Paradoxically, the decrease in repertoire only affects non-MeV-specific antibodies because a detectable increase in MeV antibodies is observed in infected individuals, suggesting that this is an off-target effect of MeV infection. Importantly, an increase in the diversity of the antibody repertoire in participants vaccinated with a measles, mumps, and rubella (MMR) vaccine was detected⁸⁰. Since both wild-type and vaccine strains of MeV are capable of replication in human hosts, the ability of wild-type to cause this state of immune suppression suggests that there are differences in wild-type and vaccine infection that could generate this phenotype.

Differences in Vaccine and Wild-type Virus

A key component of this study is to assess the differences between infection patterns and cellular responses generated by vaccine (EZ) and wild-type (FL-15) strains of MeV. Despite being a live-attenuated replication competent virus, the decrease in antibody titer, decrease in B cell diversity, and changes in the immune phenotype of the B cell compartment are not detected in those who receive the vaccine^{53, 80, 81}. Vaccine strains have been shown to have up to 14 amino acid substitutions in each protein. Twenty nucleotide substitutions which lead to changes in amino acids throughout the virus were shown to be conserved between eight different vaccine strains⁸⁴. Mutations in viral proteins has been shown to impact the virulence of virus strains⁸⁵ potentially affecting their ability to affect host cell function such as: N interfering with cytokine production⁸⁶, P protein suppressing Toll-like receptor signaling⁸⁷, V protein inhibiting inflammasome formation and IL-1 β production⁶⁰ and TLR-7/9 induction¹⁶, C protein's impact on cell growth²⁴ and IFN β production⁸⁸, M protein's impact inhibition of host cell transcription⁸⁹, and H protein's impact on

dendritic cell signaling³⁸. Sequencing of EZ and FL-15 virus show that there is approximately a 3.5% difference in the nucleotides that make up the viral genome which leads to several amino acid substitutions in the EZ virus (Figure 2). However, the exact mechanism of attenuation is not known,⁸⁴ therefore, comparing the infection of wild-type and vaccine strains in B cells and the functional impact on B cells may play a key role in fully understanding the development of immune suppression.

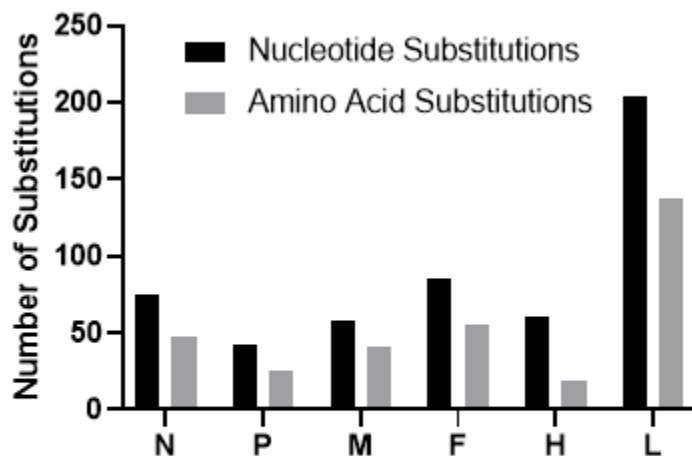


Figure 2. Substitutions in EZ Compared to FL-15

Gaps in knowledge and experimental goals

The infection of B cells *in vitro* has not been fully characterized. Replication and production of viral progeny, B cell viability, cytokine production, and interactions between infected and uninfected B cells have not been evaluated. Most importantly, the differences between wild-type and vaccine infections in these contexts have not been assessed.

Our studies aim to assess the ability of both vaccine and wild-type strains of MeV to replicate in B cells. Additionally, these studies aim to analyze consequences of infection on B cells by assessing cytokine production, interactions between infected and uninfected cells, and the viability of infected cells. The goal is to elucidate differences in the infection profiles in cells infected with vaccine or wild-type strains of measles virus. Experiments assessed MeV infection from both the viral and cellular perspective, which may guide future *in vivo* experiments to determine the mechanism of the immune suppression and modulation.

Chapter 2: Characterizing Viral Replication During the Infection of B Cells with Wild-type or Vaccine Strains of Measles Virus

This chapter is reproduced with edits from:

Characterizing infection of B cells with wild-type and vaccine strains of measles virus

Logan Melot^{1,2}, Bettina Bankamp¹, Paul A. Rota^{1,2}, Melissa M. Coughlin¹

¹Viral Vaccine Preventable Diseases Branch, Division of Viral Diseases, National Center for Immunization and Respiratory Diseases, Atlanta, GA, USA, Centers for Disease Control and Prevention. ²Emory University, Atlanta, GA, USA

ABSTRACT

Acute infection with measles virus (MeV) causes transient immunosuppression which can lead to secondary infections. MeV infection of B lymphocytes leads to changes in the antibody repertoire and memory B cell populations for which the mechanism is unknown. In this chapter, we characterize the infection of primary B cells with wild-type and vaccine strains of MeV and focus on each viruses' ability to replicate in B cells *in vitro*. Vaccine-infected B cells are characterized by a higher percentage of cells positive for viral protein, regardless of B cell subtype. Cells infected with EZ-GFP displayed higher levels of N gene transcription at 24- and 48-hours post-infection than cells infected with FL-15. Non-switched memory cells had lower levels of viral protein expression than other subtypes during EZ-GFP infection. There were slightly higher levels of viral protein detected in non-switched memory cells than in other subtypes during FL-15 infection. Despite evidence of replication, measles-infected B cells did not produce detectable virus progeny. This study furthers our understanding of the outcomes of MeV infection of human B cells.

INTRODUCTION

Measles virus (MeV) is an enveloped negative sense RNA virus in the *morbillivirus* genus of the family *Paramyxoviridae*. Measles presents with a maculopapular skin rash, a fever above 38.3°C, cough, coryza, and conjunctivitis⁹⁰. The case fatality rate for measles can range from 0.2% to 29.1% depending on the epidemiologic setting⁹¹. A highly effective vaccine for the virus was developed in 1963, and despite the estimated 31.7 million lives saved worldwide through measles vaccination⁹², there were still 149,796 cases and an estimated 60,700 deaths in 2020⁹³. The COVID-19 pandemic has further exacerbated the threat of MeV globally as surveillance and vaccination coverage have declined, with a 2% decrease in first dose measles vaccination, and a

1% decrease in second dose vaccination globally. This coincided with a 23% decrease in countries with >90% MCV1 coverage⁹³.

Individuals are infected via the respiratory route through the inhalation of respiratory droplets. MeV is lymphotropic, initially targeting signaling lymphocytic activation molecule F1 (SLAMF1, CD150)-expressing alveolar macrophages and dendritic cells in the respiratory tract followed by transmission to SLAM-expressing B and T cells in the surrounding bronchus-associated lymphoid tissue⁴⁴. Infected cells migrate to draining lymph nodes, further replicating in B and T cells leading to lymphopenia and a generalized prolonged immune suppression^{53, 94}. Following replication in the lymph nodes, MeV disseminates to the periphery, infecting nectin-4+ epithelial cells, leading to the characteristic maculopapular rash and allowing for spread through infectious respiratory droplets^{95, 96}. Measles-associated immune suppression is observed only following infection and is not observed after vaccination with the measles, mumps, and rubella (MMR) vaccine⁸⁰. MeV-induced immune suppression is characterized by increased secondary infections which are a major cause of morbidity and mortality in children⁵³. Children with measles are more likely to require prescription antivirals and antibiotics in the months and years following MeV infection⁹⁷. The mechanism by which MeV causes immune suppression is not fully understood. Studies performed *in vitro* have demonstrated immune cell dysfunction in dendritic cells and CD8+ T cells^{94, 98}. B cells are highly targeted in non-human primate models of measles infection, accounting for approximately 20-30% of infected PBMCs^{42, 99}. Importantly, infected individuals have changes in the frequency of T cell subtypes and a decrease in class-switched memory B cells, resulting in a decline in circulating non-MeV specific antibodies and an altered antibody repertoire accompanied by a decrease in B cell clonal diversity^{81, 100}. The targeting of and changes in B cell-associated immune profiles suggests that B cells could play a significant role in

measles induced immune dysregulation. This chapter aims to better understand the characteristics of B cell infection with vaccine (Edmonston-Zagreb strain, EZ) and wild-type (MVs/Florida.U.S.A./12.15 [D8], FL-15) strains of MeV. EZ expressing GFP (EZ-GFP) was used as a representative for vaccine viruses because the Edmonston-Zagreb vaccine strain has been the most widely used measles vaccine strain globally since its licensure in 1967¹⁰¹. A MeV isolate of genotype D8, FL-15, was used as a representative wild-type virus because >50% of sequences reported to the Measles Nucleotide Surveillance (MeaNS) sequence database were genotype D8 in 2018 and this percentage has continued to increase in recent years¹⁰²⁻¹⁰⁴. We assessed viral transcription and protein production in an EBV-free B cell line (BJAB cells) and primary B cells. Additionally, we assessed the production of viral progeny and infection of specific B cell subtypes. These studies were performed to determine if there were any differences between viral replication through viral transcription and protein production in B cells infected with EZ-GFP or FL-15.

METHODS

Cell Lines

Vero/hSLAM cells were passaged or maintained in DMEM supplemented with 10% heat-inactivated fetal bovine serum (HI-FBS) 0.4 mg/mL Geneticin™ (G418) (Gibco™, 10131035), 1% penicillin-streptomycin, and 1% L-glutamine)¹⁰⁵. BJAB cells (non-EBV Burkitt-lymphoma B cell line provided by Dr. Jan Vinje's lab at Centers for Disease Control and Prevention) were cultured in RPMI (10% HI-FBS, 1% penicillin-streptomycin, and 1% L-glutamine).

Primary B Cell Isolation and Culture

Whole blood from healthy human donors was collected in heparin tubes (CDC IRB Protocol #1652). Peripheral blood mononuclear cells (PBMCs) were isolated by gradient

centrifugation with Lymphocyte Separation Medium (Corning™, 25-072-CV). Blood was centrifuged for 30 minutes at room temperature at 400 x g without break. Remaining red blood cells were lysed with Ammonium-Chloride-Potassium (ACK) lysing buffer (Gibco™, A1049201). B cells were isolated using a pan human B cell isolation kit (Miltenyi Biotec, 130-101-638) and purity (88-97%) was measured via flow cytometry (Supplemental Figure 1). B cells were counted, and 250,000 cells were seeded in 96 well round-bottom plates in RPMI medium (5% HI-FBS, 1% penicillin-streptomycin, 1% L-glutamine, 50 µM 2-mercaptoethanol). Frozen B cells (StemCell™ Technologies, 70023) were stored in liquid nitrogen at -180°C before being thawed for infection and analysis.

Virus Preparation

Cells were infected with either a low passage wild-type MeV, MVs/Florida.USA/12.15 [D8] (FL-15) or a recombinant EZ virus containing a GFP reporter gene inserted after the measles P gene (EZ-GFP)¹⁰⁶. All viral stocks were prepared by infecting Vero/hSLAM cells for 72 hours (MOI < 0.01, 32°C) in DMEM (2% HI-FBS, 1% penicillin-streptomycin, 1% L-glutamine, 0.2 mg/mL G418). Cells were harvested, lysed by freeze-thaw, supernatant was clarified by centrifugation (1500 RPM, 4°C) for 5 minutes and aliquoted. Viral titer was determined by 0.5% crystal violet staining of a plaque assay after 6 days incubation in Vero/hSLAM cells using 2% carboxymethylcellulose (CMC) overlay. Plaque forming units per mL were calculated for each virus stock. Virus stock was UV inactivated at 2000 mW/cm² on ice for 4 hours (EZ and FL-15) or 8 hours (EZ-GFP). UV inactivation was confirmed by TCID₅₀¹⁰⁷.

BJAB cells or primary B cells were seeded into a 96-well round-bottom plate at 250,000 cells per well. Cells were pelleted by centrifugation at 1500 RPM for 10 minutes at 4°C. Cells were infected at an MOI of 1 by resuspension of cell pellet in virus containing RPMI (5% HI-FBS,

1% penicillin-streptomycin, 1% L-glutamine, and 50 μ M 2-mercaptoethanol) and incubated at 37°C. Infected cells were then pelleted at timepoints via centrifugation at 1500 RPM for 10 minutes at 4°C and were washed with PBS (no Mg^{2+} , Ca^{2+}) before further analysis.

Flow Cytometry

Viral protein expression in B cells was analyzed by flow cytometry using a Fortessa flow cytometer (BD Biosciences). Vaccine was detected through GFP expression and wild-type cells were detected using MeV hemagglutinin (H) protein by antibody staining using mouse anti-H (MilliporeSigma, MAB8905, clone CV1/CV4) and anti-mouse IgG fluorescein isothiocyanate (FITC) conjugated secondary antibody (eBioscience™, 11-4010-82). Immunophenotyping of B cells was performed using phycoerythrin conjugated anti-CD27 (BD Pharmigen™, 555441), allophycocyanin conjugated anti-CD19 (BD Pharmigen™, 555415), BD Horizon Brilliant Ultraviolet (BUV) 395 conjugated anti-CD20 (BD Horizon™, 563782), Alexa 700 conjugated anti-IgD (BD Pharmigen™, 561302), BD Brilliant Violet (BV) 605 conjugated anti-CD24 (BD Horizon™, 562788), BV786 conjugated anti-CD38 (BD Horizon™, 563964), and Zombie Violet viability stain (Biolegend, 423113). Positive fluorescent values were determined as signal above the isotype control for each fluorophore. Positive values for viral fluorescence were determined as the signal above cells stained for viral protein expression at 0 hours.

Preparation of RNA

Cells were pelleted by centrifugation (1500 RPM, 4°C) for 10 minutes. Cell pellets were homogenized using Qias shredder spin columns (Qiagen™, 79656). RNA was isolated from infected cells using Qiagen™ RNeasy Mini Kits (Qiagen™, 74104) according to the manufacturer's instructions at 0-, 24-, and 48-hours after infection. Viral lysates used for infection

were also assessed for presence of residual viral RNA using a QIAamp Viral RNA kit according to manufacturer's instructions (Qiagen™, 52904). Messenger RNA (mRNA) was preferentially amplified using oligo(dT)12-18 primers and SuperScript™ III (Invitrogen, 18080044) reverse transcriptase according to manufacturer's recommendation. Samples were incubated with RNase H (500 ng/μL) (Invitrogen™, 18021014) for 30 minutes at 37°C to remove residual RNA.

Detection of viral N gene via real-time polymerase chain reaction

Real-time PCR (rRT-PCR) was performed using an Applied Biosystems 7500 Fast Real-time PCR System. MeV N gene was detected using Taqman primers and probes using SuperScript™/Taq polymerase SuperScript™ III Platinum™ One-Step qRT-PCR kit (Invitrogen™, 11732020) as previously described¹⁰⁸. Samples were incubated at 48°C for 30 minutes and 95°C for 5 minutes, followed by cycling (95°C for 15 seconds, 60°C for 1 minute) 40 times. MeV N detection was normalized to a housekeeping gene, RNaseP (RPPH1).

Production of Progeny Virus

Infected cells were pelleted by centrifugation at 1500 RPM for 10 minutes at 4°C. Supernatant was collected and cells were resuspended in media equivalent to supernatant media and placed at -80°C for 24 hours to lyse the cells. Supernatants and cellular lysates from infected B cells were titrated on Vero/hSLAM cells in DMEM (2% HI-FBS, 1% penicillin-streptomycin, 1% L-glutamine, 0.2 mg/mL G418) for 6 days at 37°C. Cells were stained with crystal violet, TCID₅₀/mL was calculated by the Reed-Muench method and converted to PFU/mL by multiplying by a factor of 0.7¹⁰⁹.

Data Analysis

Flow cytometry data were collected from the BD Fortessa using FACSDiva software and analyzed using FlowJo version 10 (FlowJo™). Statistical analysis by multiple t-tests to compare differences in means of percent positive cells from 0 to 24 hours, 0 to 48 hours, and 24 to 48 hours was performed using Graphpad Prism version 8. MeV N gene expression measured by rRT-PCR was normalized to RNaseP (RPPH1) and the $2^{-\Delta Ct}$ calculated. Statistical analysis by multiple t-test to compare MeV N gene expression at 0 to 24 hours, 0 to 48 hours and 24 to 48 hours was performed using Graphpad Prism version 8. Differences were checked for significance using multiple t-tests.

RESULTS

MeV protein production and gene transcription in BJAB cells

BJAB cells, an Epstein-Barr virus-negative human B cell lymphoma cell line, were used to as a model for MeV infection of B cells *in vitro*. Viral N gene transcription and protein production were measured in BJAB cells following infection at an MOI of 1 with EZ-GFP or FL-15 strains of MeV. GFP was used to measure infection with the vaccine strain and H protein expression was used to measure infection with wild-type MeV. The levels of viral protein production following detection of GFP, or cell surface H expression were equivalent in EZ-GFP-infected BJAB cells, demonstrating that detection of GFP or H could be used to measure viral protein expression for EZ-GFP (Supplemental Fig. 2). GFP was expressed in 44.6% of EZ-GFP-infected BJAB cells at 24 hours and 78.0% at 48 hours, while H protein was expressed in 9.6% of FL-15-infected cells at 24 hours and 50.4% at 48 hours (Fig. 1A).

Real-time RT-PCR indicated that viral lysates had low levels N gene mRNA (data not shown) which accounts for detection of N gene RNA at the 0-hour timepoint. EZ-GFP infection resulted in a 15.2-fold increase in N gene mRNA transcription from 0 to 24 hours. N gene transcription in EZ-GFP infected cells continued to increase between 24- and 72- hours post-infection with a 1.73-fold change from 24 to 48 hours, and a 2.03-fold change from 48 to 72 hours (Fig. 1B). Compared to EZ-infected cells, FL-15-infected BJAB cells had significantly lower levels of N gene transcription. Additionally, unlike transcription in EZ-GFP-infected BJAB cells which continued to increase over the time-course; transcription in FL-15-infected cells increased significantly only in the first 24 hours, (2.78-fold change from 0 to 24 hours), followed by a modest but not significant increase at 48 hours (1.36-fold change from 24 to 48 hours), and no detectable increase from 48 to 72 hours (Fig. 1C). Increased mRNA transcription and protein production

demonstrated that BJAB cells allow for viral transcription and protein production following infection with EZ-GFP or FL-15 strains of MeV. However, infection with FL-15 resulted in a lower proportion of infected cells and less transcription and protein production.

Analysis of viral protein expression in infected primary B lymphocytes in vitro

MeV infection characteristics in primary cells were assessed in B cells isolated from healthy human donors. A representative gating strategy to measure viral protein production in negatively selected CD19⁺ live B cells by flow cytometry is shown (Fig. 2A). Cells stained immediately after infection (0 hours) were used to determine the lower boundary of gating for infected cells as measured by viral GFP or H expression for vaccine and wild-type virus, respectively (Fig. 2B). Two separate experiments were performed to measure viral protein expression at 0- and 24- hours (Fig. 2C and Fig. 2D) and 0- and 48- hours post-infection (Fig. 2E and 2F) due to the limited B cell recovery from donor blood. At 24 hours post-infection, 14.4% of EZ-GFP-infected B cells expressed GFP (Fig. 2C). At 48 hours post-infection, the percentage of GFP-expressing B cells increased to 26.1% (Fig. 2E). FL-15 infected B cells demonstrated a lower percentage of infected cells at 24 hours (7.7% of B cells expressing MeV-H), and no significant increase in the proportion of infected cells at 48 hours post-infection (8.23% of B cells expressing MeV-H) (Fig. 2D and 2F). Both EZ-GFP- and FL-15-infected B cells showed increased viral protein expression; however, this increase appears limited to the first 24 hours in FL-15 infected cells with minimal differences in the mean percentage of infected cells after 24 hours.

Transcription of MeV N gene in infected primary B cells

Differences in viral gene transcription in B cells infected with EZ or FL-15 at an MOI of 1 were assessed by rRT-PCR targeting N gene mRNA in B cells from two healthy human donors.

At 24 hours post-infection, there was a comparable increase in MeV N gene transcription in B cells from both donors infected with EZ-GFP, with a 1.48-fold increase in N gene transcript normalized to RNaseP in B cells from Donor 1 (Fig. 3A) and a 1.45-fold increase in cells from Donor 2 (Fig. 3B). However, FL-15-infected B cells showed no significant increase in N gene transcription from 0 to 24 hours in B cells from either donor (Fig. 3A and 3B). While detectable transcription increased in B cells from both donors 48 hours after infection with vaccine virus, cells from Donor 1 demonstrated greater increase in transcription (4.37-fold) compared to B cells from Donor 2 (2.5-fold) (Fig. 3C and 3D). This difference between donors was not detected in FL-15-infected B cells and both donors demonstrated a similar 2.4-fold increase in N gene transcription at 48 hours post-infection (Fig. 3C and 3D). These data show that B cells infected with FL-15 and EZ-GFP strains of MeV showed an increase in viral transcripts; however, FL-15 transcription occurred later post-infection and to lower abundance compared with EZ-GFP.

Infection of naïve and memory B cell subtypes

Preferential infection of B cell subtypes by MeV was evaluated by infecting freshly thawed B cells from two donors with EZ-GFP and FL-15. Results were analyzed according to the gating strategy shown in Fig. 4A and B. MeV infection of freshly isolated and frozen B cells from donors was found to be equivalent (Supplemental Fig. 3). Memory cell subtypes were determined based on IgD and CD27 expression. CD27⁺ single positive cells were identified as switched memory cells, CD27⁺IgD⁺ double positive cells were identified as non-switched memory cells, IgD⁺ single positive cells were identified as naïve cells, and cells that expressed neither marker were identified as double-negative¹¹⁰. GFP or H expression was evaluated in the B cell subtypes as a marker of MeV infection, with the lower boundary of the gate determined based on cells stained at 0-hours post-infection (Fig. 4B). Cells of all B cell subtypes infected with EZ-GFP showed a

significant increase in the percentage of GFP-expressing cells from 0 to 24 (Fig. 4C). Between 24- and 48-hours post-infection naïve, switched memory and double negative B cell subtypes showed a significant increase in the percentage of GFP positive cells following EZ-GFP infection (Fig. 4C). There was no significant increase in the frequency of infected cells from 0 to 24 hours in cells infected with FL-15; however, a significant increase was detected from 24 to 48 hours in all four subtypes (Fig. 4D). Preferences for specific subtypes was determined by comparing frequency of infected cells between each subtype using multiple t-tests. At 24 hours, there was no detectable difference between subtypes in EZ-GFP infected cells (Fig. 4E). Non-switched memory cells had a significantly lower percentage of infected cells at 48 hours when compared to naïve, switched memory, and double negative cells (Fig. 4E). In FL-15 infected B cells, the only significant difference in the frequency of infected cells was observed between switched memory double negative subtypes, with double negative cells showing a slightly lower frequency of infection (Fig. 4F). At 48-hours post-infection there were no detectable differences in the frequency of infected subtypes following infection with FL-15 (Fig. 4F). These data show that all subtypes are infected at similar frequencies but there is slightly reduced infection in non-switched memory cells at 48-hours with EZ-GFP and for double negative cells at 24-hours post-infection with FL-15.

Production of MeV from infected B cells

Viral transcription and protein expression were detected in B cells over 48 hours post-infection; therefore, the production of infectious viral particles from B cells was evaluated. Supernatants and lysates were collected at 0-, 24- and 48-hours post-infection from B cells infected with either EZ-GFP or FL-15 and titrated on Vero/hSLAM cells. Viral titer did not increase over input (0 hours post-infection) in either EZ-GFP (Fig. 5A) or FL-15 (Fig. 5B) infected cells. The potential for residual inoculum to mask small increases in viral titer was assessed by removal of

viral inoculum after 2 hours of infection from BJAB cells infected at an MOI of 1, followed by incubation for an additional 48 hours. Like the results in B lymphocytes, no detectable increase in viral titer over input was observed in EZ-GFP (Fig. 5C) or FL-15 (Fig. 5D) infected BJAB cells following inoculum removal. MeV infection of BJAB cells at a low MOI of 0.001 was evaluated to detect increases in viral titer over an extended time-course, however, similar results in viral transcription, protein expression, and the lack of detection of viral progeny above input were observed (Supplemental Fig. 4). Despite MeV protein expression and N gene transcription in MeV-infected B cells, there was no detectable increase in infectious virus in the supernatant nor in the cell lysate following 48 hours of infection with EZ or FL-15.

DISCUSSION

Despite evidence that MeV targets and induces changes in B cell repertoires *in vivo* [8], infection of human B cells with MeV has not been fully characterized. Our study showed higher levels of viral transcription and protein expression in EZ-GFP infected BJAB and primary B cells at 24- and 48-hours-post-infection compared with FL-15 infected cells, with viral transcription and the percentage of infected cells continuing to increase in EZ-GFP infected cells, but not FL-15 infected cells between 24 and 48 hours. These results demonstrate that EZ-GFP infection of B cells leads to more viral gene transcription and viral protein translation than FL-15 within the assessed time-course. While EZ-GFP infected all B cell subtypes at a higher frequency, there were some subtype target differences between vaccine and wild-type infected cells. Similar to previously published results⁹⁹, MeV comparably targeted naïve and memory cells; however, when the memory B cell population was further subtyped, some differences were noted. EZ-GFP appeared to target non-switched memory cells at 48-hours post-infection less than other B cell subtypes, whereas FL-15 appeared to target non-switched memory cells at a slightly higher, though not

significant ($p = 0.07$) frequency than other cell types. Differences similarly have been noted between T cell memory subtypes following *in vitro* infection with wild-type MeV⁹⁹. Further evaluation could focus on the potential impact of targeting non-switched memory populations during wild-type MeV infection.

While measurement of viral transcription and protein production indicate infection of target B cells, no detectable changes in viral titer above input were observed in the supernatant or infected cell lysate. There were no measles specific antibodies detected in the supernatant from infected cells, demonstrating that the lack of viral progeny was not due to the presence of neutralizing antibodies (data not shown). This suggests that measles viral components are spreading via non-canonical methods in B cells. Spread to neighboring cells has been demonstrated for MeV and pneumoviruses through the generation of synapse structures and actin mediated mechanisms. MeV synapse structures have been shown to occur between dendritic cells and T cells through the localization of cellular interaction proteins such as CD150, ICAM-1, and LFA-1 to allow transfer of viral genetic material through a “virological synapse”¹¹¹. Non-canonical spread has been shown for non-immune cells as well. Spread of viral ribonucleocapsid in MeV-infected human airway epithelial cells occurs without syncytia through actin mediated polarization^{112,113}. Non-canonical mechanisms of MeV spread are likely to play a role in infection of B cells.

Cell lines can be an important model of infection outcomes *in vitro*; this study established that BJAB cells may serve as a model for MeV infection of human B cells. Infected BJAB cells demonstrated similar levels and patterns of viral replication as observed in primary cells. BJAB cells had higher frequencies of infected cells for both EZ-GFP and FL-15 when compared to primary cells. The difference in the time course of infection between EZ-GFP and FL-15 in primary B cells was also reflected in infected BJAB cells. Additionally, previous studies have used

an infection enhancing molecule known as PHCSK4 when evaluating MeV infection of B cells¹¹⁴. Experiments were performed using PHCSK4 to evaluate enhancement of MeV infection of primary B cells and BJAB cells in this study; however little enhancement of infection was observed, and a lower percentage of wild-type infected cells were detected compared with vaccine infected cells even in the presence of PHCSK4 (data not shown). Lastly, as observed in primary cells, infected BJAB cells did not generate an increase in infectious particles above input. Therefore, data collected from BJAB cell infections can be used to inform future experiments for infection of primary B cells *in vitro*.

Further studies are needed to address the change in the B cell population following infection *in vivo*¹⁰⁰. Based on the changes in antibody repertoire seen in humans, examination of germinal center B cells, antibody secreting cells, or a more detailed analysis of class-switched B cells (IgA, IgG) is required to fully elucidate the mechanism of modulation. A limitation of our study is the inability to assess other sub-types such as those listed above due to their limited availability or unavailability in peripheral blood. Other cells such as T_{FH} cells or stromal cells are also not present *in vitro*. Studies that investigate B cells *in vivo* may reveal more information on the interaction of infected B cells with other immune cells and immune consequences of MeV infection.

The infection of B cells *in vitro* with a representative wild-type (FL-15) and vaccine (EZ-GFP) strain of MeV characterized here supports the widespread impact of MeV infection on B cell subtypes and the antibody repertoire. Comparison of infection with vaccine and wild-type infected cells highlighted interesting differences that could contribute to the immune consequences demonstrated following measles. Higher levels of protein were detected in EZ-GFP infected cells when compared to FL-15 infected cells, regardless of subtype. Higher levels of N gene

transcription were detected in EZ-GFP infected cells. Non-switched memory cells had lower levels of viral protein expression than other subtypes during EZ-GFP infection. There were slightly higher levels of viral protein detected in non-switched memory cells than in other subtypes during FL-15 infection. This chapter elucidates differences between vaccine (EZ-GFP) and wild-type (FL-15) infection.

Figure 1. MeV protein expression and transcription in infected BJAB cells

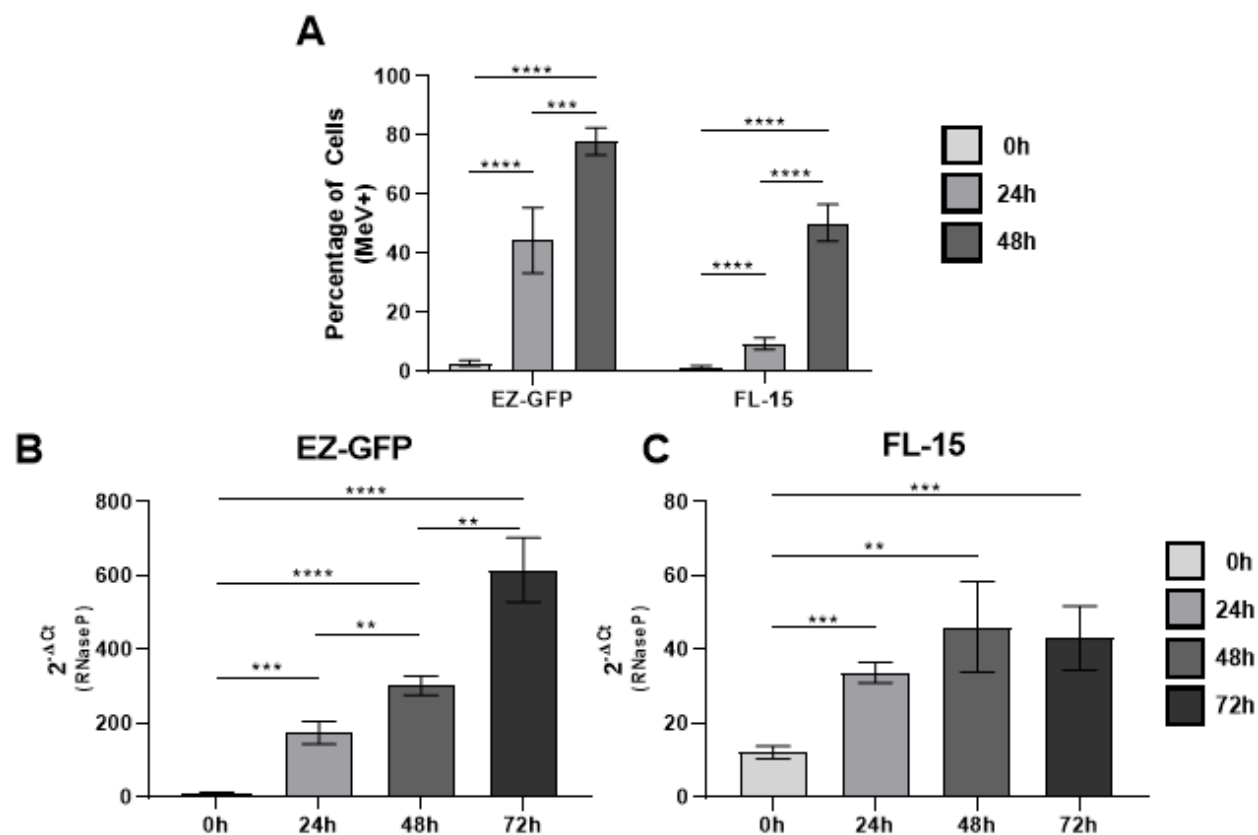


Figure 1. MeV protein expression and transcription in infected BJAB cells. Measles hemagglutinin (H) expression in FL-15 and GFP expression in EZ-GFP infected BJAB cells were analyzed by flow cytometry (A) (n=5). Transcription of MeV N gene normalized to RNaseP was measured by rRT-PCR in cells infected with EZ-GFP (B) and FL-15 (C) (n = 3). Error bars represent standard deviation (** = $p < 0.01$, *** = $p < 0.005$, **** = $p < 0.001$)

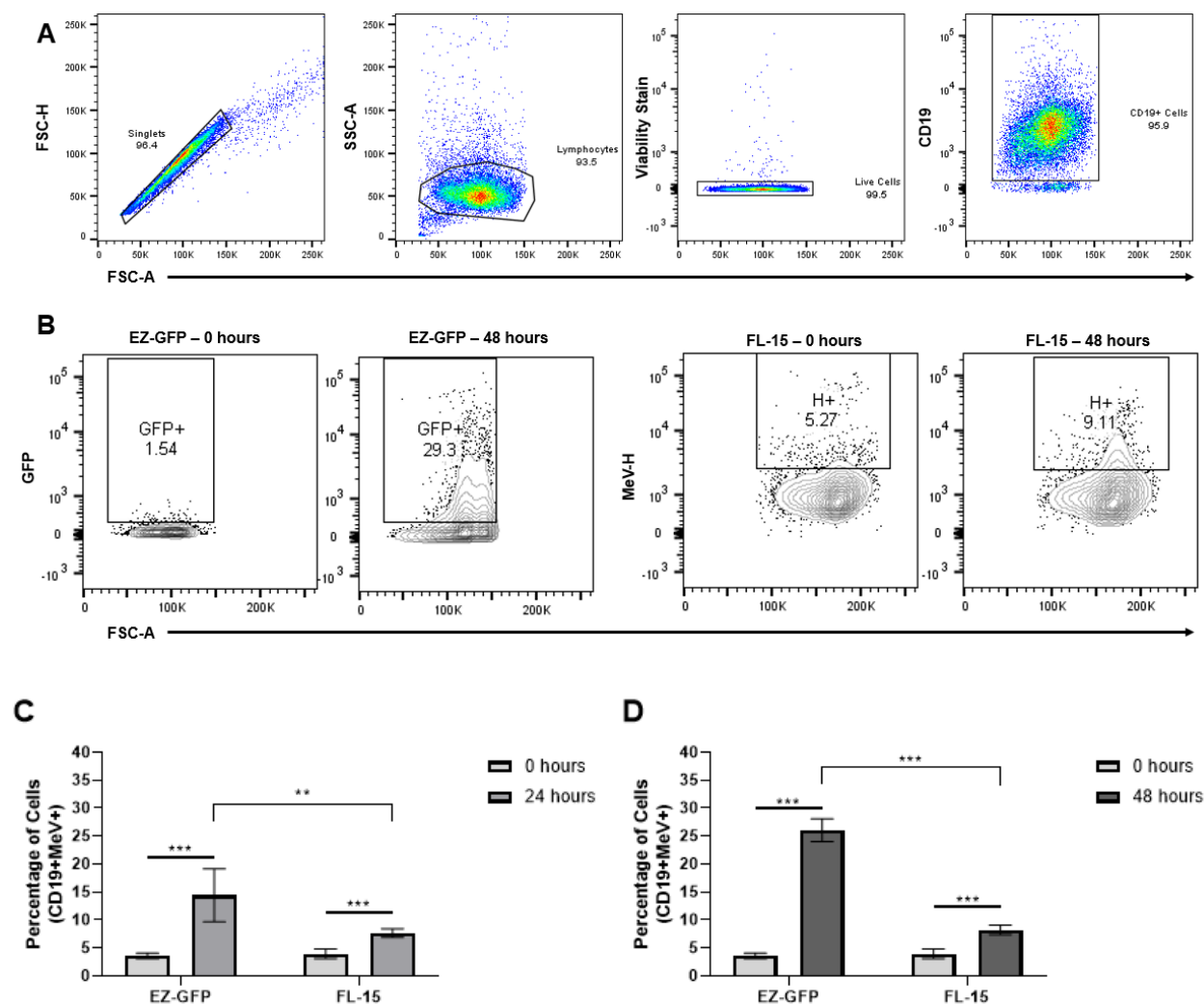
Figure 2. MeV protein expression in infected B lymphocytes

Figure 2. MeV protein expression in infected B lymphocytes. B cells from two healthy human donors were infected with EZ-GFP or FL-15. Example gating strategy used for analysis, cells were gated on singlets, lymphocytes, viability, and CD19 (A). The number of infected cells was determined relative to cells stained at 0 hours-post infection(B). For MeV vaccine infected B cells, GFP expression was measured at 0 hours and 24 hours (C) and 0 hours and 48 hours (D) in two separate infections. Surface expression of MeV H protein in wild-type MeV infected cells was measured with a mixture of CV1/CV4 antibodies directed against the H protein. Expression was measured at 0 hours and 24 hours (C) and 0 hours and 48 hours (D) in two separate infections.

Results from both donors are combined in each figure C-D. Statistical analyses were also performed to assess differences between EZ-GFP and FL-15 at 24 (C) and 48 hours (D). Error bar represents standard deviation ($n = 6$, *** = $p < 0.005$, ** = $p < 0.01$).

Figure 3. MeV N gene transcription following *in vitro* infection of human B lymphocytes

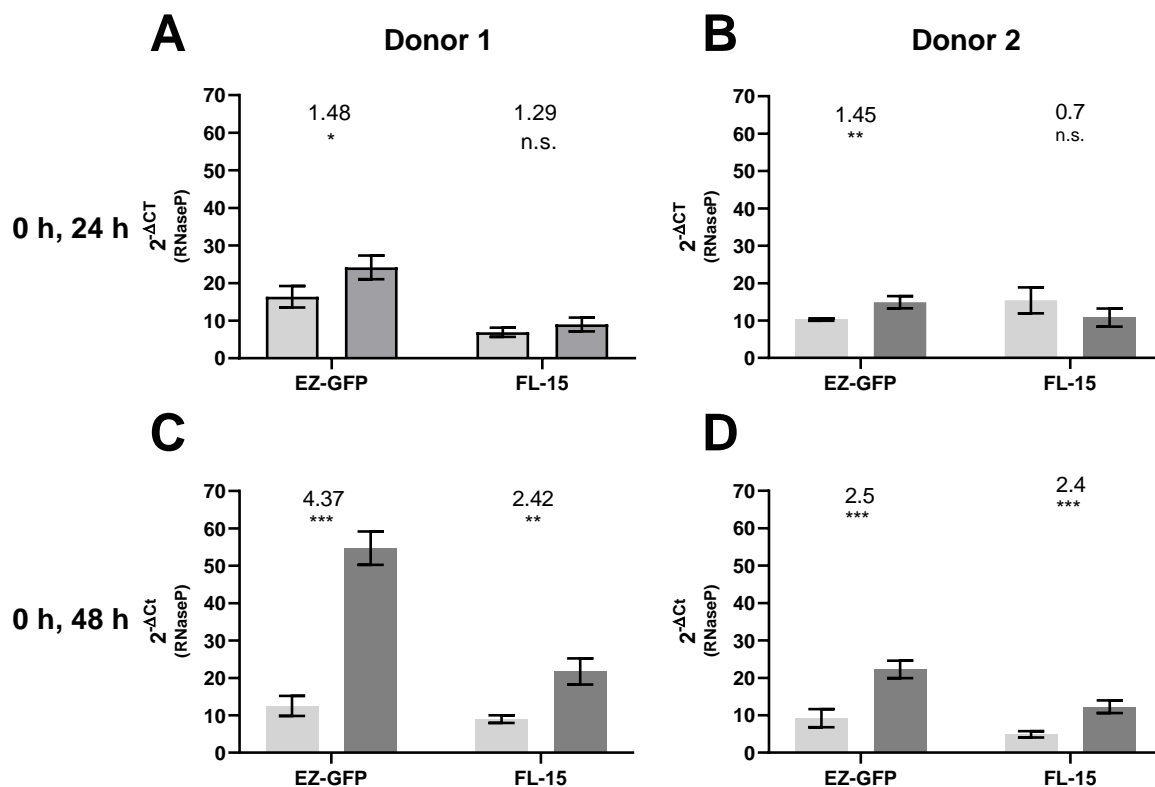


Figure 3. MeV N gene transcription following *in vitro* infection of human B lymphocytes. N gene expression was measured via rRT-PCR using RNA from B cells infected with EZ-GFP or FL-15. N gene transcription at 0 hours and 24 hours (A, B) and at 0 hours and 48 hours (C, D) was normalized to RNaseP in two separate experiments. Fold change in N gene transcription is shown above columns. Error bars represent standard deviation ($n = 6$, significance was determined by student t-test * = $p < 0.05$, ** = $p < 0.01$, *** = $p < 0.005$)

Figure 4. MeV protein expression in B cell subtypes following infection.

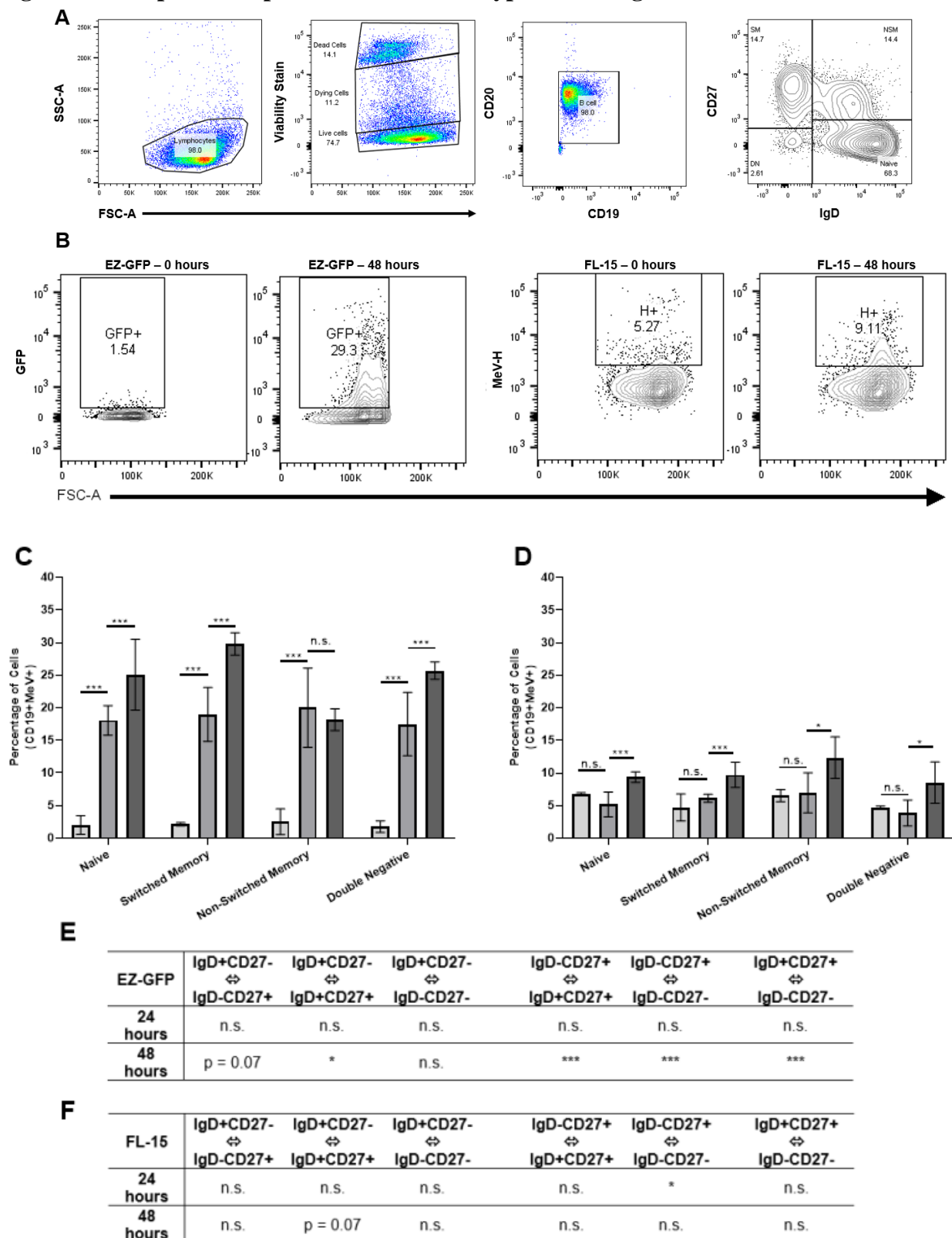


Figure 4. MeV protein expression in B cell subtypes following infection. Freshly thawed B cells from human donors were infected *in vitro*. Cells were gated on live CD19⁺CD20⁺ B cells and subdivided into memory and naive subtypes by CD27 and IgD expression (A) IgD⁻CD27⁺ (Switched Memory), IgD⁺CD27⁺ (Non-switched Memory), IgD⁺CD27⁻ (Naïve), IgD⁻CD27⁻ (Double Negative). (B) MeV H protein or recombinant GFP expression corresponding to infected cells was evaluated in each B cell subtype with the gate set based infected cells stained at 0 hours. Expression of GFP in EZ-GFP infected B cell subtypes (C) and hemagglutinin (H) in FL-15 infected B cell subtypes (D) was evaluated. Statistical analyses were performed to assess differences in infections between subtypes during infection with EZ-GFP (E) or FL-15 (F). Error bars represent standard deviation and significance was determined by t-test (n = 3 replicates per donor. n.s. = non-significant, ***** = p < 0.0001, *** = p < 0.005, ** = p < 0.01, * = p < 0.05, ó = conditions compared in the statistical analysis)

Figure 5. Measurement of progeny MeV in B lymphocytes at 48 hours infection.

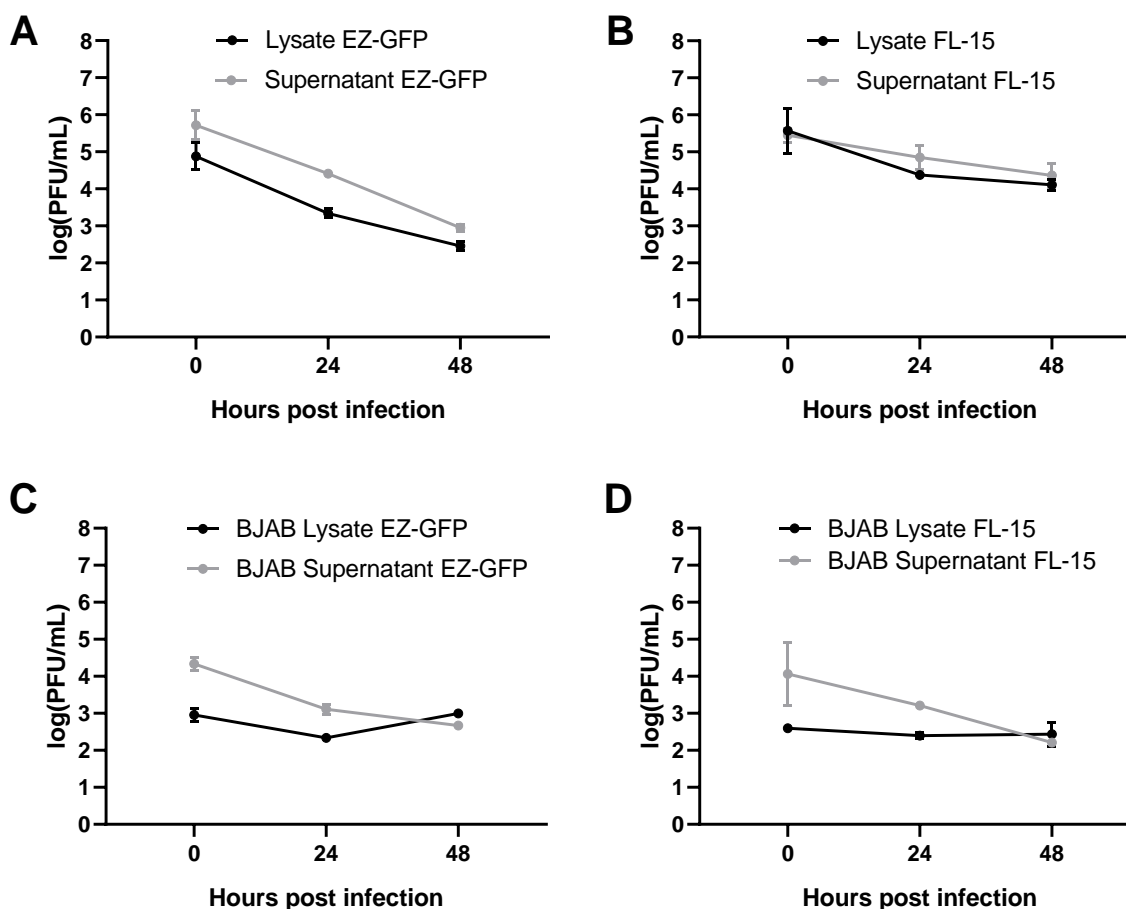
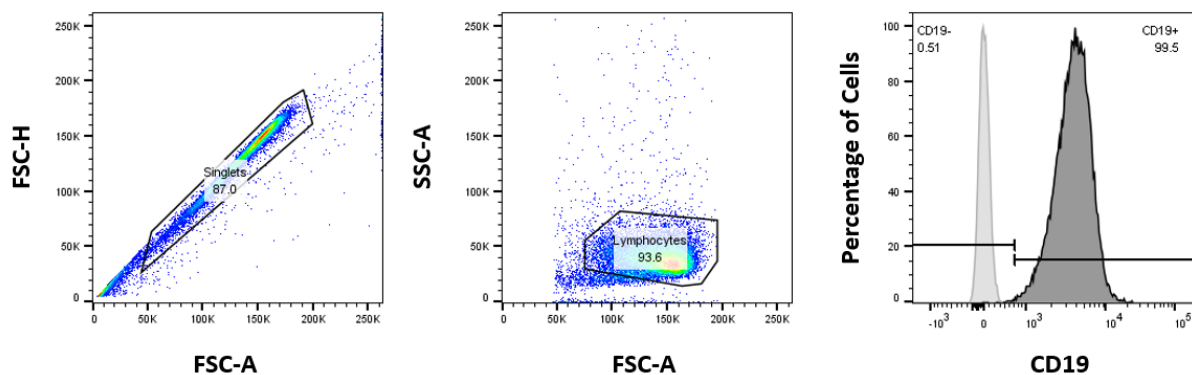


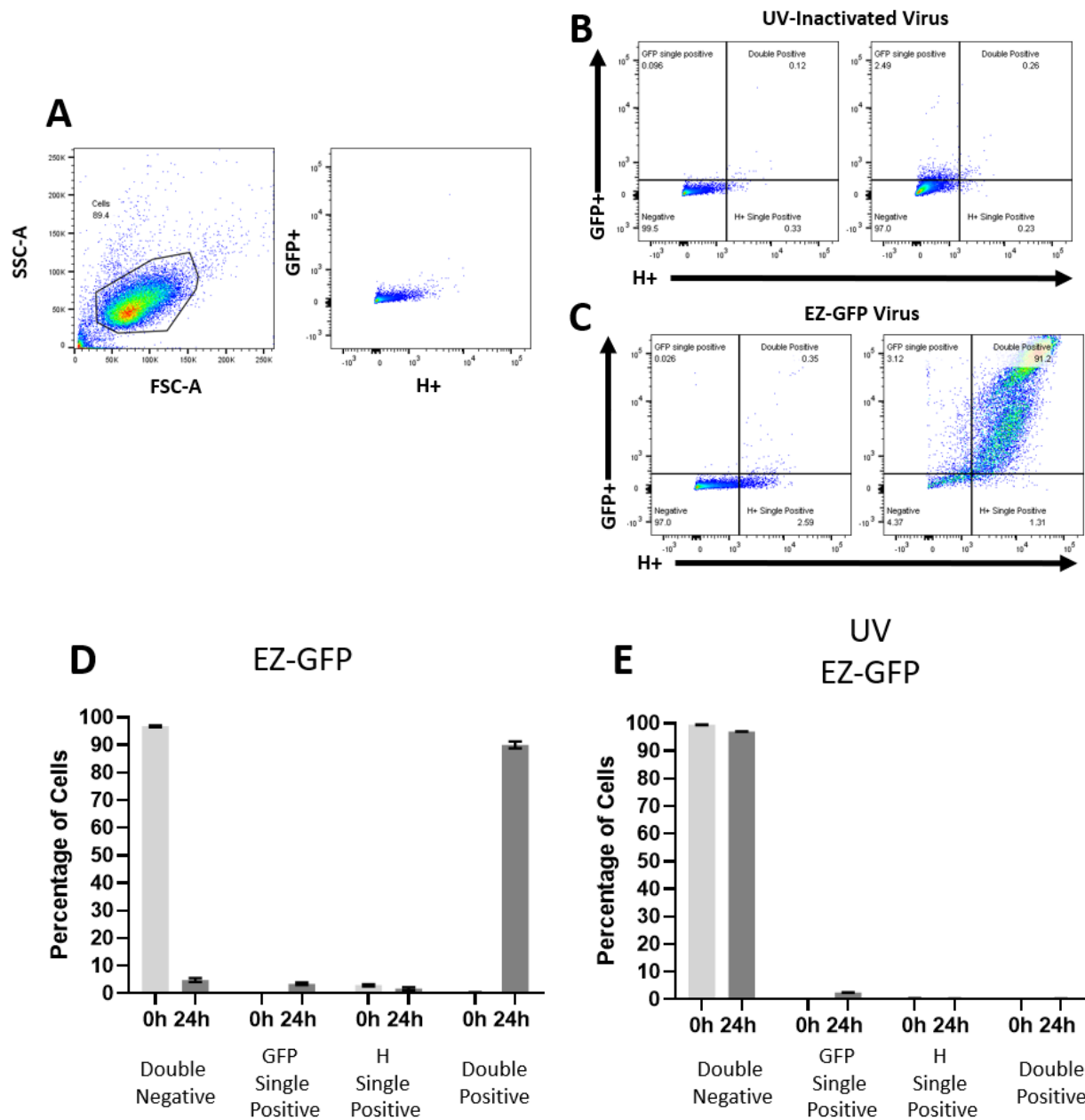
Figure 5. Measurement of progeny MeV in B lymphocytes at 48 hours infection. Viral titers in supernatant or lysate from B cells (panels A, B) or BJAB cells (panels C, D) infected with EZ-GFP (panels A, C) or FL-15 (panels B, D) was measured by endpoint dilution in using Vero/hSLAM cells. Virus inoculum was not removed from B cells (A, B) but viral inoculum was removed after 2 hours of incubation from BJAB cells (C, D). Viral titer was plotted as the log PFU/mL. Error bars represent standard deviation. Experiments were performed in triplicate.

Supplemental Figure 1. Representative B Cell Purity.

Supplemental Figure 1. Representative B Cell Purity. B cells were isolated at a purity of >88%.

The gating strategy used gating on singlets, lymphocytes, viability, and CD19. Cells were gated on positive cells to specifically assess B cells in further studies.

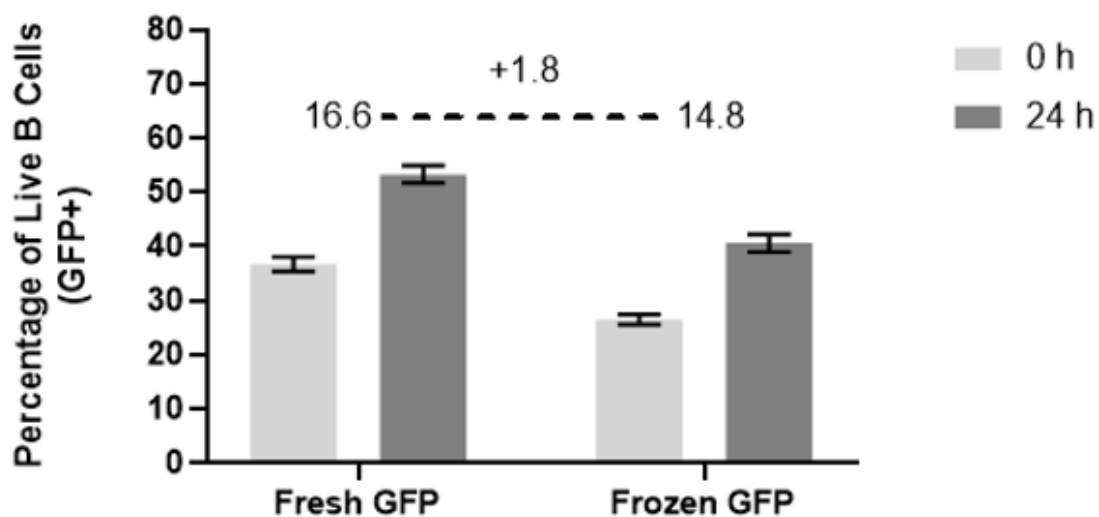
Supplemental Figure 2. Comparison of GFP expression to H expression on measles virus infected BJAB cells



Supplemental Figure 2. Comparison of GFP expression to H expression on measles virus infected BJABs. BJABs were infected at an MOI of 1 and stained for H expression using a phycoerythrin-cyanine 5 labeled secondary antibody. Gates were determined using cells that were

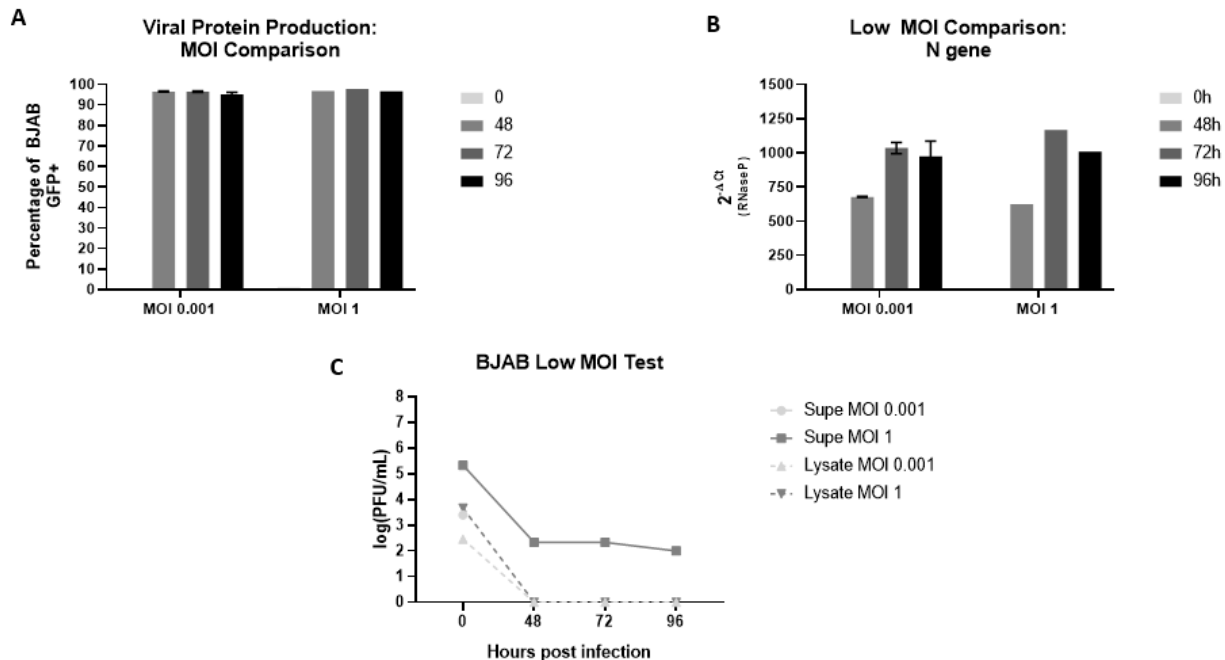
exposed to UV-inactivated GFP virus (A, B). Single and double positive cells were assessed (C) and quantified (D). Negative controls show no increase in expression of either viral protein (E).

Supplemental Figure 3. Comparing increase in frequency of infected cells in frozen and fresh B cells.



Supplemental Figure 3. Comparing increase in frequency of infected cells in frozen and fresh B cells. Fresh and frozen B cells were infected side-by-side. There was a statistically insignificant difference of 1.8%.

Supplemental Figure 4. Assessing effect on input virus on experimental outcome.



Supplemental Figure 4. Assessing effect on input virus on experimental outcome. BJABs were infected at an MOI of 1 and 0.001 to assess the impact of MOI on experimental outcome. Both MOIs show consistent levels of viral infection at 48, 72, 96 hours. This is shown via GFP expression in infected cells (A) and N gene transcription in infected cells (B). Additionally, both MOIs show no production of infectious progeny virus after 96 hours (C).

Chapter 3: Assessing Cellular Characteristics of B Cells Infected with Vaccine and Wild-type Strains of MeV

This chapter is reproduced with edits from:

Characterizing infection of B cells with wild-type and vaccine strains of measles virus

Logan Melot^{1,2}, Bettina Bankamp¹, Paul A. Rota^{1,2}, Melissa M. Coughlin¹

¹Viral Vaccine Preventable Diseases Branch, Division of Viral Diseases, National Center for Immunization and Respiratory Diseases, Atlanta, GA, USA, Centers for Disease Control and Prevention. ²Emory University, Atlanta, GA, USA

ABSTRACT

Prolonged immune suppression is a sequela associated with wild-type measles virus (MeV) infection that does not manifest in those vaccinated with the live-attenuated MeV. The immune suppression is characterized by the inability to respond to secondary infection, and specifically, in B cells, loss of antibody repertoire and memory B cell diversity. This study aims to assess characteristics of B cells infected with a vaccine strain (EZ) or wild-type (FL-15) strains of MeV. Understanding the impact of infection on the cell will play a key role in finding the mechanism of immune suppression. Here we show differences in cell viability between FL-15 and EZ infected B cells. FL-15 infected cells demonstrated lower viability as well as higher levels of MLKL phosphorylation as well as caspase-3, -8, and -9 cleavage. A difference in cytokine profiles between FL-15 and EZ infected cultures was also observed: Expression of IL-4 and IL-6 was increased in both FL-15 and EZ infected cultures. Higher levels of IL-8 were detectable in FL-15 infected cultures than in EZ infected cultures, while higher levels of TNF- α and IL-10 were measured in EZ infected cultures. Localization of nucleoprotein on the cell surface and at cellular interaction sites was observed in both FL-15 and EZ infected cultures. Localization of hemagglutinin and MeV receptor SLAM were observed in both FL-15 and EZ infected cultures, but protein reorganization occurred earlier in the course of infection in EZ infected cultures. These data help us understand the differences in cellular outcome following infection with vaccine or wild-type strains of MeV.

INTRODUCTION

MeV has been shown to impact cytokine signaling and effector function in infected primary dendritic cells and T cells¹¹⁵. MeV infected dendritic cells have a reduced capacity to provide costimulatory signals to CD4 T cells during infection and limit T cell proliferation^{115,69}. One long notable outcome of MeV infection is a suppression of the tuberculin skin test in those previously positive for the antigen¹¹⁶. This suggests that there is a breakdown in signaling between innate and adaptive immunity. As previously mentioned, evidence of immune cell dysfunction is not isolated to infected dendritic cells and T cells, B cells have been shown to have altered effector functions through changes in the diversity of peripheral antibodies and the B cell memory repertoire. These changes last longer than signals for detectable virus, suggesting that there is a prolonged alteration of signaling and immune function in addition to high levels of lymphopenia. However, these differences are not observed in vaccinated individuals, suggesting that the outcome of infection of immune cells with wild-type virus differs than what occurs when live attenuated vaccine virus targets cells. Because cytokines play a significant role in proliferation, cell communication, and immune cell function, furthering our understanding of cytokines produced by B cells during infection could elucidate some of the mechanisms behind changes observed in immune cell effector function *in vivo*.

Due to high levels of lymphopenia detected in MeV infected individuals, understanding the induction of cell death pathways following infection is key in understanding how MeV impacts cell proliferation and maintenance. Cell death pathways play an important role in the pathogenesis of viral infection. Cell death pathways are mostly mediated through signaling cascades that involve cysteine-aspartic proteases (caspases). Two of the major categories of caspases are initiator caspases and executioner caspases. This section will focus on the analysis of two initiator caspases

(caspase-8, caspase-9) and one executioner caspase (caspase-3) during infection of primary B cells with MeV. Caspases exist in a pro-protein form and are cleaved upon response to stimuli that leads to their active form. For example, pro-caspase-8 is cleaved following the binding of CD95 with its ligand¹¹⁷. Pro-caspase-9 is cleaved following damage to mitochondrial membranes and the release of cytochrome c into the cytoplasm¹¹⁸. Following cleavage of pro-caspase-8 or pro-caspase-9, pro-caspase-3 is cleaved and activated¹¹⁸. Activation of caspase-3 induces programmed cleavage of proteins that are key in regulating the survival of cells, leading to cell death, or apoptosis¹¹⁹. A second form of cell death, necroptosis, is mediated by receptor-interacting protein kinase (RIPK) 1, RIPK3, and mixed lineage kinase domain-like (MLKL) proteins. This pathway is generally pursued by the cell when apoptosis is blocked. Necroptosis leads to leakage of cellular components into the surrounding environment, causing it to be a more inflammatory form of cell death¹²⁰. MeV induces cell death in bystander, non-infected T cells, suggesting that infected cells have specific cytokine and signaling profiles that impact the viability of surrounding cells⁷⁷, which could be linked to MeV nucleoprotein inducing apoptosis and the exchange of nucleoprotein from infected to uninfected cells¹²¹. Understanding differences in the induction of caspases following infection with wild-type or vaccine can provide important information in understanding how wild-type MeV induces high levels of lymphopenia not observed in vaccinated individuals.

In chapter 2, our results showed that despite evidence of viral protein production and viral transcription, no progeny virus could be detected in culture supernatants or cell lysates, suggesting that viral components are spreading from cell-to-cell through non-canonical methods. There are several methods that permit viruses to spread from cell to cell. Viruses can spread by assembly and budding from infected cells and spreading through diffusion to uninfected cells as cell-free virus particles. Virus has been shown to spread from infected to uninfected cells through cell-cell

interactions. Several mechanisms of cell-cell infection or spread of viral components can be identified in the literature: formation of a virological synapse through binding of viral protein on the surface an infected cell to the receptor of an uninfected cell¹¹¹, generation of tunneling nanotubes (TNT) between cells which permits the transfer of viral components¹²², formation of pores and aggregation of viral components at these pores¹²³, capture of viral particles on the surface of another cell that interacts with a susceptible cell (trans-infection)¹²⁴, and the formation of filopodia that promotes rafting of viral components between cells¹²⁵. Cell-cell contact has been shown to enhance infection by allowing for spread of viral components in non-optimal conditions, such as in the presence of neutralizing antibodies^{126,127,128} and anti-viral drugs such as Oseltamivir¹²². Many of the previously mentioned mechanisms can be inhibited through blocking actin polymerization. For example, knocking out ARP-2, a protein that plays a key role in actin polymerization, caused a significant decrease in detectable respiratory syncytial virus (RSV) genomes and progeny¹²⁹. Part of this thesis aims to assess localization of viral and cellular proteins at cell-cell interfaces to determine if there is evidence of cell-cell spread of MeV between infected B cells and by which mechanism it occurs.

MeV has been shown to impact the function of immune cells, contribute to cell death, and spread between cells using non-canonical methods. In this chapter, we aim to assess the cytokine profiles, viability, and levels of proteins associated with the induction of cell death in infected cultures. Understanding differences in the induction of cell death and cytokines caused by infection with vaccine or wild-type could help further understanding changes in B cell function during infection in humans and the role B cells play in contributing to MeV induced immunosuppression. The lack of detectable virus progeny following MeV infection of B cells suggests that spread of viral components is occurring through non-canonical pathways. In this chapter, we aim to further

understand the localization of viral and cellular proteins in B cells infected *in vitro* with vaccine or wild-type strains of MeV. Assessing cytokine production, cell death, and spread of viral components in wild-type and vaccine infected cultures could elucidate differences between vaccine and wild-type infected cultures that could inform potential mechanisms that contribute to the generation of MeV associated immune suppression.

METHODS

Cell Lines

Vero/hSLAM cells were passaged or maintained in DMEM supplemented with 10% heat-inactivated fetal bovine serum (HI-FBS) 0.4 mg/mL Geneticin™ (G418) (Gibco™, 10131035), 1% penicillin-streptomycin (Gibco™, 15140122) and 1% L-glutamine (Gibco™, 25030081) ¹⁰⁵. BJAB cells (non-EBV Burkitt-lymphoma B cell line provided by Dr. Jan Vinje at Centers for Disease Control and Prevention) were cultured in RPMI (10% HI-FBS, 1% penicillin-streptomycin, and 1% L-glutamine).

Primary B Cell Isolation and Culture

Whole blood from healthy human donors was collected in heparin tubes by Emory Donor Services (CDC IRB Protocol #1652). Peripheral blood mononuclear cells (PBMCs) were isolated by gradient centrifugation with Lymphocyte Separation Medium (Corning™, 25-072-CV). Blood was centrifuged for 30 minutes at room temperature at 400 x g without break. Remaining red blood cells were lysed with Ammonium-Chloride-Potassium (ACK) lysing buffer (Gibco™, A1049201). B cells were isolated using a pan human B cell isolation kit (Miltenyi Biotec, 130-101-638) and purity (88-97%) was measured via flow cytometry (Supplemental Figure 1). B cells were counted, and 250,000 cells were seeded in 96 well round-bottom plates in RPMI medium (5% HI-FBS, 1%

penicillin-streptomycin, 1% L-glutamine, 50 μ M 2-mercaptoethanol). Alternatively, commercially available frozen B cells (StemCell™ Technologies, 70023) were stored in liquid nitrogen at -180°C before being thawed for infection and analysis.

Virus Preparation

Cells were infected with either a low passage wild-type MeV MVs/Florida.USA/12.15 [D8] (FL-15) or a recombinant Edmonston-Zagreb (genotype A) virus containing a GFP reporter gene inserted after the measles P gene (EZ-GFP)¹⁰⁶. All viral stocks were prepared by infecting Vero/hSLAM cells for 72-96 hours (MOI < 0.01, 32°C) in DMEM (2% HI-FBS, 1% penicillin-streptomycin, 1% L-glutamine, 0.2 mg/mL G418). Cells were harvested by scraping into one milliliter of media per flask, lysed by freeze-thaw, supernatant was clarified by centrifugation (1500 RPM, 4°C) for 5 minutes and aliquoted. Viral titer was determined by the addition of 110 μ L of infectious inoculum to Vero/hSLAM cells in a 24-well plate for 2 hours. One milliliter of 2% carboxymethylcellulose (CMC) overlay (Leibowitz media (Gibco™, 21083027), 5% HI-FBS, 1% penicillin-streptomycin, 1% L-glutamine, 0.5% amphotericin B (Gibco™, 15290018), 0.5% gentamicin (Gibco™, 15750060). was added and cells were incubated at 37°C for five days. CMC media was removed and plates were washed once with PBS. Wells were stained with 0.5% crystal violet by weight (5% ethanol, 12% formaldehyde, 70% water) for 10-15 minutes at room temperature in a biosafety cabinet. Cells were washed three times with PBS and air dried. Plaques were counted at five-ten-fold dilutions (10^{-4} - 10^{-8}). Plaque forming units per mL were calculated for each virus stock. UV-inactivated viruses were used as controls for infection. Virus stock was UV inactivated at 2000 mW/cm² (UVG-54 handheld UV lamp, confirmed with a shortwave UV meter from Analytik Jena) on ice for 4 hours (EZ and FL-15) or 8 hours (EZ-GFP). UV inactivation was confirmed by TCID₅₀¹⁰⁷.

B cell Infection

250,000 BJAB cells or primary B cells were seeded into a 96-well round-bottom plate. Cells were pelleted same day by centrifugation at 1500 RPM for 10 minutes at 4°C. Cells were infected at an MOI of 1 by resuspension of cell pellet in RPMI (5% HI-FBS, 1% penicillin-streptomycin, 1% L-glutamine, and 50 µM 2-mercaptoethanol) and incubated at 37°C. Infected cells were pelleted at timepoints via centrifugation at 1500 RPM for 10 minutes at 4°C and were washed with PBS (no Mg²⁺, Ca²⁺) before further analysis.

Flow Cytometry

Infected cells were pelleted at 1500 RPM at 4°C for 5 minutes and washed once with phosphate buffered saline (PBS). Biolegend Zombie Violet viability stain (Biolegend, 423113) was used to determine cellular viability. Cells were resuspended in PBS containing Zombie Violet (1:250) and incubated in the dark at room temperature for 15 minutes. Cells were then pelleted at 1500 RPM at 4°C for 5 minutes and washed twice in HI-FBS containing PBS (1%) to inactivate the stain. Positive fluorescent values were determined using uninfected 0-hour timepoints. Live cells were gated based on manufacturer's instructions for staining.

Cytokine analysis

Cytokines were measured using a Luminex FlexMap3D instrument (BioRad Laboratories). Infected cultures were centrifuged at 1500 RPM for 10 minutes at 4°C. Supernatants from infected B cells were analyzed using a 10-plex human cytokine panel to assess GM-CSF, IL-1β, IL-2, IL-4, IL-5, IL-6, IL-8, IL-10, IFNγ, and TNF-α protein production according to manufacturer's

recommendations (ThermoFisher™, LHC0001M). Protein concentration was determined using the provided standard.

Immunofluorescence Assay

B cells were seeded in 8-well glass chamber slides (ThermoFisher™, 154534) coated with poly-d-lysine (Gibco™, A3890401) in RPMI medium (5% HI-FBS, 1% penicillin-streptomycin, 1% L-glutamine, 50 µM 2-mercaptoethanol) the day prior to infection. Cells were then infected at an MOI of 1 with FL-15 or EZ-GFP for 24 and 48 hours. Cells were fixed at each timepoint using 4% paraformaldehyde (BD™, 554655) in PBS (10 minutes, room temperature) and permeabilized using 0.1% Triton X-100 in PBS (5 minutes, room temperature). Non-specific binding was blocked using a mixture of 5% normal goat serum (Gibco™, PCN5000) and 2.5% bovine serum albumin (BSA, ThermoScientific™, 37525) in PBS for one hour at room temperature. Cells were washed with PBS between each step and staining steps. Cells were then stained overnight at 4°C using one of two antibody cocktails: A) monoclonal mouse anti-CD150 (1:100) (IPO-3) (abcam™, ab2604), polyclonal rabbit anti-MeV nucleoprotein (1:100) (generated from whole virus inoculated rabbits), and monoclonal rat anti-CD19 (1:200) (6OMP31) (eBioscience™, 14-0194-82) or B) monoclonal mouse anti-MeV-H (1:100) (CV1/CV4) (MilliporeSigma, MAB8905), monoclonal rabbit anti-SLAMF1 (1:100) (MilliporeSigma, SAB2109151), and monoclonal rat anti-CD19 (1:200) (6OMP31) (eBioscience™, 14-0194-82). Slides were then washed three times with PBS. Cells were stained for 1 hour at room temperature with the following secondary antibodies: a) goat anti-mouse conjugated with Alexa Fluor™ 488 (1:200) (Invitrogen™, A28175), goat anti-rat conjugated with Alexa Fluor™ 555 (1:200) (Invitrogen™, A-21434) and goat anti-rabbit conjugated with Alexa Fluor™ 647 (1:200) (Invitrogen™, A-21245). Slides were then washed three times with PBS. Slides were stained for 5 minutes at room temperature with 1X DAPI nuclear

stain (Invitrogen™, D21490). Slides were then washed three times with PBS and once with cell-culture grade water. Slides were mounted using fluorescence mounting medium (Agilent, S302380-2) and 1.5 mm cover slips and dried overnight. Antibody dilutions were determined using serial dilutions on infected BJAB cells to optimize the signal to background ratio. Images were taken using a Zeiss LSM 800 confocal microscope.

Western Blot Assays

Cells were seeded at 400,000 cells per well in a 96-well plate and infected at an MOI of 1 as previously described. At time of analysis, cells were pelleted by centrifugation at 1500 RPM for 10 minutes at 4°C. Cells were washed with PBS and re-pelleted via centrifugation. Cells were lysed by resuspension in RIPA lysis buffer (ThermoFisher™, 89900) containing 1X Halt™ Phosphatase Inhibitor Cocktail (ThermoFisher™, 78420) and 1X Halt™ Protease Inhibitor (ThermoFisher™, 87786) and agitation for 10 minutes at room temperature. Protein concentrations were determined using a BCA protein standard according to manufacturer's instructions (ThermoFisher™, J63283-QA). Samples were then prepared by diluting in NuPAGE™ LDS Sample Buffer (Invitrogen™, NP0007) containing 1X NuPAGE™ Sample Reducing Agent (Invitrogen™, NP0004) and heating to 95°C for 10 minutes. Samples were loaded into a NuPAGE™ 4-12%, Bis-Tris, 15 well, 1.5 mm mini protein gel (Invitrogen™, NP0336) at 20 ng/well. Samples were run side-by-side with a 10-250 kilodalton (kD) Precision Plus Protein™ standard at 50V for 5 minutes followed by 130V for 70 minutes in 1X NuPage™ MOPS SDS Running Buffer (Invitrogen™, NP0001). Protein was blotted using an iBlot™ 2 (Invitrogen™, IB21001) dry blot system. Protein was blotted onto a nitrocellulose membrane using iBlot™ 2 nitrocellulose transfer stacks (Invitrogen™, IB23002) at 20V for 1 minute, then 23V for 4 minutes, and finally 25V for 3 minutes according to manufacturer guidance. Blots were rinsed with Tris-

buffered saline (TBS) containing 0.1% Tween-20 (Sigma-Aldrich™, P1379) (TBST). Blots were blocked with 5% powdered milk in TBST for one hour at room temperature. Blots were washed with TBST three times for 5 minutes. TBS containing 1% bovine serum albumin (BSA) was used to dilute rabbit anti-human monoclonal antibodies directed against GAPDH (1:1000) (Cell Signaling Technology™ [CST], clone D16H11, 5174), caspase-3 (1:1000) (CST, clone D3R6Y, 14220), caspase-8 (1:1000) (CST, clone D34G2, 4790), caspase-9 (1:1000) (CST, clone D8I9E, 20750), and MLKL (1:500) (CST, clone D2I6N, 14993). Mouse anti-MeV-nucleoprotein (1:1000) (SigmaAldrich, clone 83KKII, MAB8906) was included to detect MeV protein. Antibody dilutions were optimized by serial dilution on BJAB cell protein lysates treated with staurosporine (1 μ M, CST™, 9953) plus recombinant human TNF α (20 ng/mL, PeproTech™, 300-01A) to induce caspase-3 and caspase-9 cleavage and anti-CD95 (APO-1, ThermoFisher™, 16-0958-81) plus human TNF α (20 ng/mL, PeproTech™, 300-01A) was used to induce caspase-3 and caspase-8 cleavage as a positive control. Concentrations of apoptosis induction molecules were based on CST manufacturer guidelines for positive controls. Blots were incubated with this mixture overnight at 4°C. Blots were washed three times with TBST. Blots were incubated in 5% milk powder in TBST containing goat-anti-mouse (Invitrogen™, 31430) and goat-anti-rabbit (Invitrogen™, 31460) antibodies tagged with horseradish peroxidase (HRP) at room temperature for an hour. Blots were washed three times with TBST. Blots were incubated for 5 minutes with SignalFire™ Plus ECL Reagent at room temperature. Blots were washed one time with TBST. Blots were then imaged on a ChemiDoc (Bio-Rad™) imaging system.

Data Analysis

Cells determined as viable or dead/dying (Zombie Violet positive) were graphed and compared using multiple t-tests at 0-, 24-, and 48-hours post infection. Cytokine MFI was converted to pg/mL

concentration using the included standard according to manufacturer's recommendations. Increases in cytokine concentration were determined by subtracting detectable cytokine at 0-hour timepoints. Statistical analyses were performed using GraphPad Prism 7.0 software. Statistical analyses for cytokine production were performed to determine differences between infection with EZ-GFP compared to infection with FL-15 or changes within each condition between 24- and 48-hours-post-infection. Western blot protein bands were analyzed by densitometry. Bands were normalized to the expression of GAPDH in each sample and fold change was calculated from a 0-hour timepoint. Differences were checked for significance using multiple t-tests. Immunofluorescence assays were assessed by determining localization of viral proteins and cellular proteins in response to infection. Infected cells were compared to uninfected cells to determine differences.

RESULTS

Cellular viability of B cells during infection with MeV

Cellular viability was evaluated in infected B cells (MOI of 1) at 0, 24, and 48 hours (Fig. 1) in EZ-GFP and FL-15-infected cells using the gating strategy shown in chapter 2 (Ch. 2: Fig. 4A). Loss of viability was interpreted as dead or dying cells. An overall 10.7% loss of viability in B cells as a result of culture was detected at 24 hours and 16.5% at 48 hours. An increase in cell death was observed in EZ-GFP infected cells compared to uninfected cells with 29.3% dead or dying cells at 24 hours post-infection; however, this did not continue to increase significantly at 48 hours post-infection (27.9%). FL-15 infected cells had less cell death at 24 hours (15.1%) than vaccine infected cells. However, FL-15-infected cells had a significantly more cell death (43.9%) than EZ-GFP-infected cells at 48 hours, despite lower levels of viral gene transcription and protein

expression than EZ-GFP infected cells (chapter 2). Infected cells were also assessed for changes in caspase-3, caspase-8, caspase-9, and MLKL expression (Fig. 1C) and nucleoprotein expression after 48 hours (Fig. 2D). Protein expression at 48-hours-post infection values were determined by normalizing densitometry values to GAPDH and comparing to a 0-hour timepoint. FL-15 cultures had a stronger, more significant ($p < 0.05$) fold decrease in caspase-3 (-2.06-fold), caspase-8 (-1.34-fold), caspase-9 (-1.99-fold), and MLKL (-1.86-fold) expression when compared to EZ-GFP infected cultures (-1.16, 1.51, 1.18, and -1.25-fold respectively) (Supplemental Figure 1). Despite increased cell death and cleavage of cell death associated proteins in FL-15 infected cultures, EZ-GFP infected cultures had higher expression of MeV nucleoprotein (69.03-fold) than FL-15 (16.5-fold) infected cultures (Fig. 1D).

Cytokine production in B cells infected with MeV

Cytokine expression was evaluated in EZ-GFP or FL-15 infected B cells (MOI of 1) at 24- and 48-hours post-infection (Fig. 2A-2E). A significant increase in most cytokines were measured in EZ-GFP infected cells compared to mock infected cells at 24- and 48-hours post-infection. However, fewer cytokines (IL-6, IL-8, and IL-10) were expressed significantly higher ($p < 0.05$) compared to mock infected cells at these same timepoints in FL-15 infected cells. TNF- α , IL-4, IL-6, and IL-8 continued to increase in the supernatant of EZ-GFP infected cells between 24- and 48-hours post-infection ($p < 0.05$) (Fig. 2A-D), but this was not observed in IL-10 expression (Fig. 2E). A significant increase ($p < 0.05$) in IL-8 expression was detected from 24- to 48-hours post-infection with FL-15 infected cells (Fig 2D), and a significant decrease ($p < 0.05$) in production of IL-10 was detected (Fig. 2E), concentrations of all other cytokines evaluated did not change in the supernatant of FL-15 infected cells between 24- and 48-hours post-infection. The level of TNF- α measured in EZ-GFP infected cells was significantly higher ($p < 0.05$) in EZ-GFP infected cells

than in FL-15 infected cells at both 24- and 48-hours post-infection, with IL-10 also demonstrating significantly higher ($p < 0.05$) levels in EZ-GFP infected cells at 48-hours post-infection (Fig. 2A and 2E). A single cytokine, IL-8, demonstrated significantly higher ($p < 0.05$) expression in FL-15 infected cells compared to EZ-GFP infected cells at both 24- and 48-hours post-infection (Fig. 2D).

Identifying cellular interactions and changes in morphology of infected BJAB cells

Cellular interactions were initially assessed using a B cell line. BJAB cells were seeded and adhered to an 8-well chamber slide prior to infection. BJAB cells were infected with FL-15 for 24 hours and stained for DAPI (not shown), CD19, and MeV nucleoprotein (Fig. 3A). Sites of cellular interactions between infected cells and neighboring cells are marked with a white arrow. Results show that infected cells interact with other cells. BJAB cells were also infected with EZ-GFP and stained with DAPI to assess additional changes in cellular morphology (Fig. 3B). Cellular extensions are denoted with a white arrow. Generation of cellular extensions are detected in B cell cultures infected with EZ-GFP.

Localization of MeV nucleoprotein in infected primary B cells

Localization of viral nucleoprotein was assessed via confocal microscopy in B cells infected with EZ or FL-15. Cell cultures were stained for DAPI (not shown), CD19, and MeV nucleoprotein. Images were taken at 24 hours-post infection (Fig. 4A, 4C) and 48 hours-post infection (Fig. 4B, 4D) using a 40X objective lens. Images were taken with 2X zoom (Fig. 4A, 4B) and 6X zoom (Fig. 4C, 4D) to assess cellular interactions more closely during infection. Nucleoprotein expression in infected cells localized to both internal and cellular surfaces (Fig. 4D). Nucleoprotein can be visualized at cellular interfaces as well as extensions of the cellular

membrane (Fig. 4C, 4D). There were no significant differences detected in the localization of nucleoprotein when comparing EZ and FL-15 infected cells.

Localization of MeV hemagglutinin and cellular SLAM in infected primary B cells

Localization of viral hemagglutinin was assessed via confocal microscopy in B cells infected with EZ or FL-15. Cells were stained for DAPI (not shown), CD19, MeV hemagglutinin, and SLAM. Images were taken at 24 hours-post infection (Fig. 5A, 5C) and 48 hours-post infection (Fig. 5B, 5D) using a 40X objective lens. Images were taken with 2X zoom (Fig. 5A, 5B) and 6X zoom (Fig. 5C, 5D) to assess cellular and protein interactions more closely. Compared to uninfected and FL-15 infected cells, EZ infected cells show increased SLAM reorganization at 24-hours-post infection (Fig. 5C). MeV hemagglutinin is localized at surfaces of cellular interaction (Fig. 5C) in both EZ and FL-15 infected cells. At 48 hours-post infection, increased reorganization of SLAM is detected on both EZ and FL-15 infected cells (Fig. 5D). High levels of hemagglutinin expression can be detected at cellular interfaces in both EZ and FL-15 infected cells (Fig. 5D). Colocalization of SLAM and hemagglutinin can be detected at 24-hours-post infection in EZ infected cells (Fig. 5D) and increases at 48-hours-post infection (Fig. 5D). Colocalization of SLAM and hemagglutinin is not detected in FL-15 infected cells until 48-hours-post infection.

DISCUSSION

Studies of measles infections in humans demonstrated a loss of antibody repertoire after recovery from measles⁸⁰, but vaccination is not associated with immunosuppression. Though there is a baseline level of viability loss in uninfected primary B cells during culture, infected cultures have a significantly higher level of cell death ($p < 0.05$). This was particularly evident in FL-15 infected cells, which had 1.6 times more cell death than EZ-GFP infected cells, suggesting that wild-type virus induces more cell death in B cells, specifically bystander cells. In addition to higher

levels of cell death, FL-15 infected cultures showed a stronger decrease in the pro-caspase -3, -8, and -9 expression, indicating cleavage and activation^{130, 131}. A marked decrease in caspase expression in FL-15 infected cells suggests that there are higher levels of activated caspase likely resulting in the observed increased cell death. Additionally, FL-15 cells expressed a decrease in the expression of the mixed lineage kinase domain-like (MLKL) protein, a protein involved in the induction of necroptosis¹³². While still a form of cell death, necroptosis is often thought to be immunogenic and potentially beneficial to host control of viruses¹³³. The decreased expression of MLKL in EZ-GFP infected cells compared to FL-15 infected cells, suggests that necroptosis may not play a large role in the development of immune suppression following MeV infection. Increased cell death in wild-type infected B cells may impact MeV induced immunosuppression by contributing to lymphopenia and alterations in percentages of antigen specific cells within the B cell repertoire, both of which may be masked through the expansion of measles specific adaptive immune cells in response to infection^{53, 80, 81, 100}. Our observations suggest that infection of B cells alone is not enough to induce these changes in memory populations since immunosuppression is not observed following vaccination and could be dependent on differences in cell death and signaling. Infection with wild-type viruses may induce differential cytokine profiles that lead to higher degrees of cell death *in vivo* or changes in signaling profiles that effect the survival and reconstitution of B cell populations.

Ferrets vaccinated with live attenuated influenza virus (LAIV) following infection with CDV showed the inability to respond to influenza challenge, suggesting functional immune response defects following morbillivirus infection⁸⁰. Function changes of B cells following MeV may be supported by the timing of viral clearance (20 days post infection in rhesus macaque model) and lymphopenia recovery (within 3 months) compared to extended immune suppression for

several months beyond that reaching estimated timeframes of several years^{53, 134, 135}. Extended immune suppression suggests that other mechanisms beyond cell loss may contribute to functional changes within B cells^{53, 80}.

Such functional changes in B cells, and other surrounding immune cells, could result from altered cytokine production. IL-10 is an important negative regulator of the immune response and has been shown to play a role in T cell exhaustion, apoptosis, and expansion of regulatory T cells. In rhesus macaques infected with wild-type MeV, viral RNA is detectable for several months after the clearance of viremia and the lack IL-10 production has been associated with other viral persistence models, such as LCMV^{135, 136}. Lower levels of IL-10 production in FL-15 infected B cells could contribute to the persistence of MeV RNA¹³⁷. Additionally, production of IL-10 by B cells positively impacts the proliferation of Treg cells, and Treg levels are higher in patients following MeV infection¹⁰⁰. Both vaccine and wild-type infected B cells produced IL-10 *in vitro*, however, IL-10 production in vaccine infected B cells was also associated with higher levels of the pro-inflammatory cytokine TNF- α , not observed in wild-type infected cells. This suggests that a differential balance in pro-inflammatory and anti-inflammatory cytokines could influence B cell function and induction of Treg cells seen in wild-type infection. Furthermore, TNF- α has been linked to B cell survival signaling akin to that of IL-2 in T cells and lower levels of TNF- α led to decreased B cell survival¹³⁸. Higher levels of TNF- α expression in vaccine infected B cells could contribute to B cell survival, lower observed cell death, and the absence of selected loss of infected cells during vaccination. IL-8 is also differentially produced in B cells infected with wild type and vaccine strains, with higher production seen in wild type infected cells. Increased IL-8 production in FL-15 infection could be linked to the binding of MeV hemagglutinin to TLR-2 which is sufficient for cytokine signaling in B cells^{139, 140}. TLR-2 signaling induces IL-8 signaling in

peripheral B cells ¹⁴¹, and increased levels of IL-8 from wild-type infected B cells could suggest that IL-8 plays a role in the development of a modified B cell response. IL-8 has been shown to impact production of cytokines from B cells and induce chemotaxis of B cells and other cells in the germinal center ^{142, 143}. Further investigation of the impact of MeV infection on the IL-8 signaling pathway could elucidate the impact of IL-8 production on surrounding cells, the germinal center reaction, and the impact these factors have on B cell reconstitution following MeV infection *in vivo*.

Unlike the cytokines discussed above, IL-4 and IL-6 are not differentially produced in wild-type and vaccine infected B cells. Regardless, they may play a role in pathogenesis and potentially tipping the scales in a pro-inflammatory route, as demonstrated by a more characteristic inflammatory response in vaccine infected B cells compared to wild-type infected cells. *In vitro* cytokine evaluation as shown here can define potential targets for *in vivo* analyses to assess the impact of cytokine expression on non-measles specific memory cells and antibody secreting cells. Experiments that focus on understanding the scale to which EZ-GFP or FL-15 impact cell signaling pathways need to be performed to assess the full impact of infection on intra- and intercellular signaling.

Lack of viral progeny as shown in chapter 2 suggests that measles viral components are spreading via non-canonical methods in B cells. Previous studies evaluating cell-to-cell spread have shown that MeV synapse structures occur between dendritic cells and T cells through the localization of cellular interaction proteins such as CD150, ICAM-1, and LFA-1 to allow transfer of viral genetic material through a “virological synapse” ¹¹¹. Non-canonical spread has been shown for non-immune cells as well. Spread of viral ribonucleocapsid in MeV-infected human airway epithelial cells occurs through pore formation mediated by actin polarization ^{112, 113}. Initially,

BJAB cells were assessed for localization of viral proteins during infection, showing localization of nucleoprotein at sites of interaction. High levels of nucleoprotein could be detected at sites of interaction with uninfected cells, suggesting exchange of viral components could be occurring between neighboring cells. Morphological changes were observed in BJAB in which cellular membranes in infected cells were visualized forming “dendritic-like” structures in the direction of uninfected cells. The localization of viral nucleoprotein at sites of interaction in infected cells as well as the dendritic-like structures suggest there may be exchange of viral components between cells through cell-to-cell contact.

MeV may be spreading between cells through interactions in infected cells expressing MeV-H on the surface and binding to neighboring, SLAM expressing cells. Since binding of SLAM on B cells affects responses to signaling associated with proliferation and antibody production^{144, 145}, studies were performed to assess the localization of SLAM and MeV-H during infection of B cells. SLAM binding has also been linked to changes in differentiation and expansion^{146, 147}, cell function¹⁴⁸, and cell death pathways⁸⁰. Understanding the interactions of B cells infected with MeV and expressing surface H may be key in understanding changes in signaling observed in wild-type infected individuals. In both EZ and FL-15 infected cells, expression of surface H can be detected at 24- and 48-hours post infection. H is detected at both sites of cellular interaction and localized with SLAM receptor on the infected cells as well as neighboring cells. Interestingly, at 24-hours-post infection, there is reorganization of SLAM protein in EZ infected cells not observed in uninfected or in FL-15 infected cells. At 48-hours-post infection, this relocalization intensifies in EZ infected cells and as it begins in FL-15 infected cells, showing that both EZ and FL-15 infected cells have interactions with neighboring cells with colocalization of SLAM and MeV-H. Infection with EZ seems to induce reorganization of cellular

protein at a higher rate, suggesting that signaling cascades induced by EZ activate more quickly. Since there are detectable differences in localization of proteins in cells infected with EZ or FL-15, that implies that there may be differences in the viral proteins involved in the cellular response mechanisms. Further studies should be performed to understand if MeV-H protein alone can induce changes in signaling of B cells as well as induce reorganization of cellular proteins, and studies to understand the differences in vaccine H vs. wild-type H and how these changes can alter cellular responses to viral proteins.

Assessment of viral protein localization at 24- and 48-hours-post infection in primary B cells show evidence of protein localization at cellular interfaces as well as co-localization of SLAM and MeV-H. Nucleoprotein can also be observed intracellularly as well as on the surface of the cell in both EZ and FL-15 infected cells. Nucleoprotein was detected at sites of cellular interaction and cellular extensions connecting neighboring cells. Nucleoprotein is theorized to be present in the endolysosomal compartment, allowing for interaction with Fc gamma receptors (Fc γ R) where it is then exported to the cell surface or released from MeV infected lymphocytes⁸⁶. Nucleoprotein attachment to Fc γ R could also lead to uptake of nucleoprotein into neighboring cells which has been linked to changes in death as well as cellular transcription and translation¹²¹. These data suggest that the uptake of nucleoprotein into neighboring, uninfected cells correlates with the induction of cell pathways in uninfected cells which could contribute to the significant cell death in FL-15 cultures despite lack of MeV+ cells detected via flow cytometry. Expression of nucleoprotein on Fc γ RIIB has been linked to decreased antibody production from human B cells¹⁴⁹, suggesting that understanding how viral components impact cell function without infection could elucidate potential mechanisms for changes detected in the B cell compartment after MeV infection.

In addition to the differences observed in the infection of B cells with FL-15 or EZ, there are differences in the cellular response to MeV infection. Despite lower levels of infection in FL-15 infected cultures, there are higher levels of cell death and induction of cell death pathways. Additionally, cytokine production by EZ-GFP infected cells suggested a more canonical anti-viral response was produced, while FL-15 infection could dampen the inflammatory response and may have implications in MeV RNA persistence and expansion of regulatory cells. Differences in the cytokine profiles of EZ-GFP or FL-15 infected cultures combined with the localization of viral proteins (MeV-N and MeV-H) and localization of SLAM on the surface of cells infected suggests that there could be mutations in the viral proteins that will impact cellular signaling. If viral proteins alone induce these changes in signaling and viability, understanding the mutations in viral proteins and their potential impact on cellular signaling and cell-to cell interactions may contribute to understanding the differences observed between infected and vaccinated individuals and the development of immune suppression.

Figure 1

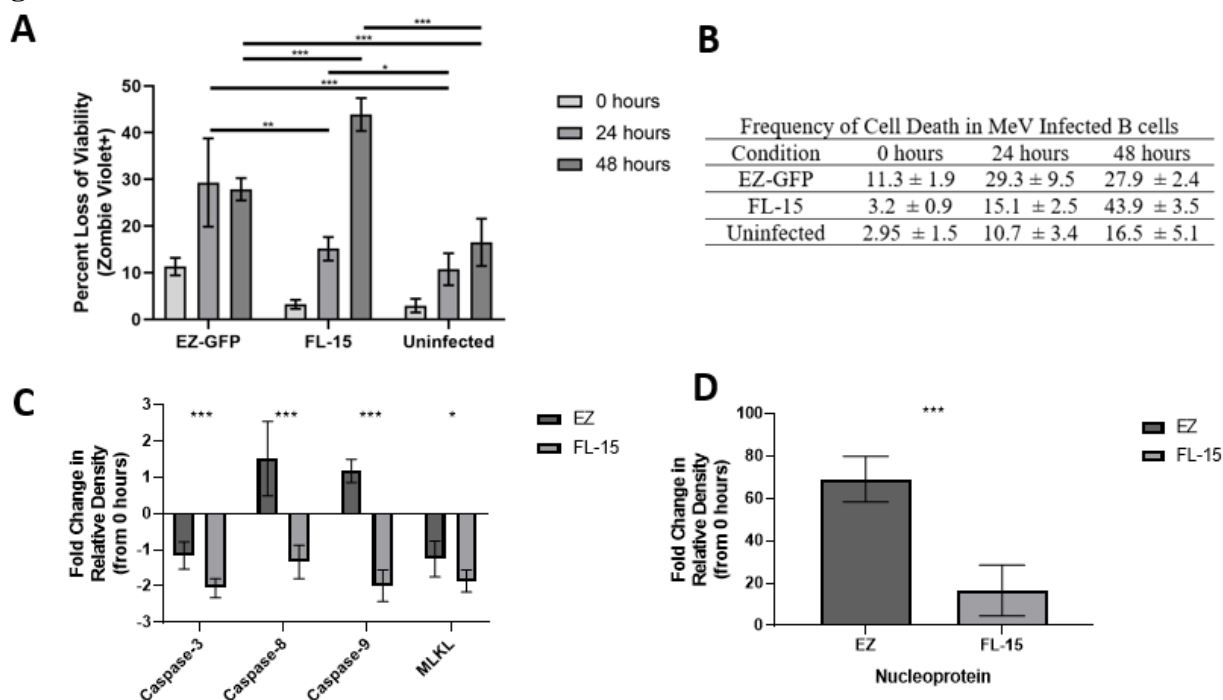


FIG 1. Cell viability following MeV infection. B cells from healthy human donors were infected with EZ-GFP and FL-15. A) Infected cells were assessed for viability using a fluorescent amine-reactant dye, Zombie Violet (n=8). The gating strategy from Chapter 2: Fig 4A was used to determine boundaries for loss of viability. Loss of viability included dying and dead cells measured at 0, 24, and 48 hours in infected and uninfected cells. (B) Frequency of cell death at each time point notated in a table format. (C) Changes in caspase expression from 0 to 48 hours relative to GAPDH were measured via Western Blot using densitometry. Values were measured as fold change from 0 hours. (D) Levels of nucleoprotein in infected cells were assessed at 48 hours post-infection via Western Blot. Error bars represent standard deviation. Statistics were determined using multiple t-tests (***) = $p < 0.001$, ** = $p < 0.01$, * = $p < 0.05$, n = 4).

Figure 2. Cytokine protein production in B cells following MeV infection.

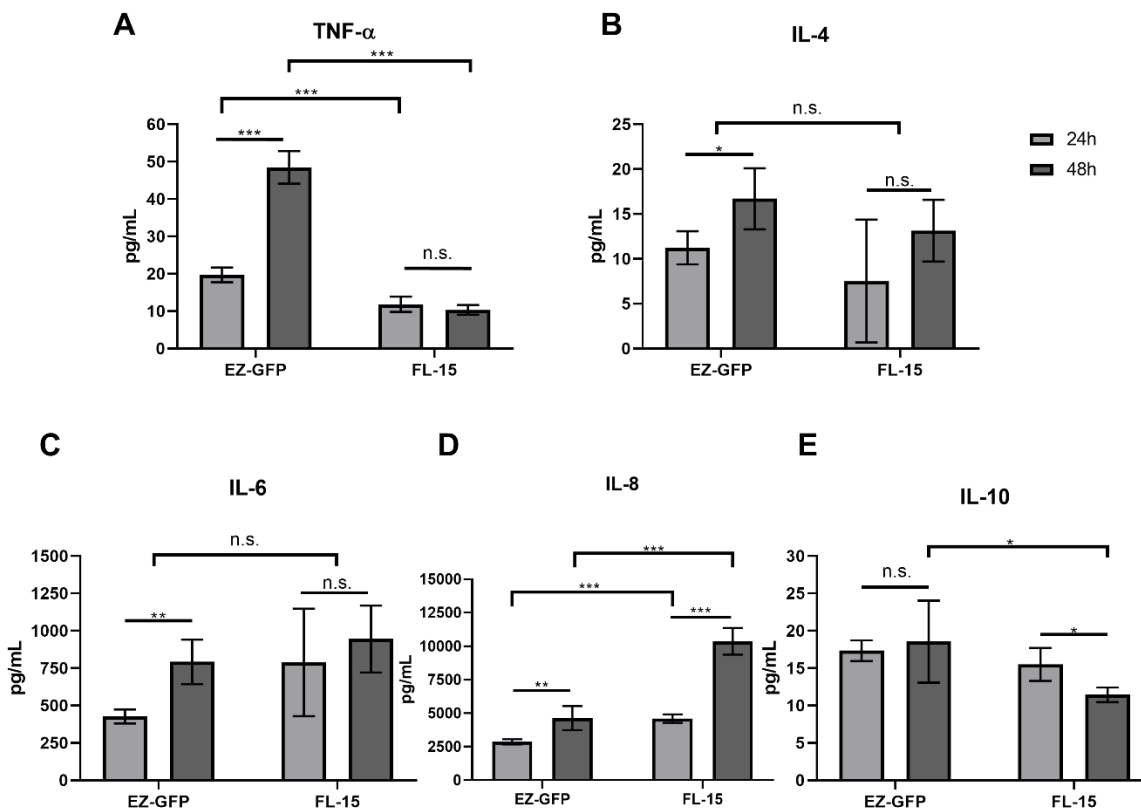


Figure 2. Cytokine protein production in B cells following MeV infection. Previously frozen B cells from 3 healthy donors were infected with EZ-GFP or FL-15 at an MOI of 1. Supernatants were collected and stored at -80°C . Supernatants from 24 hours post-infection 48 hours post-infection were assessed for TNF- α (A), IL-4 (B), IL-6 (C), IL-8 (D), and IL-10 (E) using a multiplex bead based Luminex assay. Statistical differences between each condition were assessed at individual timepoints. using multiple t-tests between each condition and from 24- to 48- hours post-infection. (***) = $p < 0.001$, (**) = $p < 0.01$, (*) = $p < 0.05$, $n = 4$).

Figure 3. Fluorescence microscopy on MeV infected BJAB cells.

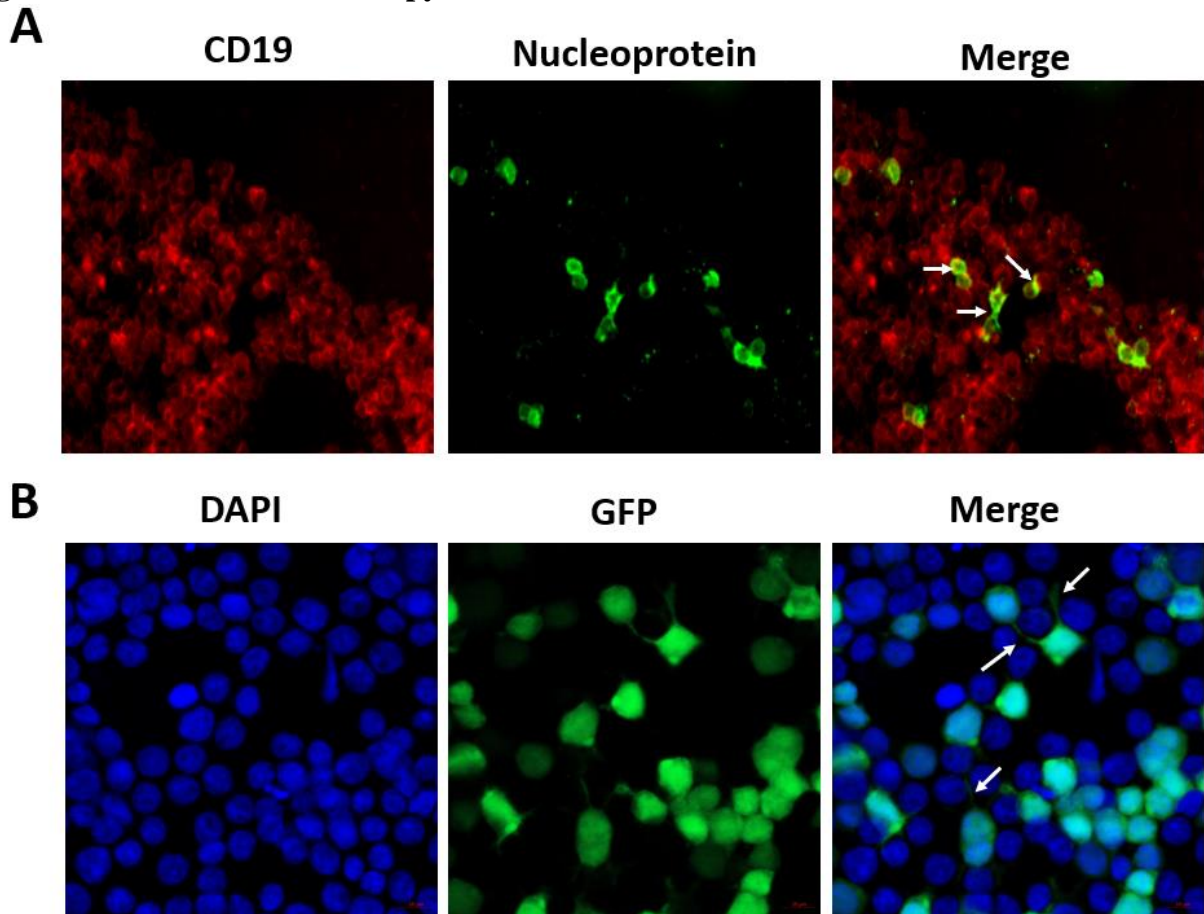
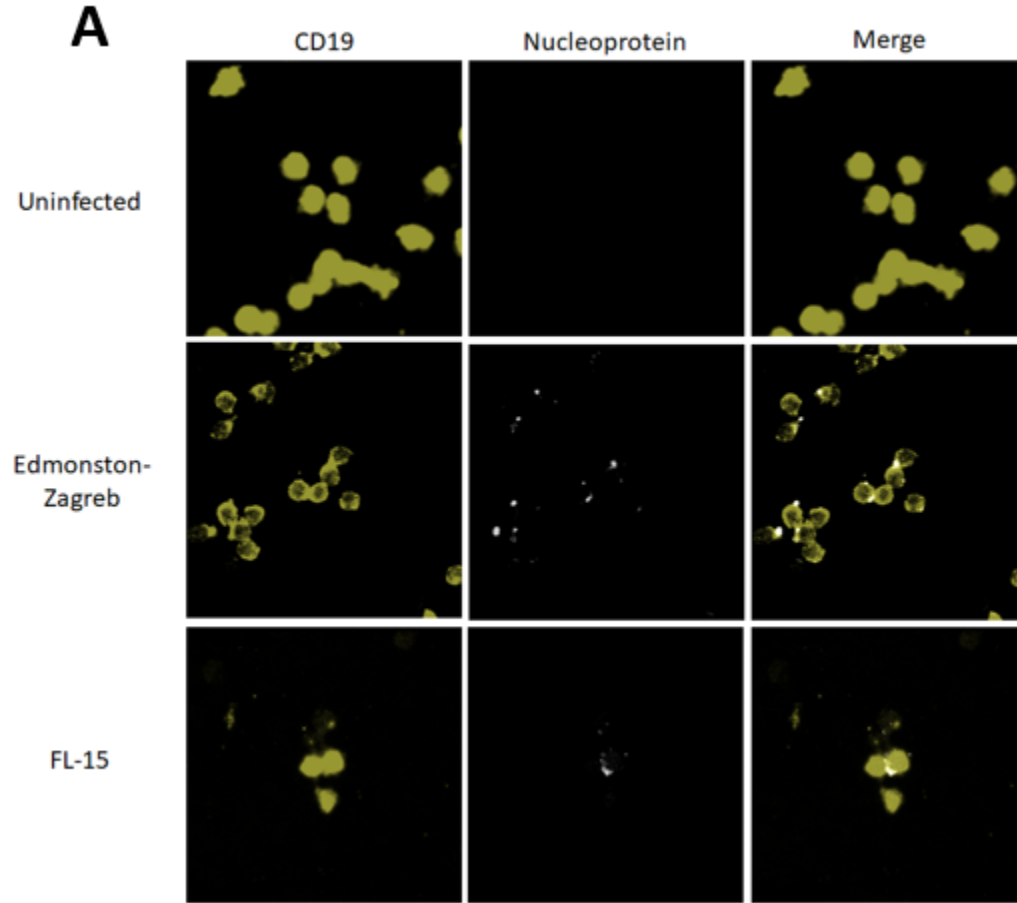
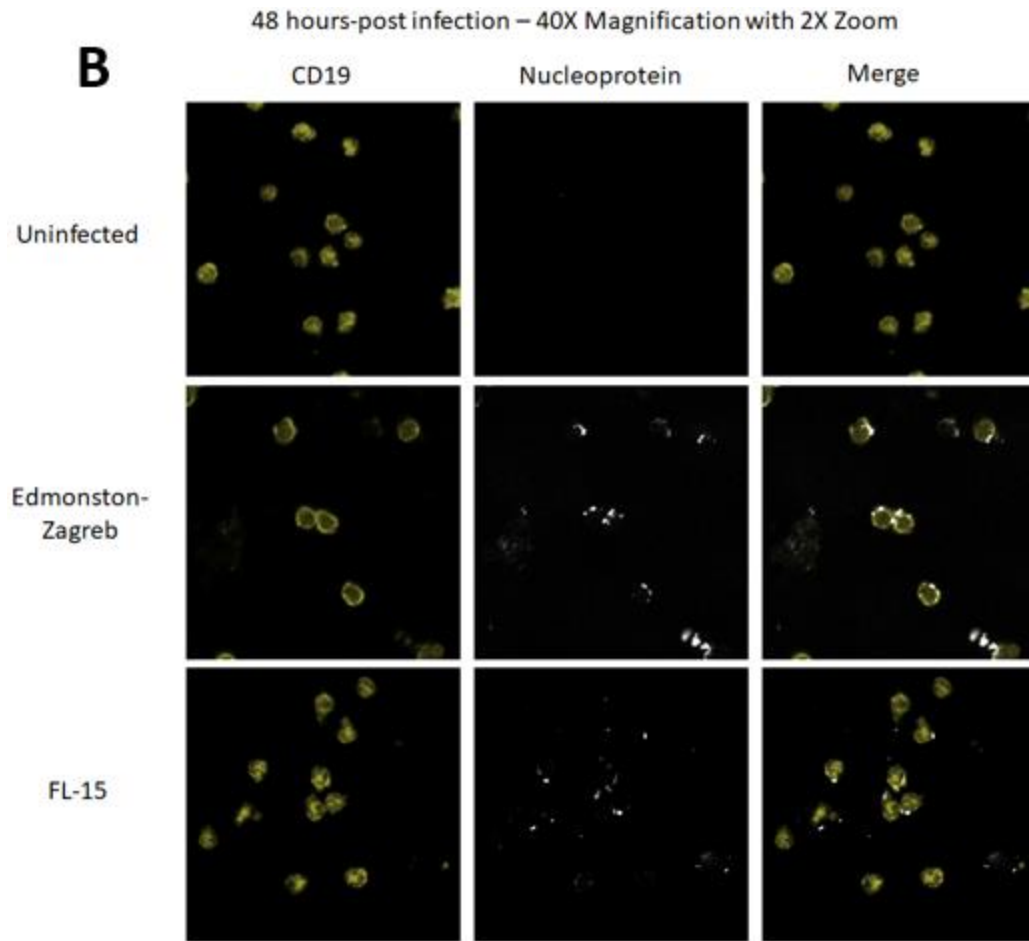
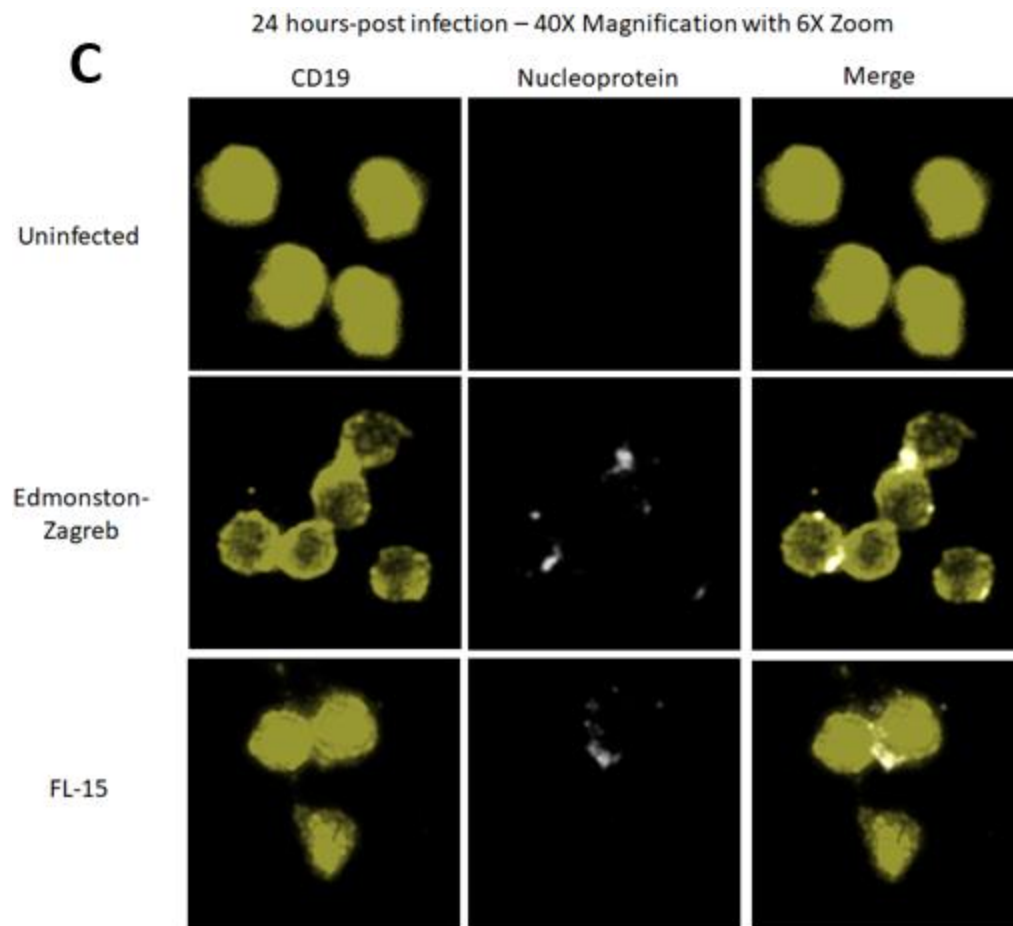


Figure 3. Fluorescence microscopy on MeV-infected BJAB cells. After overnight adherence, BJAB cells were infected after adherence to an 8-well chamber slide. (A) BJAB cells were infected with FL-15 and stained for CD19 and nucleoprotein and imaged at 20X to identify localization of nucleoprotein in infected cells. Points of cellular interactions between infected cells and neighboring cells are marked with a white arrow. (B) BJAB cells were infected with EZ-GFP, stained with DAPI, and imaged at 40X to assess the existence of cellular extensions during infection. Cellular extensions are highlighted by white arrows. (n=4)

Figure 4. Fluorescent imaging of MeV nucleoprotein in infected B cells.
24 hours-post infection – 40X Magnification with 2X Zoom







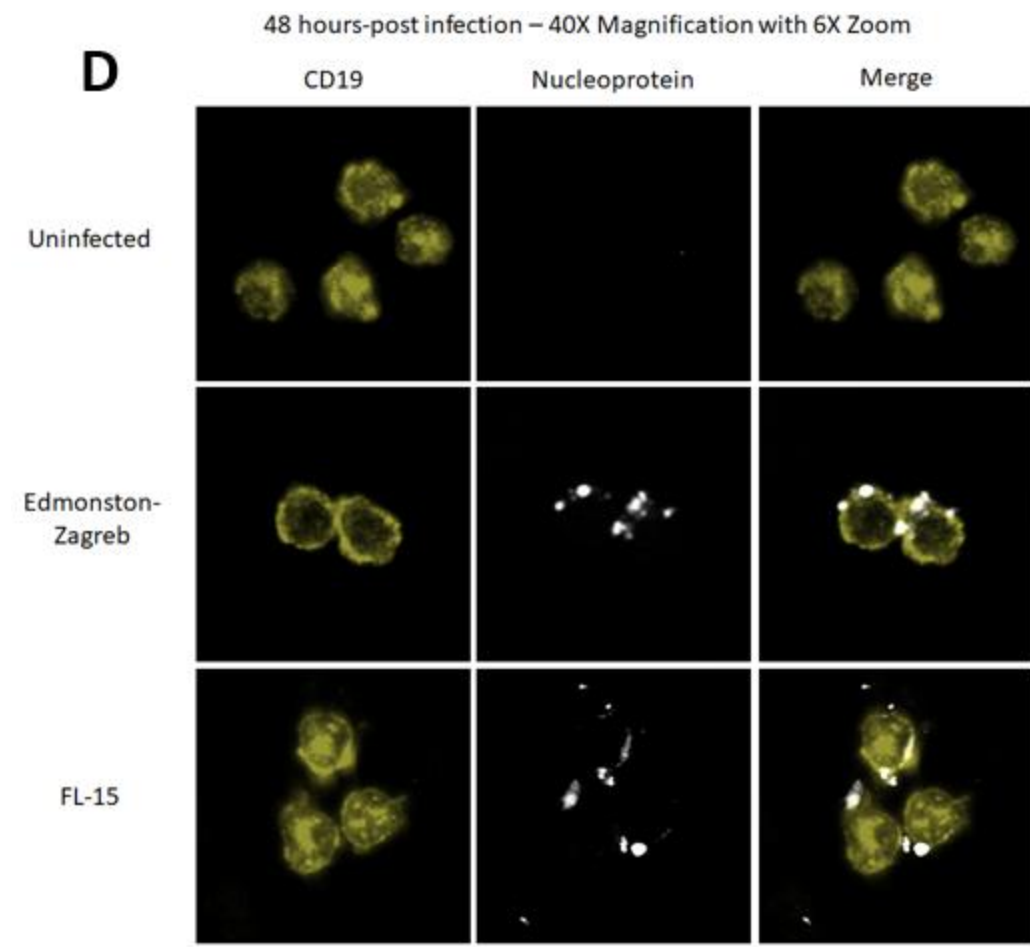
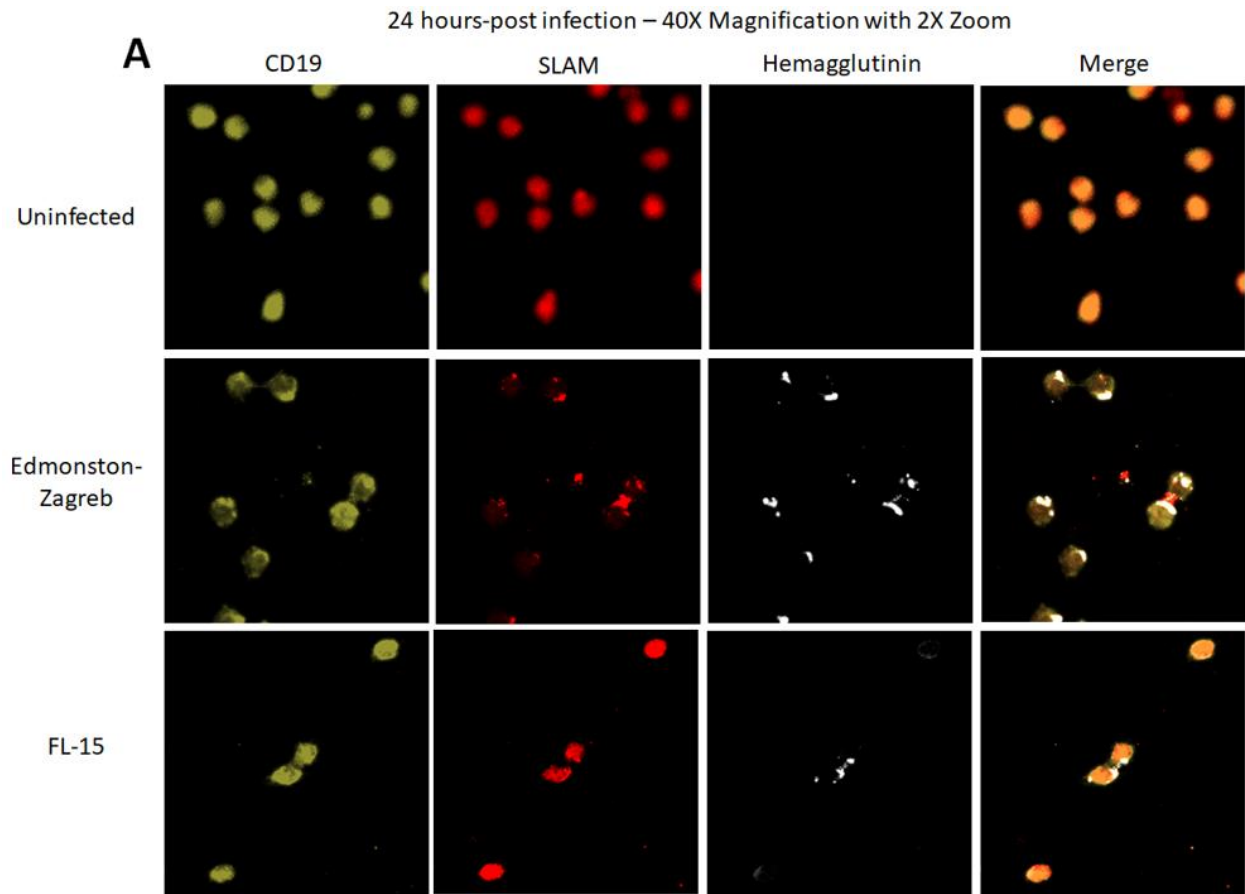
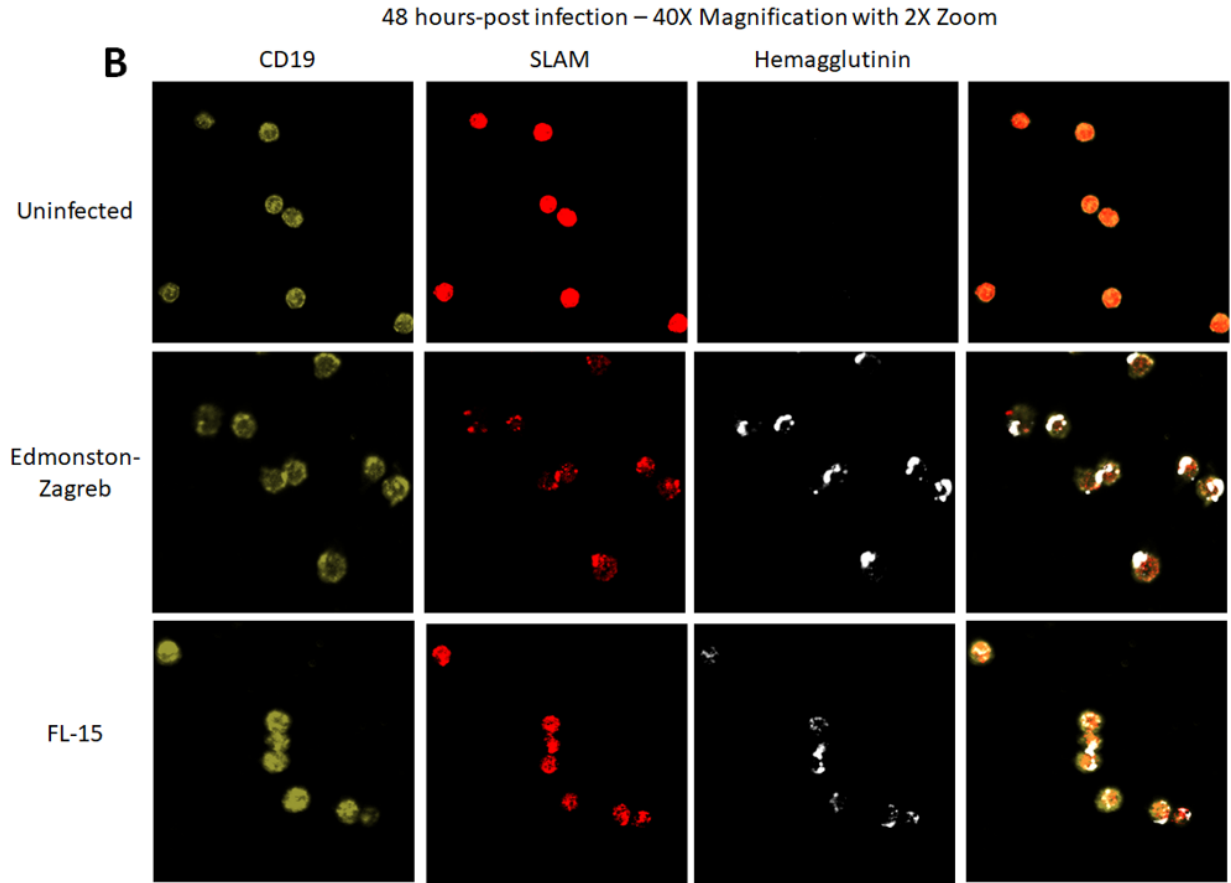
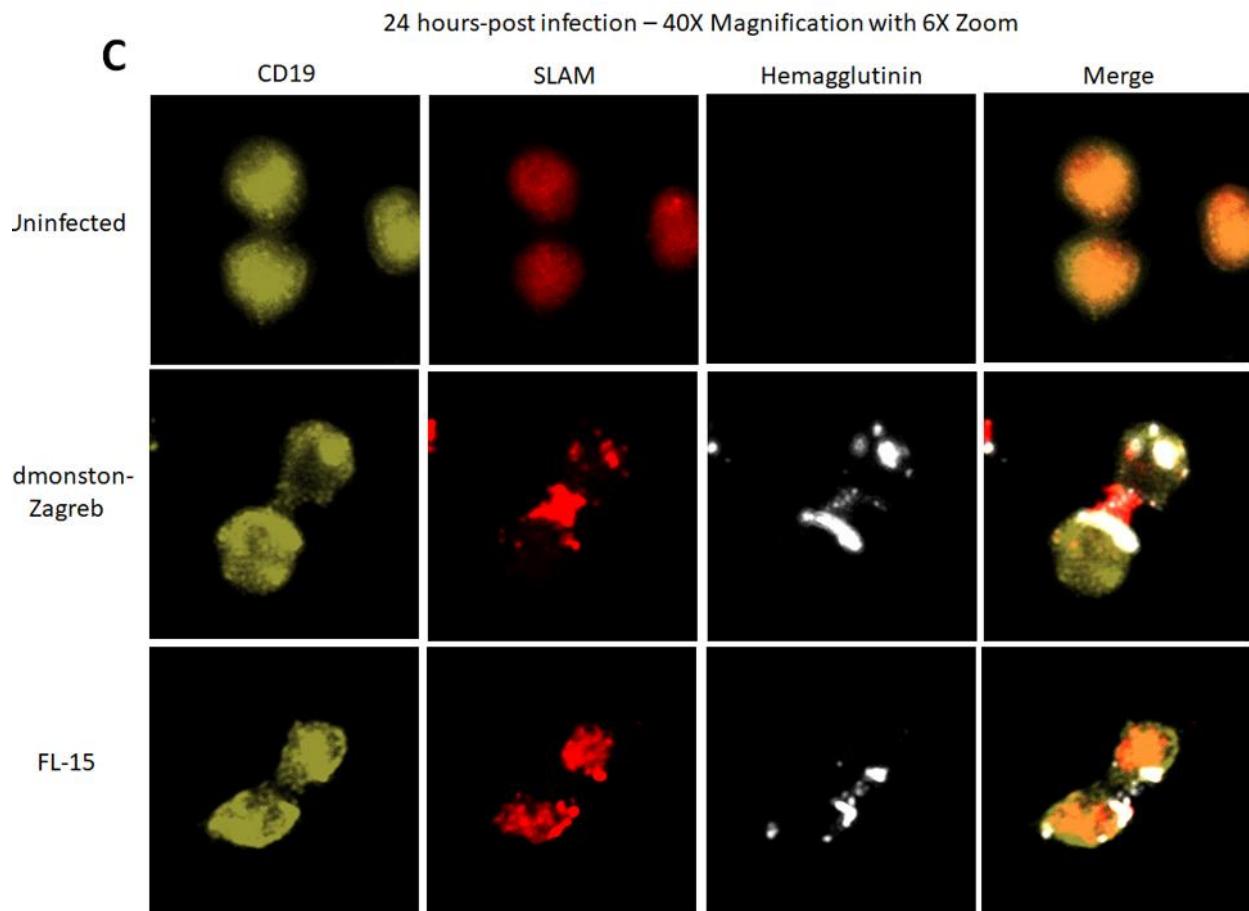


Figure 4. Fluorescent imaging of MeV nucleoprotein in infected B cells. Healthy donor human B cells were infected in 8-well chamber slides following overnight adherence and stained for MeV nucleoprotein and CD19 at 24 (A, C) and 48 (B, D) post-infection. Cells were imaged at 40X magnification while using 2X (A, B) and 6X (C, D) zoom. Images are representative of infection replicates (n=4).

Figure 5. Fluorescent imaging to assess localization of MeV hemagglutinin and cellular SLAM in infected B cells







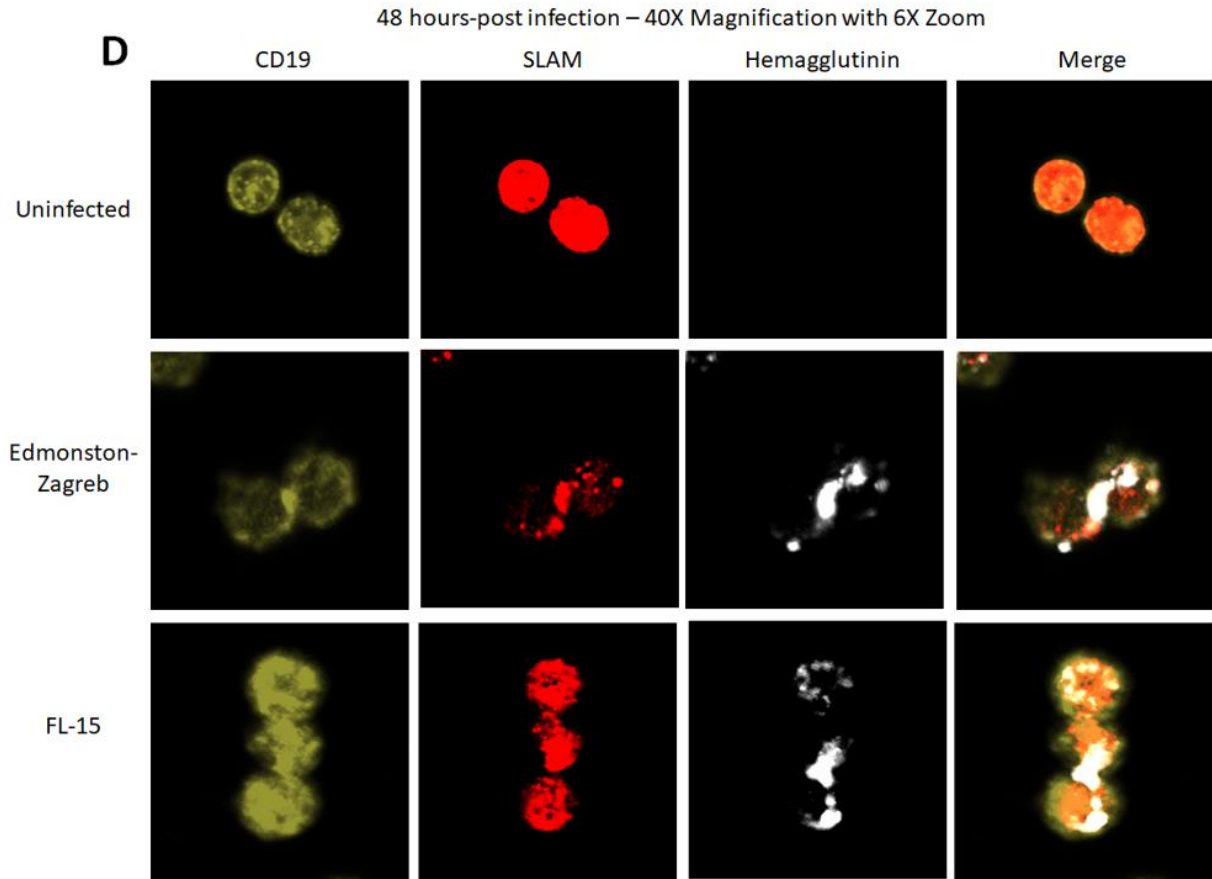
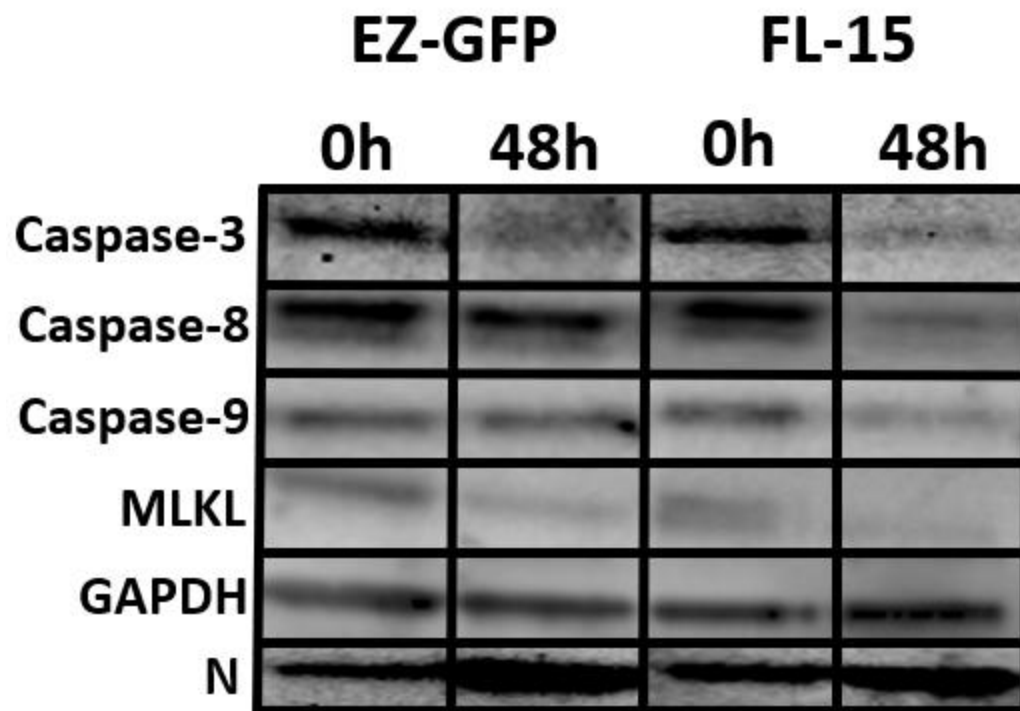


Figure 5. Fluorescent imaging to assess localization of MeV hemagglutinin and SLAM in infected B cells. Healthy human B cells were infected in 8-well chamber slides following overnight adherence and stained for CD19, SLAM, and MeV hemagglutinin at 24 (A, C) and 48 (B, D) post-infection. Cells were imaged at 40X magnification while using 2X (A, B) and 6X (C, D) zoom. Images are representative of infection replicates (n=4).



Supplemental Figure 1. Representative bands for densitometry to determine densitometry of cell death associated proteins. Donor B cells from StemCell were seeded at 400,000 cells per well and infected with EZ-GFP or FL-15. Protein was isolated and processed for SDS-PAGE electrophoresis using 20 ng protein per well. Protein was transferred to a nitrocellulose membrane, blocked using 5% milk powder in TBST, and stained with primary antibody for pro-caspase-3, pro-caspase-8, pro-caspase-9, MLKL, GAPDH, and MeV-N followed by secondary HRP expressing antibody to assess expression at 0h and 48h (n=4).

Chapter 4: Discussion and Conclusions

DISCUSSION

The goal of these studies was to determine if there were differences in the infection of B cells with vaccine (EZ) or wild-type (FL-15) strains of MeV. Previous work shows that B cells are infected by MeV at a high frequency⁸², and individuals who are infected with MeV show changes in their immune profile⁷⁴, antibody repertoire⁸⁰, and have incomplete reconstitution of B cell diversity following infection⁸¹. Importantly, the immune suppression observed following infection is not observed in individuals who have received the live-attenuated MeV virus from the MMR vaccine. The lack of immune suppression suggests that despite being replication competent, vaccine virus behaves and impacts infected cells differently. To address these potential differences, healthy human B cells were infected with EZ-GFP or FL-15 strains of MeV and assessed for infection frequency, viral gene transcription, production of progeny virus, preferential infection of specific B cell subtypes, cytokine profiles, cell death, and localization of cellular and viral proteins. These studies aim to elucidate differences in the assessed parameters to further our understanding of how MeV infection affects B cells and the contribution of infected B cells to the pathogenesis of immune suppression .

BJAB cells as a model of infection for MeV

One of the first goals was to assess an EBV(-) B cell line (BJAB cells) as a model for MeV infection. Due to the low frequency of B cells present in the periphery (5-10% of PBMCs)¹⁵⁰, it is important to have a model for studies requiring high cell numbers. Our studies showed that BJAB cells can be infected with EZ-GFP and FL-15. Infected cells show detectable increases in viral protein expression at 24- and 48-hours-post infection with EZ-GFP cultures having a higher frequency of infected cells than FL-15 infected cultures. Viral gene transcription was also

measured in these cells. We observed that there are increases in N gene transcription at 24-, 48-, and 72- hour-post infection for EZ-GFP infected BJAB cells but only to 48-hours-post infection for FL-15 infect cells. Due to the higher frequency of infection detected in BJAB cells over primary cells, BJAB cells were used to further asses the production of viral progeny from infected cells. Infectious inoculum was removed from BJAB cells to determine if the residual virus was impacting detection of new progeny virus. Results show that even with the removal of inoculum, with and without lowering the MOI, there was no detection of an increase in viral titer above input. Lastly, BJAB cells were used as a proof of concept to determine if there was evidence of non-canonical MeV virus spread via fluorescence microscopy. BJAB cells were infected and it was observed that there was evidence of morphological changes in cell structure that likely contributed to the cell-to-cell spread of viral content and localization of viral proteins at sites of cellular interaction. These results were consistent with published literature that show that MeV can transfer viral components to neighboring cells through the formation of cellular pores or virological synapse through actin polymerization or interaction between cell surface molecules on neighboring cells^{111, 112}. Despite evidence of viral replication, BJAB cells were not used to assess cell death or cytokine production due to lack of cytokine production under stimulation¹⁵¹ and potential differences in caspase induction since it is an immortalized cell line. BJAB cells were infected with EZ-GFP and FL-15 and showed similar patterns of infection as primary cells *in vitro* suggesting that they are a good model to understand differences in infection characteristics of MeV.

Comparison of wild-type and vaccine replication in B cells

There is published evidence of B cell infection *in vivo* but the characteristics of infection in B cells are not fully understood. We infected human B cells *in vitro* with EZ-GFP or FL-15 to

further our understanding of the characteristics of these infections. We detected increases in the frequency of virus positive cells present in infected cultures at 24- and 48-hours-post infection for both EZ-GFP and FL-15; however, at both time points, EZ-GFP-infected cells were detected at a higher frequency than FL-15-infected cells. Additionally, there was an increase in N gene transcription detected in EZ-GFP-infected cultures at both 24- and 48-hours-post infection but only at 48-hours for FL-15-infected cultures. These data suggest that infection of B cell cultures with EZ-GFP more readily replicate viral components than FL-15 infected cultures. We refined the analysis of infection characteristics by assessing the propensity for MeV to infected specific subtypes of B cells. To do this, we analyzed the infection of four B cell subtypes: naïve (IgD+CD27-), non-class switched memory (IgD+CD27+), class switched memory (IgD-CD27+), and double negative (IgD-CD27-). we observed similar frequencies of naïve and memory subtypes being infected⁷⁶, which is concordant with published results for frequencies of naïve and memory subtypes after infection. However, within the memory compartment, EZ-GFP targeted non-switched memory cells at a lower frequency at 48-hours-post infection than other cell types while FL-15 appeared to target non-switched memory cells at a higher, though non-significant ($p = 0.07$), frequency. Circulating CD19+IgD+IgM+CD27+ cells have been observed to have a similar phenotype to marginal zone B cells¹⁵². Marginal zone B cells are responsible for large amounts of the IgM produced in humans which protect against commonly occurring antigens in bacteria and viruses, playing an important role in mounting an immune response to pathogens¹⁵³. Preferential targeting of this cell-type by wild-type infection *in vivo* may lead to extensive cell death in this compartment which would impact the ability of MeV infected individuals to respond to secondary infections which correlates with the increased susceptibility to secondary infections following MeV infection⁹⁷. Our data show that as in studies performed in T cells showing difference in

frequency of infection within the memory compartment⁷⁶, there are differences in infection frequency within B cell memory compartment. Further experimental evaluation could elucidate the targeting of non-switched memory B cell subtype as well as other memory B cell subtypes during and following *in vivo* infections to further our understanding of how these cell types could be differentially infected by vaccine or wild-type MeV leading to the phenotypic outcome observed in wild-type infection. Because of the observed changes in an already existing antibody repertoire⁸⁰, changes in diversity of memory B cells⁸¹, and changes in the frequency of certain B cell subtypes following infection⁷⁴, studies should be performed to assess differences in infection characteristics in memory subtypes such as IgG or IgA B cells compared to IgM B cells. Additionally, understanding how the infection can spread in a germinal center to impact antibody production and clonal diversity is key in understanding the mechanism behind the development of immune suppression. The limitation of this study was that we did not assess changes in these compartments due to the lack of availability and different phenotypes of B cells in the periphery as well as lack of access to tissue samples with germinal center formations. Examination of the targeting of these different B cell subtypes during infection could improve our understanding of the targeting of specific B cell subtypes during MeV infection and the role of these subtypes in the development of immune suppression.

Assessing cell death in MeV infected B cell cultures infected

Due to the differences detected in infection characteristics, we assessed the differences in the outcome of the infected B cell cultures, including cell death. A higher level of cell death was detectable in infected cells with FL-15 infected cells demonstrating the highest frequency of cell death. Despite lower levels of infection and viral transcription, FL-15 infected B cells resulted in greater cell death. Viral protein and infection can lead to the induction of cell death pathways such

as apoptosis and necroptosis¹⁵⁴. FL-15 infected cell cultures show more activation of caspase-3, caspase-8, caspase-9, and MLKL proteins which are all associated with cell death pathways. MLKL activation was not exclusively detected in FL-15 infected cultures. Due to the higher rates of survival in EZ-GFP infected cultures, lack of immune suppression following vaccination, and necroptosis being linked to a more immunogenic form of cell death¹³³, necroptosis likely does not play a role in the development of immune suppression. The development of MeV induced immune suppression is often theorized to be caused by high levels of lymphopenia that occur during infection. However, virus is cleared within 20 days and lymphopenia is generally recovered within 3 months^{134, 135}. Additionally, studies show that morbillivirus infected models show an inability to respond to stimuli⁸⁰ and mathematical models predict MeV induced immune suppression could last for several years⁵³. The time frame of these factors combined with extensive bystander cell death in FL-15 infected cultures suggest that there could be other mechanisms that are impacting the longevity of the immune suppression

Cytokine expression in MeV infected B cell cultures

Our studies also assessed the cytokine profile of B cell cultures infected with EZ-GFP or FL-15. Understanding the differences in cytokine production in cells infected with FL-15 or EZ-GFP is key in understanding how infection with each of these viruses may differentially impact cell function. Lower levels of IL-10 expression in FL-15 cells could promote persistence of MeV RNA and skew cellular populations following infection. EZ-GFP infected cultures expressed more IL-10 along with higher levels of TNF- α . Expression of IL-10 and TNF- α suggest EZ-GFP infected cultures could contribute to B cell survival accounting for the lower levels of cell death observed in EZ-GFP infected cultures. FL-15 infected cultures produced higher levels of IL-8, which could be linked to the binding of MeV to TLR-2 which is sufficient for cytokine signaling in B cells¹³⁹.

IL-8 has been shown to impact chemotaxis of cells as well as production of cytokines from B cells in the germinal center¹⁴². IL-8 production from FL-15 infected cultures suggest that IL-8 production *in vivo* may impact the populations of B cells present following reconstitution of cells after MeV infection. Unlike IL-8, IL-10, and TNF- α , IL-4 and IL-6 were not differentially produced between the two infections but show a detectable increase over input. The combination of cytokines produced by EZ-GFP infected cultures (IL-4, IL-6, IL-10, and TNF- α) suggests a more controlled, inflammatory route of response to the vaccination which may have implications in preventing the development of immune suppression. These cytokines may provide targets for more in-depth analysis in future *in vivo* studies.

Production of viral progeny and non-canonical viral spread

Despite evidence of viral replication as demonstrated by the transcription of viral genes and increases in the frequency of infected cells over the time-course, there was no detectable increase in viral titer produced over input. Viral titer was assessed using TCID₅₀ and Reed-Muench calculations to determine PFU/mL with no detectable increase in viral titer above input in either FL-15 or EZ-GFP infected cultures. To examine if inoculum was masking the growth of new virus BJAB cells were infected and the inoculum was removed. Additionally, infections were performed at an MOI of 0.001 and an MOI of 1.0 with an incubation time of 96 hours to determine if extending the infection course would permit production of viral progeny. Extending the time course, lowering the MOI, and removing the inoculum on infected BJAB cells did not produce an increase in titer at any of the time points. Increased percentages of antigen-positive cells over time despite the lack of a detectable increase in viral titer in every condition suggests that MeV is spreading between B cells in a non-canonical fashion. MeV has been shown to spread viral components through binding of SLAM expressed on uninfected cells to neighboring infected cells expressing MeV-H¹¹¹,

cellular pores at sites of cellular interaction, and actin bridges formed by infected cells, permitting replication and viral signaling in cells that were not infected by a viral particle¹¹². We used confocal microscopy to investigate the potential for non-canonical spread by demonstrating localization of nucleoprotein in infected cells as well as localization of hemagglutinin and SLAM on infected and uninfected cells.

We first used BJAB cells to visualize localization of viral and cellular proteins. BJAB cells were infected with FL-15 and stained for CD19 and nucleoprotein and imaged via fluorescence microscopy. These cultures showed evidence of nucleoprotein collecting at the interfaces of infected cells with other cells. BJAB cells were also infected with EZ-GFP to investigate potential changes in cellular morphology. Infected cells showed a propensity for formation of “dendrite-like” structures that often extended towards uninfected cells. The localization of nucleoprotein as well as the dendrite-like extensions suggest that there are non-canonical mechanisms being used for the spread of MeV viral components from cell-to-cell. To further investigate non-canonical methods, primary B cells were infected and imaged using confocal microscopy to assess SLAM, nucleoprotein, and hemagglutinin localization. In both EZ and FL-15 infected cultures, nucleoprotein can be detected at sites of cell-to-cell interaction. Additionally, nucleoprotein can be detected on the surface of the cell and on cellular extensions visualized through CD19 staining. Nucleoprotein has been shown to be exported to the surface of cells that express Fc γ R which may have implications in the production of immunoglobulin and cytokines that impact T cell differentiation^{86, 149}. Additionally, presence of nucleoprotein on the surface of cells has been linked to uptake of nucleoprotein on neighboring, uninfected cells that express Fc γ R which leads to cell death and further changes in effector function such as antibody production or attenuated signaling by binding to Fc γ RIIB^{121, 155}. These findings could be linked to the increased cell death and

differential cytokine profiles detected in FL-15 cultures despite lower frequencies of viral proteins detected in these cultures. In primary B cell cultures stained for SLAM and MeV-H, SLAM and H can be detected at cellular interfaces. At 24-hours-post infection, EZ-infected cultures show reorganization of SLAM to be more colocalized with MeV-H. Protein reorganization is even more apparent at 48-hours post-infection in EZ-infected cultures. This phenomenon is not detected in FL-15-infected cultures at 24-hours-post infection. At 48-hours-post infection, reorganization of SLAM can be detected in FL-15 infected cultures, but not to the degree that it is in EZ infected cultures at 24- or 48-hours-post infection. Infection with EZ appears to induce increased reorganization of cellular protein, suggesting that there may be differences in the hemagglutinin produced by EZ or FL-15 which impact the interactions with SLAM and thus downstream signaling following binding of MeV. SLAM binding has been linked to both activation and attenuation of T cell receptor and BCR signaling cascades under certain conditions, suggesting that viral components may have an impact on the signaling induced by SLAM binding on infected cells¹⁵⁶. Furthermore, MeV-H has also been linked to changes in co-stimulatory molecule expression, Akt and ERK1/2 activity, and an overall decrease in *in vivo* inflammatory response in mice³⁸. Furthering our understanding of how MeV-H interactions with SLAM may differentially impact signaling cascades depending on the strain of MeV could provide insight into the impact on inflammatory signaling cascades caused by MeV-H binding. Additionally, since nucleoprotein is present on the surface of B cells infected with EZ or FL-15 but FL-15 infected cultures have higher levels of cell death and a less inflammatory cytokine profile, this suggests that there may be differences in the nucleoprotein generated from these viruses, leading to differential impact on the infected cell's signaling cascades as well as cells in their environment. Understanding the impact of mutations present in vaccine virus proteins and how these could affect the ability of

MeV to induce an immunosuppressive state both *in vitro* and *in vivo* may provide insight into how wild-type virus induces a state of immune suppression.

Understanding differences in protein localization contributes to our understanding of how viral components may be transferred via cell-to-cell interactions. Since both EZ and FL-15 infected cells produce nucleoprotein and express it on the cellular surface, further studies need to be performed to assess potential differences in the nucleoproteins expressed by each virus and how these may differentially impact cellular function. Understanding how nucleoprotein alone may impact an uninfected cell will give insight into the transfer of nucleoprotein from cell-to-cell as well as the changes in cytokine and immunoglobulin production caused by this viral protein. Similar experiments that further our understanding of the impact on MeV-H binding to SLAM and how this may vary with different strains of MeV will give additional insight into how wild-type induces immune suppression and vaccine does not.

Impact and future studies

Our studies have shown that there are detectable differences in viral replication between EZ and FL-15 infected cells, cell targeting, cell viability, and cytokine profiles in infected B cell cultures. We have also shown that the rate of protein reorganization during infection varies despite similar expression patterns for nucleoprotein and hemagglutinin, suggesting there may be differences in not only replication of each virus but also protein expression. These findings can be used to inform future studies, particularly experiments to compare viral protein expression and *in vivo* infection models between wild-type and vaccine strains of MeV. The rate at which the SLAM on infected cells reorganizes suggests that the signaling cascades induced by vaccine and wild-type infection may be different and understanding how each virus' hemagglutinin may bind to

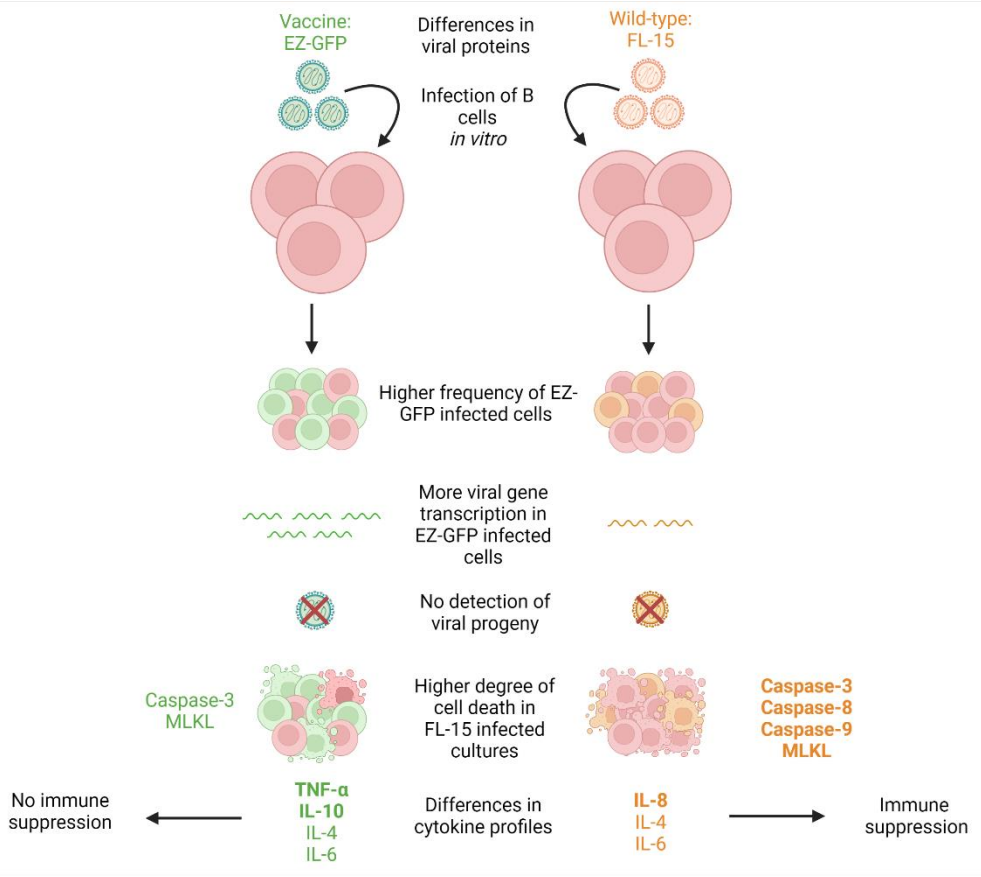
SLAM could elucidate how downstream signaling influences B cell function observed following MeV infection.

Further studies to assess variations in viral proteins between EZ and FL-15 and the role of these mutations in the cellular response to MeV infection may clarify the mechanism of MeV induced immune suppression and the role of B cells in mediating immune suppression following infection. In addition to potential mutations present in MeV-H and MeV-N, mutations present in non-structural proteins such as the V protein have been shown to impact its ability to inhibit IFN α production²³, suggesting that the impact of even non-structural proteins may vary between strains of MeV. Due to the heavy involvement of many MeV proteins in controlling the host cell response, it is important to understand how the mutations present in each protein of vaccine strains of MeV impacts the pathogenesis of MeV in B cells to limit the development of immune suppression.

Passaging MeV in different cell lines has an impact on the ability of MeV to produce viral proteins, such as the V protein, generating a quasispecies of MeV¹⁵⁷. Evidence of these quasispecies suggests that infection of B cells may impact each strain of virus differently, changing the genetic characteristics and ability of the virus to infect or transfer its viral material to other cells. Sequencing viruses that are used to infect and comparing those sequences to genomes after infection may be informative in understanding how B cells may impact the genetic characteristics of each strain as shown in another B cell tropic virus, Epstein Barr Virus (EBV)¹⁵⁸. Furthermore, studies using live cell imaging of infected cultures could evaluate the impact of cell-to-cell interactions and trace the spread of virus from infected to uninfected cells, providing evidence for the spread of viral components through cell interactions.

Lastly, MeV infection causes differences in the frequency of detectable sub-types of circulating immune cells following infection, suggesting that changes caused by infection may

impact different immune cell sub-types to varying degrees⁷⁴. Due to the difficulty of obtaining these sub-types, it was outside the scope of this thesis work. There are detectable decreases in certain sub-types of B cells following infection such as IgA and IgG B cells⁷⁴. Our data shows that there are differences in the frequency of infection in some sub-types of B cell, suggesting MeV may target B cell sub-types differently at the various stages in the B cell differentiation and development processes. Infection of B cells at different stages in B cell development could impact the genetic composition of MeV, impacting the ability of MeV to infect other cells and its ability to inhibit host-cell responses. Understanding the consequence of how MeV may impact B cell sub-types and how this could vary based on sub-type could help elucidate the role of B cells in the development of MeV induced immune suppression. Additionally, studies focused on understanding the infection specifically in cells that impact the antibody repertoire such as cells involved in the germinal center reaction and plasma cells may contribute to understanding the loss of antibody repertoire and effector function following wild-type infection. Our studies aim to leverage the comparison of B cells infected with a vaccine strain of MeV with B cells infected with wild-type MeV to further understand the contribution of B cells to MeV induced immune suppression.



Graphical Abstract for Thesis Findings

REFERENCES

1. Griffin, D.E., *Measles*, in *Fields Virology*, D.M. Knipe and P.M. Howley, Editors. 2013, Lippincott Williams & Wilkins: Wolters Kluwer Health. p. 1042-1069.
2. Williams, D., et al., *Update: circulation of active genotypes of measles virus and recommendations for use of sequence analysis to monitor viral transmission*. Weekly Epidemiological Record, 2022. **39**: p. 485-492.
3. Neverov, A.A., et al., *Genotyping of measles virus in clinical specimens on the basis of oligonucleotide microarray hybridization patterns*. J Clin Microbiol, 2006. **44**(10): p. 3752-9.
4. Moss, W.J. and D.E. Griffin, *Global measles elimination*. Nature Reviews Microbiology, 2006. **4**(12): p. 900-908.
5. World Health Organization. *Measles*. 2018; Available from: <https://www.who.int/teams/health-product-policy-and-standards/standards-and-specifications/vaccine-standardization/measles>.
6. Wise, J., *Finnish study confirms safety of MMR vaccine*. BMJ, 2001. **130**: p. 322.
7. Food and Drug Administration, *Priorix*. 2022.
8. Bennett, J.V., F.T. Cutts, and S.L. Katz, *Edmonston-Zagreb Measles Vaccine: A Good Vaccine With an Image Problem*. Pediatrics, 1999. **104**(5): p. 1123-1123.
9. Plumet, S., W.P. Duprex, and D. Gerlier, *Dynamics of viral RNA synthesis during measles virus infection*. J Virol, 2005. **79**(11): p. 6900-8.
10. Calain, P. and L. Roux, *Generation of measles virus defective interfering particles and their presence in a preparation of attenuated live-virus vaccine*. J Virol, 1988. **62**(8): p. 2859-66.
11. Genoyer, E. and C.B. López, *The Impact of Defective Viruses on Infection and Immunity*. Annual Review of Virology, 2019. **6**(1): p. 547-566.
12. Ader-Ebert, N., et al., *Sequential Conformational Changes in the Morbillivirus Attachment Protein Initiate the Membrane Fusion Process*. PLOS Pathogens, 2015. **11**(5): p. e1004880.
13. Herschke, F., et al., *Cell-cell fusion induced by measles virus amplifies the type I interferon response*. J Virol, 2007. **81**(23): p. 12859-71.
14. Cattaneo, R., et al., *Measles virus editing provides an additional cysteine-rich protein*. Cell, 1989. **56**(5): p. 759-64.
15. Parisien, J.P., et al., *A shared interface mediates paramyxovirus interference with antiviral RNA helicases MDA5 and LGP2*. J Virol, 2009. **83**(14): p. 7252-60.
16. Pfaller, C.K. and K.K. Conzelmann, *Measles virus V protein is a decoy substrate for I κ B kinase alpha and prevents Toll-like receptor 7/9-mediated interferon induction*. J Virol, 2008. **82**(24): p. 12365-73.
17. Caignard, G., et al., *Measles virus V protein blocks Jak1-mediated phosphorylation of STAT1 to escape IFN-alpha/beta signaling*. Virology, 2007. **368**(2): p. 351-62.
18. Palosaari, H., et al., *STAT protein interference and suppression of cytokine signal transduction by measles virus V protein*. J Virol, 2003. **77**(13): p. 7635-44.
19. Ramachandran, A., J.P. Parisien, and C.M. Horvath, *STAT2 is a primary target for measles virus V protein-mediated alpha/beta interferon signaling inhibition*. J Virol, 2008. **82**(17): p. 8330-8.
20. Devaux, P., et al., *Attenuation of V- or C-Defective Measles Viruses: Infection Control by the Inflammatory and Interferon Responses of Rhesus Monkeys*. Journal of Virology, 2008. **82**(11): p. 5359-5367.
21. Takeuchi, K., et al., *Stringent requirement for the C protein of wild-type measles virus for growth both in vitro and in macaques*. J Virol, 2005. **79**(12): p. 7838-44.
22. Nakatsu, Y., et al., *Measles virus circumvents the host interferon response by different actions of the C and V proteins*. J Virol, 2008. **82**(17): p. 8296-306.

23. Sparrer, K.M.J., C.K. Pfaller, and K.-K. Conzelmann, *Measles Virus C Protein Interferes with Beta Interferon Transcription in the Nucleus*. Journal of Virology, 2012. **86**(2): p. 796-805.
24. Yokota, S., T. Okabayashi, and N. Fujii, *Measles virus C protein suppresses gamma-activated factor formation and virus-induced cell growth arrest*. Virology, 2011. **414**(1): p. 74-82.
25. Ravel, K., et al., *Measles virus nucleocapsid protein binds to FcγRII and inhibits human B cell antibody production*. J Exp Med, 1997. **186**(2): p. 269-78.
26. Marie, J.C., et al., *Mechanism of measles virus-induced suppression of inflammatory immune responses*. Immunity, 2001. **14**(1): p. 69-79.
27. Marie, J.C., et al., *Cell Surface Delivery of the Measles Virus Nucleoprotein: a Viral Strategy To Induce Immunosuppression*. Journal of Virology, 2004. **78**(21): p. 11952-11961.
28. Iwasaki, M., et al., *The matrix protein of measles virus regulates viral RNA synthesis and assembly by interacting with the nucleocapsid protein*. J Virol, 2009. **83**(20): p. 10374-83.
29. Division of Viral Diseases/National Center for Immunization and Respiratory Diseases. *Measles History*. 2020; Available from: <https://www.cdc.gov/measles/about/history.html>.
30. Pan-American Health Organization. *Measles*. 2020; Available from: <https://www.paho.org/en/topics/measles>.
31. World Health Organization, *Implementing the Immunization Agenda 2030*. 2021.
32. *Framework for verifying elimination of measles and rubella*. Wkly Epidemiol Rec, 2013. **88**(9): p. 89-99.
33. National Center for Immunization and Respiratory Diseases/Division of Viral Diseases. *Measles Cases and Outbreaks*. 2022 January 6, 2023; Available from: <https://www.cdc.gov/measles/cases-outbreaks.html>.
34. Patel, M.K., et al., *Progress Toward Regional Measles Elimination - Worldwide, 2000-2019*. MMWR Morb Mortal Wkly Rep, 2020. **69**(45): p. 1700-1705.
35. Minta, A., et al., *Progress Toward Regional Measles Elimination — Worldwide, 2000–2021*. MMWR Morb Mortal Wkly Rep, 2022. **71**: p. 1489-1495.
36. Browning, M.B., et al., *The T cell activation marker CD150 can be used to identify alloantigen-activated CD4(+)25+ regulatory T cells*. Cell Immunol, 2004. **227**(2): p. 129-39.
37. De Salort, J., et al., *Expression of SLAM (CD150) cell-surface receptors on human B-cell subsets: from pro-B to plasma cells*. Immunol Lett, 2011. **134**(2): p. 129-36.
38. Romanets-Korbut, O., et al., *Measles virus hemagglutinin triggers intracellular signaling in CD150-expressing dendritic cells and inhibits immune response*. Cell Mol Immunol, 2016. **13**(6): p. 828-838.
39. Ferreira, C.S., et al., *Measles virus infection of alveolar macrophages and dendritic cells precedes spread to lymphatic organs in transgenic mice expressing human signaling lymphocytic activation molecule (SLAM, CD150)*. J Virol, 2010. **84**(6): p. 3033-42.
40. Cannons, J.L., S.G. Tangye, and P.L. Schwartzberg, *SLAM family receptors and SAP adaptors in immunity*. Annu Rev Immunol, 2011. **29**: p. 665-705.
41. de Witte, L., et al., *Measles virus targets DC-SIGN to enhance dendritic cell infection*. J Virol, 2006. **80**(7): p. 3477-86.
42. de Vries, R.D., et al., *In vivo tropism of attenuated and pathogenic measles virus expressing green fluorescent protein in macaques*. J Virol, 2010. **84**(9): p. 4714-24.
43. Yanagi, Y., et al., *Measles virus receptors*. Curr Top Microbiol Immunol, 2009. **329**: p. 13-30.
44. Lemon, K., et al., *Early target cells of measles virus after aerosol infection of non-human primates*. PLoS Pathog, 2011. **7**(1): p. e1001263.
45. Ludlow, M., et al., *Pathological consequences of systemic measles virus infection*. J Pathol, 2015. **235**(2): p. 253-65.

46. Mateo, M., et al., *Different Roles of the Three Loops Forming the Adhesive Interface of Nectin-4 in Measles Virus Binding and Cell Entry, Nectin-4 Homodimerization, and Heterodimerization with Nectin-1*. Journal of Virology, 2014. **88**(24): p. 14161-14171.
47. Racaniello, V., *An Exit Strategy for Measles Virus*. Science, 2011. **334**(6063): p. 1650-1651.
48. Rota, P.A., et al., *Measles*. Nat Rev Dis Primers, 2016. **2**: p. 16049.
49. Baxby, D., *The diagnosis of the invasion of measles from a study of the exanthema as it appears on the buccal mucous membrane* By Henry Koplik, M.D. Reproduced from Arch. Paed. 13, 918-922 (1886). Rev Med Virol, 1997. **7**(2): p. 71-74.
50. Ferren, M., B. Horvat, and C. Mathieu, *Measles Encephalitis: Towards New Therapeutics*. Viruses, 2019. **11**(11).
51. National Institute of Neurological Disorders and Stroke. *Subacute Sclerosing Panencephalitis*. 2022 July 25, 2022; Available from: <https://www.ninds.nih.gov/health-information/disorders/subacute-sclerosing-panencephalitis>.
52. Griffin, D.E., *Measles virus-induced suppression of immune responses*. Immunol Rev, 2010. **236**: p. 176-89.
53. Mina, M.J., et al., *Long-term measles-induced immunomodulation increases overall childhood infectious disease mortality*. Science, 2015. **348**(6235): p. 694-9.
54. Gadroen, K., et al., *Impact and longevity of measles-associated immune suppression: a matched cohort study using data from the THIN general practice database in the UK*. BMJ Open, 2018. **8**(11): p. e021465.
55. Davis, M.E., et al., *Antagonism of the phosphatase PP1 by the measles virus V protein is required for innate immune escape of MDA5*. Cell Host Microbe, 2014. **16**(1): p. 19-30.
56. Schuhmann, K.M., C.K. Pfaller, and K.K. Conzelmann, *The measles virus V protein binds to p65 (RelA) to suppress NF-kappaB activity*. J Virol, 2011. **85**(7): p. 3162-71.
57. Wang, J., et al., *NF-kappa B RelA subunit is crucial for early IFN-beta expression and resistance to RNA virus replication*. J Immunol, 2010. **185**(3): p. 1720-9.
58. Kessler, J.R., J.R. Kremer, and C.P. Muller, *Interplay of measles virus with early induced cytokines reveals different wild type phenotypes*. Virus Res, 2011. **155**(1): p. 195-202.
59. Shivakoti, R., et al., *Limited in vivo production of type I or type III interferon after infection of macaques with vaccine or wild-type strains of measles virus*. J Interferon Cytokine Res, 2015. **35**(4): p. 292-301.
60. Komune, N., et al., *Measles virus V protein inhibits NLRP3 inflammasome-mediated interleukin-1 β secretion*. J Virol, 2011. **85**(24): p. 13019-26.
61. Zilliox, M.J., W.J. Moss, and D.E. Griffin, *Gene expression changes in peripheral blood mononuclear cells during measles virus infection*. Clin Vaccine Immunol, 2007. **14**(7): p. 918-23.
62. ten Oever, J., et al., *Characterization of the Acute Inflammatory Response in Measles Infection*. Journal of the Pediatric Infectious Diseases Society, 2013. **3**(3): p. 197-200.
63. Dubois, B., et al., *Measles virus exploits dendritic cells to suppress CD4+ T-cell proliferation via expression of surface viral glycoproteins independently of T-cell trans-infection*. Cell Immunol, 2001. **214**(2): p. 173-83.
64. Hahm, B., N. Arbour, and M.B. Oldstone, *Measles virus interacts with human SLAM receptor on dendritic cells to cause immunosuppression*. Virology, 2004. **323**(2): p. 292-302.
65. Fugier-Vivier, I., et al., *Measles virus suppresses cell-mediated immunity by interfering with the survival and functions of dendritic and T cells*. J Exp Med, 1997. **186**(6): p. 813-23.
66. Servet-Delprat, C., et al., *Measles virus induces abnormal differentiation of CD40 ligand-activated human dendritic cells*. J Immunol, 2000. **164**(4): p. 1753-60.

67. Hahm, B., J.H. Cho, and M.B. Oldstone, *Measles virus-dendritic cell interaction via SLAM inhibits innate immunity: selective signaling through TLR4 but not other TLRs mediates suppression of IL-12 synthesis*. *Virology*, 2007. **358**(2): p. 251-7.
68. Abt, M., E. Gassert, and S. Schneider-Schaulies, *Measles virus modulates chemokine release and chemotactic responses of dendritic cells*. *J Gen Virol*, 2009. **90**(Pt 4): p. 909-914.
69. Grosjean, I., et al., *Measles virus infects human dendritic cells and blocks their allostimulatory properties for CD4+ T cells*. *J Exp Med*, 1997. **186**(6): p. 801-12.
70. Avota, E., et al., *Disruption of Akt kinase activation is important for immunosuppression induced by measles virus*. *Nat Med*, 2001. **7**(6): p. 725-31.
71. Kaiko, G.E., et al., *Immunological decision-making: how does the immune system decide to mount a helper T-cell response?* *Immunology*, 2008. **123**(3): p. 326-38.
72. Roscic-Mrkic, B., et al., *Roles of macrophages in measles virus infection of genetically modified mice*. *J Virol*, 2001. **75**(7): p. 3343-51.
73. Permar, S.R., et al., *Role of CD8(+) lymphocytes in control and clearance of measles virus infection of rhesus monkeys*. *J Virol*, 2003. **77**(7): p. 4396-400.
74. Laksono, B.M., et al., *Studies into the mechanism of measles-associated immune suppression during a measles outbreak in the Netherlands*. *Nat Commun*, 2018. **9**(1): p. 4944.
75. Borysiewicz, L.K., et al., *The immunosuppressive effects of measles virus on T cell function--failure to affect IL-2 release or cytotoxic T cell activity in vitro*. *Clin Exp Immunol*, 1985. **59**(1): p. 29-36.
76. de Vries, R.D., et al., *Measles immune suppression: lessons from the macaque model*. *PLoS Pathog*, 2012. **8**(8): p. e1002885.
77. Vuorinen, T., P. Peri, and R. Vainionpää, *Measles virus induces apoptosis in uninfected bystander T cells and leads to granzyme B and caspase activation in peripheral blood mononuclear cell cultures*. *Eur J Clin Invest*, 2003. **33**(5): p. 434-42.
78. Mueller, N., et al., *Neutral sphingomyelinase in physiological and measles virus induced T cell suppression*. *PLoS Pathog*, 2014. **10**(12): p. e1004574.
79. McChesney, M.B., et al., *Measles virus infection of B lymphocytes permits cellular activation but blocks progression through the cell cycle*. *J Virol*, 1987. **61**(11): p. 3441-7.
80. Mina, M.J., et al., *Measles virus infection diminishes preexisting antibodies that offer protection from other pathogens*. *Science*, 2019. **366**(6465): p. 599-606.
81. Petrova, V.N., et al., *Incomplete genetic reconstitution of B cell pools contributes to prolonged immunosuppression after measles*. *Sci Immunol*, 2019. **4**(41).
82. Laksono, B.M., et al., *In Vitro Measles Virus Infection of Human Lymphocyte Subsets Demonstrates High Susceptibility and Permissiveness of both Naive and Memory B Cells*. *J Virol*, 2018. **92**(8).
83. Zhao, J., et al., *Pathogenesis of canine distemper virus in experimentally infected raccoon dogs, foxes, and minks*. *Antiviral Res*, 2015. **122**: p. 1-11.
84. Bankamp, B., et al., *Genetic characterization of measles vaccine strains*. *J Infect Dis*, 2011. **204 Suppl 1**: p. S533-48.
85. Bankamp, B., et al., *Genetic changes that affect the virulence of measles virus in a rhesus macaque model*. *Virology*, 2008. **373**(1): p. 39-50.
86. Marie, J.C., et al., *Cell surface delivery of the measles virus nucleoprotein: a viral strategy to induce immunosuppression*. *J Virol*, 2004. **78**(21): p. 11952-61.
87. Yokota, S., et al., *Measles virus P protein suppresses Toll-like receptor signal through up-regulation of ubiquitin-modifying enzyme A20*. *Faseb j*, 2008. **22**(1): p. 74-83.
88. Sparrer, K.M., C.K. Pfaller, and K.K. Conzelmann, *Measles virus C protein interferes with Beta interferon transcription in the nucleus*. *J Virol*, 2012. **86**(2): p. 796-805.

89. Yu, X., et al., *Measles Virus Matrix Protein Inhibits Host Cell Transcription*. PLoS One, 2016. **11**(8): p. e0161360.
90. Hutchins, S.S., et al., *Evaluation of the measles clinical case definition*. J Infect Dis, 2004. **189** **Suppl 1**: p. S153-9.
91. Salama, P., et al., *Malnutrition, measles, mortality, and the humanitarian response during a famine in Ethiopia*. Jama, 2001. **286**(5): p. 563-71.
92. Wolfson, L.J., et al., *Has the 2005 measles mortality reduction goal been achieved? A natural history modelling study*. Lancet, 2007. **369**(9557): p. 191-200.
93. Dixon, M.G., et al., *Progress Toward Regional Measles Elimination - Worldwide, 2000-2020*. MMWR Morb Mortal Wkly Rep, 2021. **70**(45): p. 1563-1569.
94. Nelson, A.N., et al., *Evolution of T Cell Responses during Measles Virus Infection and RNA Clearance*. Sci Rep, 2017. **7**(1): p. 11474.
95. Singh, B.K., et al., *Cell-to-Cell Contact and Nectin-4 Govern Spread of Measles Virus from Primary Human Myeloid Cells to Primary Human Airway Epithelial Cells*. Journal of Virology, 2016. **90**(15): p. 6808-6817.
96. Mühlebach, M.D., et al., *Adherens junction protein nectin-4 is the epithelial receptor for measles virus*. Nature, 2011. **480**(7378): p. 530-3.
97. Gadroen, K., et al., *Impact and longevity of measles-associated immune suppression: a matched cohort study using data from the THIN general practice database in the UK*. BMJ Open, 2018. **8**(11): p. e021465.
98. Romanets-Korbut, O., et al., *Measles virus hemagglutinin triggers intracellular signaling in CD150-expressing dendritic cells and inhibits immune response*. Cellular & Molecular Immunology, 2016. **13**(6): p. 828-838.
99. de Vries, R.D., et al., *Measles Immune Suppression: Lessons from the Macaque Model*. PLOS Pathogens, 2012. **8**(8): p. e1002885.
100. Laksono, B.M., et al., *Studies into the mechanism of measles-associated immune suppression during a measles outbreak in the Netherlands*. Nature Communications, 2018. **9**(1): p. 4944.
101. Beck, M., et al., *Immune response to Edmonston-Zagreb measles virus strain in monovalent and combined MMR vaccine*. Dev Biol Stand, 1986. **65**: p. 95-100.
102. Brown KE, R.P., Goodson JL, et al., *Genetic Characterization of Measles and Rubella Viruses Detected Through Global Measles and Rubella Elimination Surveillance, 2016–2018*. MMWR Morb Mortal Wkly Rep, 2019(68): p. 587-591.
103. World Health Organization, *Genetic diversity of wild-type measles viruses and the global measles nucleotide surveillance database (MeaNS)*. Wkly Epidemiol Rec, 2015(90): p. 373-380.
104. Williams, D., et al., *Update: circulation of active genotypes of measles virus and recommendations for use of sequence analysis to monitor viral transmission* Weekly Epidemiological Record, 2022. **39**.
105. Ono, N., et al., *Measles viruses on throat swabs from measles patients use signaling lymphocytic activation molecule (CDw150) but not CD46 as a cellular receptor*. J Virol, 2001. **75**(9): p. 4399-401.
106. Rennick, L.J., et al., *Live-attenuated measles virus vaccine targets dendritic cells and macrophages in muscle of nonhuman primates*. J Virol, 2015. **89**(4): p. 2192-200.
107. Lei, C., et al., *On the Calculation of TCID₅₀ for Quantitation of Virus Infectivity*. Virol Sin, 2021. **36**(1): p. 141-144.
108. Hummel, K.B., et al., *Development of quantitative gene-specific real-time RT-PCR assays for the detection of measles virus in clinical specimens*. J Virol Methods, 2006. **132**(1-2): p. 166-73.
109. Ramakrishnan, M.A., *Determination of 50% endpoint titer using a simple formula*. World J Virol, 2016. **5**(2): p. 85-6.

110. Wu, Y.-C.B., D. Kipling, and D. Dunn-Walters, *The Relationship between CD27 Negative and Positive B Cell Populations in Human Peripheral Blood*. *Frontiers in Immunology*, 2011. **2**.
111. Koethe, S., E. Avota, and S. Schneider-Schaulies, *Measles virus transmission from dendritic cells to T cells: formation of synapse-like interfaces concentrating viral and cellular components*. *J Virol*, 2012. **86**(18): p. 9773-81.
112. Singh, B.K., et al., *Measles Virus Ribonucleoprotein Complexes Rapidly Spread across Well-Differentiated Primary Human Airway Epithelial Cells along F-Actin Rings*. *mBio*, 2019. **10**(6): p. e02434-19.
113. Singh, B.K., et al., *Cell-to-Cell Contact and Nectin-4 Govern Spread of Measles Virus from Primary Human Myeloid Cells to Primary Human Airway Epithelial Cells*. *J Virol*, 2016. **90**(15): p. 6808-6817.
114. Nguyen, D.T., et al., *The synthetic bacterial lipopeptide Pam3CSK4 modulates respiratory syncytial virus infection independent of TLR activation*. *PLoS Pathog*, 2010. **6**(8): p. e1001049.
115. Hahm, B., et al., *Measles virus infects and suppresses proliferation of T lymphocytes from transgenic mice bearing human signaling lymphocytic activation molecule*. *J Virol*, 2003. **77**(6): p. 3505-15.
116. Starr, S. and S. Berkovich, *EFFECTS OF MEASLES, GAMMA-GLOBULIN-MODIFIED MEASLES AND VACCINE MEASLES ON THE TUBERCULIN TEST*. *N Engl J Med*, 1964. **270**: p. 386-91.
117. Kober, A.M., et al., *Caspase-8 activity has an essential role in CD95/Fas-mediated MAPK activation*. *Cell Death Dis*, 2011. **2**(10): p. e212.
118. Avrutsky, M.I. and C.M. Troy, *Caspase-9: A Multimodal Therapeutic Target With Diverse Cellular Expression in Human Disease*. *Front Pharmacol*, 2021. **12**: p. 701301.
119. Strasser, A., S. Cory, and J.M. Adams, *Deciphering the rules of programmed cell death to improve therapy of cancer and other diseases*. *Embo j*, 2011. **30**(18): p. 3667-83.
120. Chen, J., et al., *Molecular Insights into the Mechanism of Necroptosis: The Necrosome As a Potential Therapeutic Target*. *Cells*, 2019. **8**(12).
121. Bhaskar, A., et al., *Expression of Measles Virus Nucleoprotein Induces Apoptosis and Modulates Diverse Functional Proteins in Cultured Mammalian Cells*. *PLOS ONE*, 2011. **6**(4): p. e18765.
122. Kumar, A., et al., *Influenza virus exploits tunneling nanotubes for cell-to-cell spread*. *Sci Rep*, 2017. **7**: p. 40360.
123. Singh, B.K., et al., *Correction for Singh et al., The Nectin-4/Afadin Protein Complex and Intercellular Membrane Pores Contribute to Rapid Spread of Measles Virus in Primary Human Airway Epithelia*. *J Virol*, 2016. **90**(6): p. 3278.
124. McDonald, D., *Dendritic Cells and HIV-1 Trans-Infection*. *Viruses*, 2010. **2**(8): p. 1704-1717.
125. Mehedi, M., et al., *Actin-Related Protein 2 (ARP2) and Virus-Induced Filopodia Facilitate Human Respiratory Syncytial Virus Spread*. *PLoS Pathog*, 2016. **12**(12): p. e1006062.
126. Roberts, K.L., B. Manicassamy, and R.A. Lamb, *Influenza A virus uses intercellular connections to spread to neighboring cells*. *J Virol*, 2015. **89**(3): p. 1537-49.
127. El Najjar, F., et al., *Human metapneumovirus Induces Reorganization of the Actin Cytoskeleton for Direct Cell-to-Cell Spread*. *PLoS Pathog*, 2016. **12**(9): p. e1005922.
128. Guo, R., et al., *Porcine Reproductive and Respiratory Syndrome Virus Utilizes Nanotubes for Intercellular Spread*. *J Virol*, 2016. **90**(10): p. 5163-5175.
129. Mehedi, M., et al., *Actin-Related Protein 2 (ARP2) and Virus-Induced Filopodia Facilitate Human Respiratory Syncytial Virus Spread*. *PLOS Pathogens*, 2016. **12**(12): p. e1006062.
130. Widmann, C., *Caspase 8*. Elsevier 2007.
131. Brentnall, M., et al., *Caspase-9, caspase-3 and caspase-7 have distinct roles during intrinsic apoptosis*. *BMC Cell Biology*, 2013. **14**(1): p. 32.

132. Hildebrand, J.M., et al., *Activation of the pseudokinase MLKL unleashes the four-helix bundle domain to induce membrane localization and necroptotic cell death*. Proc Natl Acad Sci U S A, 2014. **111**(42): p. 15072-7.
133. Balachandran, S. and G.F. Rall, *Benefits and Perils of Necroptosis in Influenza Virus Infection*. Journal of Virology, 2020. **94**(9): p. e01101-19.
134. Tamashiro, V.G., H.H. Perez, and D.E. Griffin, *Prospective study of the magnitude and duration of changes in tuberculin reactivity during uncomplicated and complicated measles*. Pediatr Infect Dis J, 1987. **6**(5): p. 451-4.
135. Nelson, A.N., et al., *Association of persistent wild-type measles virus RNA with long-term humoral immunity in rhesus macaques*. JCI Insight, 2020. **5**(3).
136. Richter, K., G. Perriard, and A. Oxenius, *Reversal of chronic to resolved infection by IL-10 blockade is LCMV strain dependent*. Eur J Immunol, 2013. **43**(3): p. 649-54.
137. Lin, W.H., et al., *Prolonged persistence of measles virus RNA is characteristic of primary infection dynamics*. Proc Natl Acad Sci U S A, 2012. **109**(37): p. 14989-94.
138. Boussiotis, V.A., et al., *Tumor necrosis factor alpha is an autocrine growth factor for normal human B cells*. Proceedings of the National Academy of Sciences, 1994. **91**(15): p. 7007-7011.
139. Bieback, K., et al., *Hemagglutinin protein of wild-type measles virus activates toll-like receptor 2 signaling*. J Virol, 2002. **76**(17): p. 8729-36.
140. Agrawal, S. and S. Gupta, *TLR1/2, TLR7, and TLR9 Signals Directly Activate Human Peripheral Blood Naive and Memory B Cell Subsets to Produce Cytokines, Chemokines, and Hematopoietic Growth Factors*. Journal of Clinical Immunology, 2011. **31**(1): p. 89-98.
141. Ganley-Leal, L.M., X. Liu, and L.M. Wetzler, *Toll-like receptor 2-mediated human B cell differentiation*. Clinical Immunology, 2006. **120**(3): p. 272-284.
142. Baggolini, M. and I. Clark-Lewis, *Interleukin-8, a chemotactic and inflammatory cytokine*. FEBS Lett, 1992. **307**(1): p. 97-101.
143. Jinqun, T., et al., *Chemotaxis and IL-8 receptor expression in B cells from normal and HIV-infected subjects*. The Journal of Immunology, 1997. **158**(1): p. 475-484.
144. Sidorenko, S.P. and E.A. Clark, *Characterization of a cell surface glycoprotein IPO-3, expressed on activated human B and T lymphocytes*. J Immunol, 1993. **151**(9): p. 4614-24.
145. Punnonen, J., et al., *Soluble and membrane-bound forms of signaling lymphocytic activation molecule (SLAM) induce proliferation and Ig synthesis by activated human B lymphocytes*. J Exp Med, 1997. **185**(6): p. 993-1004.
146. Cocks, B.G., et al., *A novel receptor involved in T-cell activation*. Nature, 1995. **376**(6537): p. 260-263.
147. Castro, A.G., et al., *Molecular and functional characterization of mouse signaling lymphocytic activation molecule (SLAM): differential expression and responsiveness in Th1 and Th2 cells*. J Immunol, 1999. **163**(11): p. 5860-70.
148. Henning, G., et al., *Signaling lymphocytic activation molecule (SLAM) regulates T cellular cytotoxicity*. European Journal of Immunology, 2001. **31**(9): p. 2741-2750.
149. Ravanel, K., et al., *Measles Virus Nucleocapsid Protein Binds to FcγRII and Inhibits Human B Cell Antibody Production*. Journal of Experimental Medicine, 1997. **186**(2): p. 269-278.
150. Miltenyi Biotec. *Blood*. 2023; Available from: <https://www.miltenyibiotec.com/US-en/resources/macs-handbook/human-cells-and-organs/human-cell-sources/blood-human.html#gref>.
151. Miyauchi, K., et al., *Cytokine signatures of transformed B cells with distinct Epstein-Barr virus latencies as a potential diagnostic tool for B cell lymphoma*. Cancer Sci, 2011. **102**(6): p. 1236-41.
152. Weller, S., et al., *Human blood IgM "memory" B cells are circulating splenic marginal zone B cells harboring a prediversified immunoglobulin repertoire*. Blood, 2004. **104**(12): p. 3647-54.

153. Cerutti, A., M. Cols, and I. Puga, *Marginal zone B cells: virtues of innate-like antibody-producing lymphocytes*. Nat Rev Immunol, 2013. **13**(2): p. 118-32.
154. Mocarski, E.S., J.W. Upton, and W.J. Kaiser, *Viral infection and the evolution of caspase 8-regulated apoptotic and necrotic death pathways*. Nat Rev Immunol, 2011. **12**(2): p. 79-88.
155. Rohrschneider, L.R., et al., *Structure, function, and biology of SHIP proteins*. Genes Dev, 2000. **14**(5): p. 505-20.
156. Gartshteyn, Y., A.D. Askanase, and A. Mor, *SLAM Associated Protein Signaling in T Cells: Tilting the Balance Toward Autoimmunity*. Frontiers in Immunology, 2021. **12**.
157. Donohue, R.C., C.K. Pfaller, and R. Cattaneo, *Cyclical adaptation of measles virus quasispecies to epithelial and lymphocytic cells: To V, or not to V*. PLoS Pathog, 2019. **15**(2): p. e1007605.
158. Hutt-Fletcher, L.M., *The Long and Complicated Relationship between Epstein-Barr Virus and Epithelial Cells*. J Virol, 2017. **91**(1).